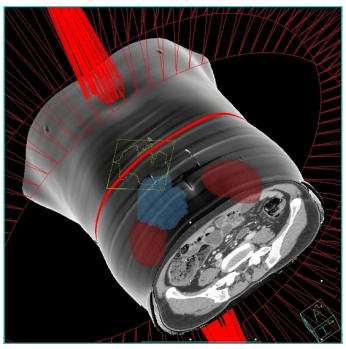

Clinical implementation of Monte Carlo simulations of a Varian TrueBeam unit

Jorge Eduardo Nunes Oliveira
Mestrado em Física médica
Departamento de Física e Astronomia
2017

Orientador
Alessandro Esposito, PhD, Faculdade de Ciências do Porto

Coorientador
João Miranda Santos, PhD, Instituto Português de Oncologia do Porto

Todas as correções determinadas pelo júri, e só essas, foram efetuadas.

O Presidente do Júri,

Porto, _____/_____/_____

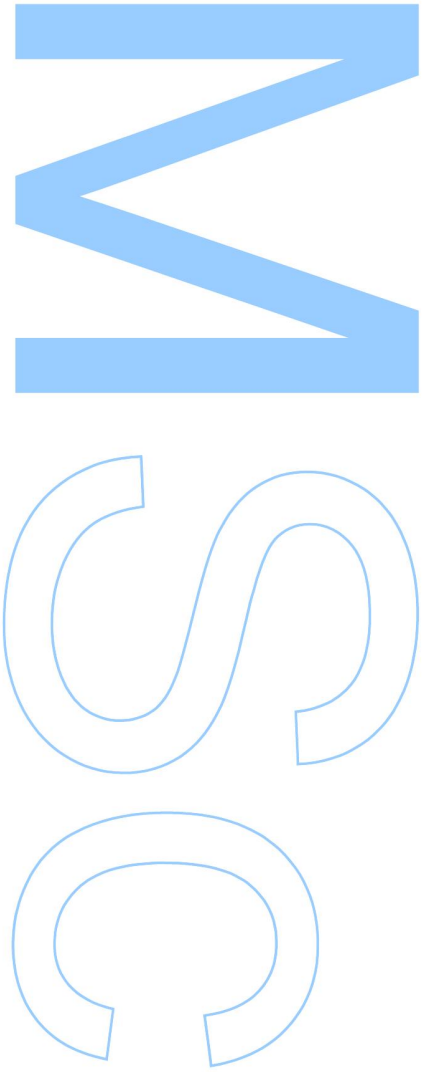

Acknowledgments

The work that you will find in this document is merit of several people who gave support to this endeavour and who at the right moments were there for me and never let me down.
To my dearest ones, wife, mother and father, who during this time suffered from my absence, to my supervisor who although the physical distance always gave his best effort, guidance and encouragement, THANK YOU.
To my co-supervisor and to the medical physics team at IPO that during this time made me feel at home and never said no to my help requests i also say THANK YOU. This work is also yours.

Abstract

The advanced modalities of radiotherapy like the Volumetric Modulated Arc Therapy (VMAT) use non-uniform intensity fields allowing complex dose distribution patterns. The intensity modulation is obtained through the motion of the beam modifiers and, in concrete, in the case of the VMAT therapy through the synchronized motion between the Multileaf Collimator (MLC) motion and the Gantry rotation. The introduction of continuous motion with continuous treatment delivery introduces uncertainties and pose difficulties in the dose distribution calculation by Treatment Planning Systems (TPS). In order to deal with the uncertainties introduced a dedicated Quality Assurance (QA) program and patient-specific dose verifications are requested which besides capturing the staff to perform the QAs it also consumes a precious time that could be used in effective treatment. A viable alternative as a recognized golden standard for dose calculation given its most detailed description of radiation-matter interaction could be through the use of Monte Carlo (MC) methods. The caveats to this method are the not trivial set-up of the RT model and treatment and also the time needed for execute the calculation. These caveats have prevented the routinely use in clinic of this method, but recently, the PRIMO software was proposed, providing several built-in RT units models, including TrueBeam, and with a user interface that facilitates this work. Nevertheless, VMAT is not implemented yet and the core of this work is about the feasibility of using PRIMO for advanced dynamic MC simulations.

With this purpose, a TrueBeam was simulated in PRIMO using 6 and 10MeV in Flatness Filter Free mode and at 15MeV with Flatness Filter. The results were validated by Gamma Function (2%, 2mm) based on reference measurements in water tank.

Since PRIMO can deal with multiple static fields, following a Position Probability Sampling (PPS), the dynamic treatment delivery is divided into a customizable number of probabilistically sampled static configurations of jaws, leaves and gantry angles. In-house algorithms were developed to interpolate the LINAC geometrical information along the procedure once the planned information is retrieved from the DICOM plan file. A graphical user interface (GUI) was developed to assist non-expert users to configure PRIMO to simulate complex deliveries.

Static simulations in reference conditions showed always $>$ 97% of Gamma points $<$ 1 for PDD and profiles at various depths and fields sizes for the 6, 10 and 15MeV primary beam respectively. The GUI properly read, manipulated and wrote the configuration data in a .ppj format, which was accepted by PRIMO. The MLC model was validated against gafchromic measure for the 6 and 10 MeV energies in FFF mode. The GUI successfully automatized the needed tasks like the TPS treatment plan import, the dynamic treatment sampling, the primo file configuration, the several PRIMO output dose files integration and the export of the result in DICOM

format.

Several tests were made to validate the sampling algorithm and the suggested workflow to implement the VMAT simulation with the aid of PRIMO. The results obtained from gamma comparisons gave reliable outcome and great expectations for future work.

Keywords: FFF; PPS; VMAT; IMRT, MC; Dynamic, Motion; Radiotherapy; Sampling; Algorithm; Advanced treatment; Matlab; PRIMO; PENELOPE

Resumo

As modalidades avançadas de tratamento radioterapêutico, como é exemplo a técnica volumetric modulated arc therapy (VMAT), utilizam modulação não uniforme de intensidade, permitindo assim a construção de padrões complexos de distribuições de dose. A modulação de intensidade é conseguida à custa do movimento dos elementos modificadores de feixe e, no caso concreto da terapia VMAT, através da sincronização entre o movimento do multileaf collimator (MLC) e o movimento da Gantry. A introdução do movimento contínuo sem interrupção do tratamento introduz incertezas no processo e coloca dificuldades no cálculo por parte do treatment planning system (TPS). De modo a controlar o processo um programa dedicado de Controlo de Qualidade (QA) para verificação de dose é efetuado para todos os tratamentos e pacientes, procedimento que além de cativar recursos humanos para a sua realização retira tempo de disponibilidade ao Linac, tempo esse que poderia ser utilizado para tratamento efetivo. Uma alternativa viável, reconhecida como standard para calculo de dose, dada descrição detalhada de interação radiação-matéria pode ser conseguida através da utilização do Método e de Monte Carlo. Algumas dificuldade na utilização deste método são a complexidade na configuração do modelo da unidade de RT bem como do plano de tratamento e o elevado tempo normalmente necessário para a realização do cálculo. Estas dificuldades têm contribuído para limitar a sua utilização na rotina clinica, no entanto, recentemente, o software PRIMO foi sugerido para ultrapassar estas limitações uma vez que tem pré-definidos vários modelos de unidades de RT, incluindo o TrueBeam, e expõe uma interface gráfica e funcionalidades que facilitam este trabalho. No entanto o tratamento VMAT não está ainda implementado e é precisamente a determinação da exequibilidade de utilizar o PRIMO para simular tratamentos dinâmicos avançados em MC que constitui o núcleo deste trabalho.

Com este propósito foi simulada uma unidade TrueBeam em PRIMO, usando as energias de 6 e 10 MeV sem filtro aplanador e energia 15MeV com filtro. Os resultados obtidos da simulação foram validados com a função Gamma (2%, 2 mm) tendo por referência as medidas em tanque de água do comissionamento da unidade.

O software PRIMO permite calcular a dose de vários campos estáticos, daí que para simular o tratamento dinâmico, seguindo a abordagem Position Probability Sampling (PPS), o tratamento é dividido num número customizado de configurações estáticas obtidas por amostragem probabilística da posição das jaws, das folhas do MLC e do ângulo da Gantry. Foram desenvolvidos algoritmos proprietários para interpolar a informação geométrica do LINAC durante o processo, a partir da informação extraída do ficheiro DICOM do planeamento.

Foi também desenvolvida uma aplicação com interface gráfica (GUI) para auxiliar um utilizador genérico a configurar o PRIMO para realizar tratamentos complexos.
Simulações estáticas realizadas em condições de referência mostraram sempre $>$ 97% de pontos gamma $<$ 1 quer para PDD quer para os perfis laterais, isto para várias profundidades e tamanhos de campo e energias 6, 10 e 15 MeV. A GUI permite manipular e escrever os dados de configuração no formato .ppj, formato esse aceite pelo PRIMO. O modelo do colimador MLC foi validado tendo por referência medições com gafchromic para as energias de 6 e 10 MeV. A aplicação GUI automatiza várias tarefas necessárias, tais como, importar o ficheiro de plano do tratamento, amostrar o tratamento dinâmico, configurar o ficheiro .ppp do PRIMO para a simulação, integrar os vários ficheiro de dose e exportar os resultados em formato DICOM. Foram realizados vários testes para validar o algoritmo de amostragem e para validar o workflow desenhado para implementar a simulação VMAT com recurso ao PRIMO. Os resultados obtidos nas comparações gamma deixam antever expectativa favorável para a realização de trabalhos futuros.

Palavras-chave: FFF; PPS; VMAT; IMRT, MC; Dynamic, Motion; Radiotherapy; Sampling; Algorithm; Advanced treatment; Matlab; PRIMO; PENELOPE

Contents

List of Tables

List of Figures

Acronyms

3DCRT Three-dimensional conformal radiation therapy.

ART Arc Radiotherapy.

BEV Beam's Eye View.

CAX central axis.

CPDF Cumulative Probability Distribution Function.

CPE Charged particle equilibrium.

CT computed tomography.

DTA Distance To Agreement.

FF Flatness Filter.

FFF Flatness Filter Free.

FWHM Full width at half maximum.

HU Hounsfield Units.

IAEA International Atomic Energy Agency.

ICRU Commission on Radiological Units and Measurements.

IM intensity modulated.

IMRT Intensity Modulated Radiation Therapy.

LINAC Linear electron accelerator.

MC Monte Carlo.

MLC multileaf collimator.

OD Optical Density.

PDD Percentage Depth Dose.

PHSP phase space file.

PPS Position Probability Sampling.

PTV Planning Tumor Volume.

QA quality assurance.

RNG Random Number Generator.

RT External Radiotherapy.

SCS Static Component Simulation.

SSD source surface distance.

TB TrueBeam.

TPS treatment planning system.

VRT Variance Reduction Technique.

1. Introduction

1.1 Motivation

In External Radiotherapy (RT), the idea of modulating the radiation field through a collimation system motion developed into the Intensity Modulated Radiation Therapy (IMRT) concept. IMRT is an advanced RT technique, which makes use of collimation system movement to modulate the radiation field in intensity. IMRT allows creating complex dose delivered distributions patterns, at the price of great complexity, to achieve practical clinical gain. Arc Radiotherapy (ART) is an extension of the IMRT technique, which introduces the rotation of he gantry dynamically during the treatment. In Medical Physics, several dosimetric problems have been approached by means of the Monte Carlo (MC) simulation method [1]. MC approach is considered [2][3] as the golden standard method for dose calculation. In some cases it is the only one to perform absorbed dose calculations because it provides the most detailed and complete description of the radiation fields and of the particle transport in tissues. Several codes have been available for simulation in the field of RT, such as GEANT4, EGSnrc/BEAMnrc, PENELOPE, FLUKA and MCNP. Recently, PRIMO, a new software simulation system that makes use of the PENELOPE features, was developed [4]. This software has a user-friendly approach, which is a suitable and competitive characteristic for clinical activity. Nevertheless, advanced features such as IMRT/ART are not yet introduced.

Among the different LINAC models provided in the actual PRIMO release, Varian FakeBeam is an available model of the Varian TrueBeam unit. TrueBeam has very peculiar features such as the possibility of work in Flatness Filter Free (FFF) mode, respiratory gating and a real-time tracking system. TrueBeam can be used for a wide range of RT applications, including stereotactic and ART techniques. A version of PRIMO is installed at Instituto Português de Oncologia (IPO-PORTO), where previous experience on radiation beam modelling has been developed. Different attempts have been made to simulate IMRT/ART treatment with different approaches. The most common techniques are Static Component Simulation (SCS) [5] and the Position Probability Sampling (PPS)[6].

Since a Varian TrueBeam unit was installed in IPO-Porto and some tests of Monte Carlo (MC) of dynamic treatments with PRIMO were also already made in-house, the conditions were set for the development of this thesis.

1.2 Objectives

This thesis pretends to accomplish the following objectives:

- To create a fully detailed and validate model of the Varian TrueBeam unit
- To perform a feasibility study of VMAT simulation with PRIMO
- To optimize the algorithm to drive the PRIMO to simulate dynamical rotational procedures
- To assist the Medical Physics Department of the IPO in evaluating the quality of treatment delivery
- To perform some treatment plans simulations for specific case with the aim of implementing the procedure in the clinical activity.

1.3 Thesis Outline

This thesis is divided in 5 major chapters. Starting by this one where the theme is introduce and the objectives delineated. Chapter 2 provides the theoretical background, approaching the physics of radiation, the Linacs, advanced treatment techniques, Monte Carlo method and principal codes used in radiotherapy, and the methods for dynamic treatment sampling. In chapter 3 is described the implementation, with the materials used and the method followed. Chapter 4 shows the results and in chapter 5 the final conclusions are drawn.

2. Background

2.1 Radiotherapy Physics and dosimetry

2.1.1 Interaction of charged particle with matter

Charged particles incident on matter undergo inelastic and elastic interactions with atomic electrons and nuclei, that is, other charged entities. Inelastic interactions include collisional and radiative process and results in energy loss by the particle. In an elastic interaction the particle is scattered by an atomic electron or nucleus, resulting in a change of direction for the particle but no energy loss. The interaction probability for charged particles is effectively 1; an incident charged particle interact at every opportunity.

Light Charged Particle Interaction: Electrons

The electron mass is small compared with any atomic mass, and incident electrons undergo four types of particle interactions with a large amount of scattering, Figure 2.1. Collisional type interactions result in energy loss, causing ionization or excited states (higher electron orbits). The collisional losses increase as the electron velocity decreases, and decrease as the absorber atomic number increases. Radiative type interactions result in x-ray emissions. The incident electron penetrates the electron cloud and interacts with the nucleus positive electrical field, undergoing abrupt deceleration with energy loss and a change in direction. The energy is released in the form of x-rays, called bremsstrahlung (or braking) radiation. With an incident mono energetic electron fluency, a continuous x-ray spectrum is emitted because the probability of any energy loss, large or small, is equal per interaction. Successive bremsstrahlung interactions may occur as the electron loses its energy; a bremsstrahlung x-ray spectrum has a maximum energy equal to the initial electron energy and all other x-ray energies below this maximum to zero. The radiative interactions are important as they are the mechanism by which bremsstrahlung x-rays are produced in diagnostic x-ray tubes and linear accelerators. Bremsstrahlung production increase at higher incident electron energies and higher Z of the absorber.

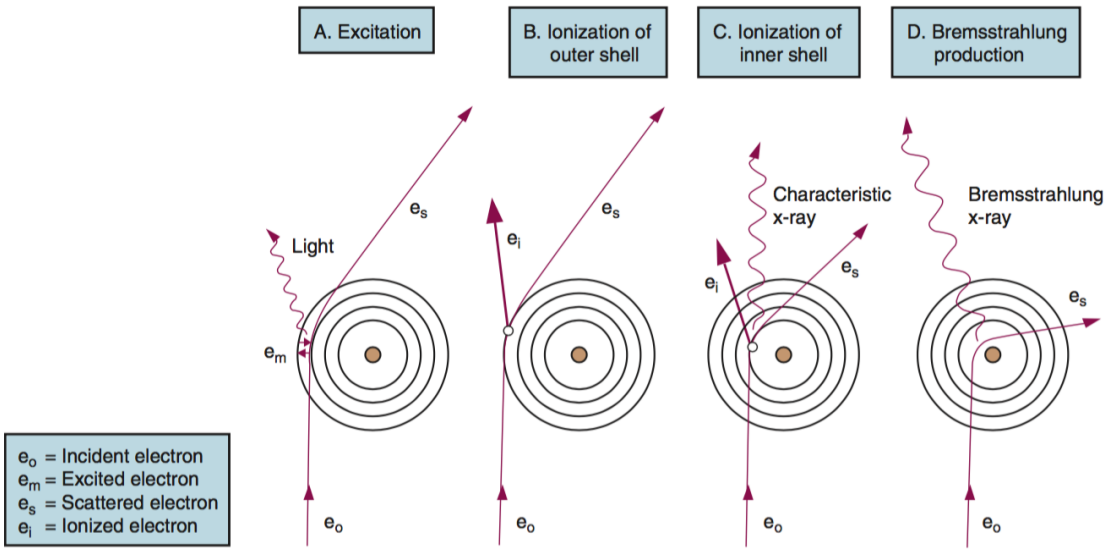

Fig. 2.1. Electron interactions. **A**, Excitation. **B**, Ionization of outer shell. **C**, Ionization of inner shell. **D**, Bremsstrahlung production.

2.1.2 Interaction of photons with matter

Photons are considered indirectly ionizing radiation, neutral particles which interact with the medium following a two steps process:

i energy transfer to charged particles in medium and.

ii energy deposition in the medium by the resulting released charged particle.

In medical imaging and treatment of diseases (radiotherapy), high-energy photons, such X-rays and γ-rays, are commonly used. When a photon passes through some medium, three different results may occur: the photon does not interact with the material; the interaction happens and the photon is totally absorbed by the medium or the photon interacts depositing some of its energy but its original trajectory is changed. The probability of occurring photon interactions with matter depends on the photon energy, density of the medium and its atomic number.

Cross section

The interaction of photons with matter is a stochastic phenomenon and the probability of each event to occur is driven by the cross section. The cross section is the parameter used to express the probability of interaction for photon radiation. It is important to point out that, as the interactions are stochastic phenomena, the particles in a photon beam, do not undergo the same interaction with the matter as the type and parameters of the interactions follow specific probabilities density functions. When considering the interactions of photons in an atomic scale, the cross section is generally defined as the atomic cross section and it can be related to the

effective area for an interaction between an X-ray photon and an atom of a particular material.

In general, the probability of occurrence of interactions depends both on photon energy and atomic number of the medium. For the energy range applied in radiotherapy, the interactions that show the highest probability to occur are the photoelectric absorption effect, incoherent (Compton) scattering, pair production and coherent (Rayleigh) scattering, Figure 2.2.

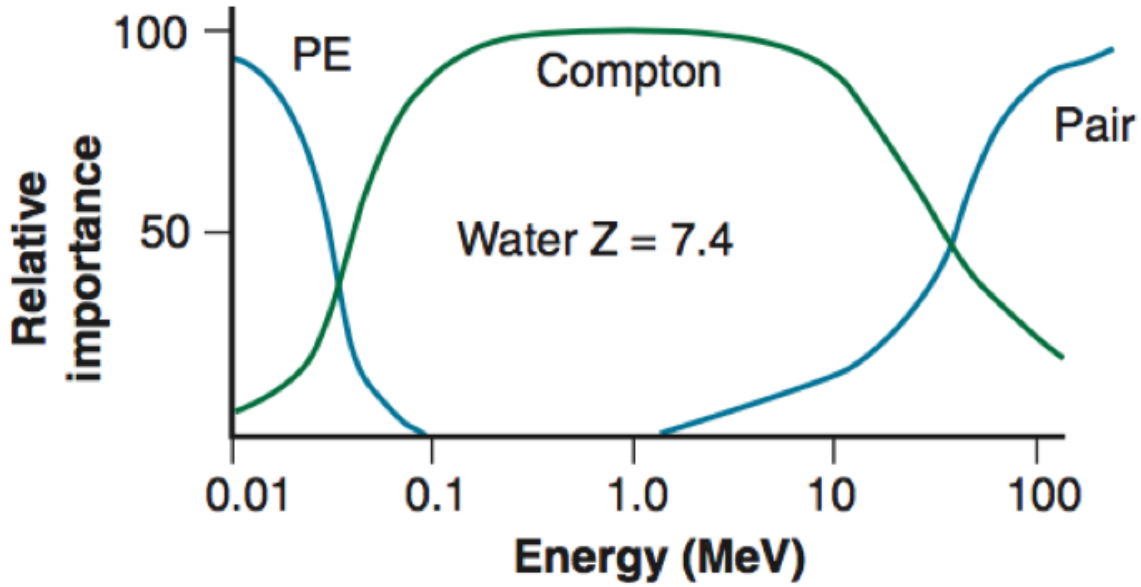

Fig. 2.2. Relative importance of photon interactions as a function of photon energy.

However, among this, only the first three interactions lead to energy deposition, as they result in the transfer of energy to electrons which will then impart it to matter in small Coulomb-force interactions along their tracks. The Rayleigh scattering, being an elastic interaction where the photon looses almost no energy and only the direction of the incident photons changes is a process that do not contribute to the transfer of energy to the medium. Figure 2.3 illustrates a scheme of these four processes.

Photoelectric absorption

The photoelectric effect is the predominant mode of interaction for photons of low energy, in the energy range of several eV to around 0.1 MeV. In this process, the incident photon interacts with a tightly bound electron (inner shells as K, L, M or N) and it is completely absorbed in the interaction and the electron (named photoelectron) is ejected from the atom In order for the photoelectric effect to occur, the incident photon energy has to be higher than the binding energy of the electron. Thus, part of the photon energy is used to overcome the binding energy and free the electron from the atom and the residual energy is transferred to the kinetic energy of the escaping electron. As result of the emission of the electron, the atom is left in an excited

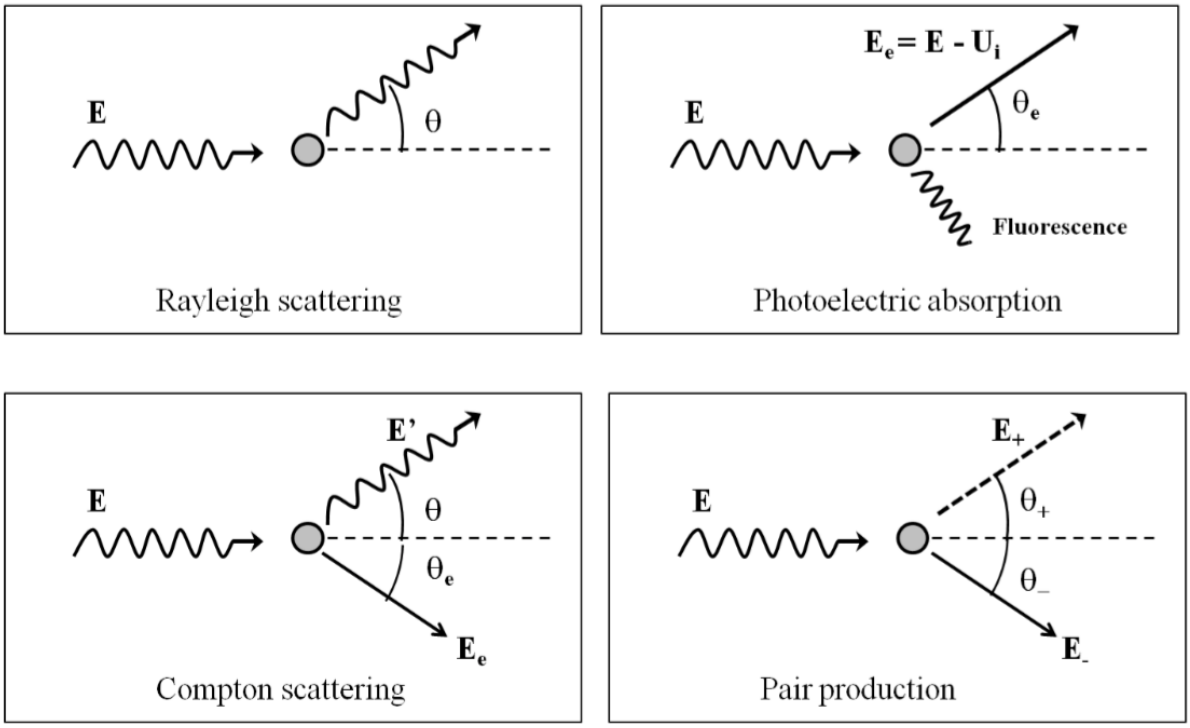

Fig. 2.3. Schematic diagrams of the main interaction processes of the photons with matter: Rayleigh scattering, Photoelectric effect, Compton scattering and Pair production.

state with a vacancy in the ionized shell. This vacancy can be quickly filled through the capture of an outer orbital electron and, therefore, one or more characteristic X-ray photons (fluorescent photons) may also be generated. In some fraction of the cases, the emission of Auger electrons may substitute for the characteristic X-ray in carrying away the atomic excitation energy. The probability of occurrence of the photoelectric effect varies roughly whit the energy of the incident photon and the atomic number Z of the medium, the photoelectric effect will be enhanced for photons of relatively low energy and for materials of high atomic number Z. The angular distribution of the emitted electrons depends on the energy of the incident photon. For low photon energy, the electrons are predominantly ejected at 90° relative to the photon direction. With increasing the photon energy, the electrons are emitted in more forward directions [7].

Incoherent (Compton) scattering

In this case the photon interacts with a free electron or with an electron which binding energy is negligible with respect to the incident photon. In this interaction the electron receives a fraction of the photon energy and moves to a certain direction, while the photon is scattered in another direction. This effect is predominant in low Z medium (e.g. human body) and at the usual energies used in radiotherapy (from the order of magnitude of some MeV).

Pair production

If the photon has energy larger than 1.02 MeV and passes near the nucleus it can interact with its electric field and the result is the disappearance of the photon and the production of an electron-positron pair. These two particles will move in opposite directions and each will carry a kinetic energy of 0.511 MeV. The positron, the antiparticle of an electron, slows down quickly and annihilates with a free electron giving off two 0.511 MeV photons that travel in opposite directions. The probability of this interaction increases with Z^2.

Coherent (Rayleigh) scattering

This interaction is purely elastic and of less importance for radiotherapy since there is no local energy transfer, only scattering of the incident photon.

2.1.3 Photon attenuation coefficients

As it passes through the material, photons may undergo one or more interactions with the atoms of the medium and some of them are absorbed or scattered leading to their removal from the initial beam. The information about the passage of the photon beam through the bulk material is given by the linear and mass attenuation coefficients. Both the primary and the scattered photons are contained in the information provided by these coefficients.

Total attenuation coefficient

As the photon beam goes through the material its attenuation is a result from the effect of all possible interaction processes and the total attenuation coefficient is expressed as the sum of the individual coefficients.

2.1.4 Fundamentals of radiation dosimetry

The result of the interaction of the radiation with matter is the transfer of a certain amount of energy to the matter through the processes of ionization and excitation. Based on this consideration, there are many different quantities and units commonly used to describe and quantify this energy transfer. An important basis for these concepts was provided in the 60's and 70's by the International Commission on Radiological Units and Measurements (ICRU). The ICRU has developed and recommended a set of fundamental quantities and units in dosimetry which has been in wide use for decades and has been vital to the successful exchange of information, and comparison of results.

Quantities and units

Generally, radiation fields are specified with two classes of radiometric quantities referring either to the number of particles or to the energy transported by these particles. These are widely used in practical applications of ionizing radiation as they provide a complete description of the field.

Fluence and energy fluency

The particle fluence Φ gives the number of particles dN that cross a sphere of unit cross-sectional dA:

$$\Phi = \frac{dN}{dA}$$

which is usually expressed in units of cm^{-2}.

The energy fluence Ψ, which is a measure of the total amount of energy entering or leaving a small volume, is defined as

$$\Psi = \frac{dR}{dA}$$

where dR denotes the radiant energy incident on a spherical volume of cross-sectional area dA. The unit for energy fluence is J m^{-2}. By radiant energy R it means the energy (excluding rest energy) of the particles emitted, transferred or received by all the particles striking the spherical volume.

Kerma

The *Kerma* (K) quantity, acronym for ***K**inetic **e**nergy **r**eleased per unit **ma**ss*, is defined as the total initial kinetic energy of the charged particles released by uncharged particles and can be written as:

$$K = \frac{dE_{tr}}{dm}$$

in which dE_{tr} is the expectation value of the energy transferred to the charged particles in a finite volume V at a point P and dm is the mass of the volume V where the energy was transferred. The unit for kerma is the same as for dose, that is, the Gray (Gy) with 1 Gy = 1 J/kg. As this charged particle can loose their energy through collision or by radiative interaction, the Kerma is usually separated into two components:

$$k = K_c + K_r$$

where K_c and K_r refer to the collision and radiative interactions, respectively.

Charged particle equilibrium

Charged particle equilibrium (CPE) is an important concept in external dosimetry, especially for photon radiation, since it allows establishing the relations between certain basic quantities. The basis of the CPE is the existence of an energy balance in a volume that will exist if each charged particle of a given type, energy and direction leaving the volume is replaced by an identical particle of the same type and energy entering the volume. One important consequence of the CPE conditions is the equivalence of the absorbed dose and the kerma. In general, the transfer of energy (kerma) from a photon beam to charged particles at a particular location does not lead to the absorption of energy by the medium (absorbed dose) at the same location, basically due to the finite range of the secondary electrons released by photon interactions but in CPE conditions it is possible to relate absorbed dose usually to collisional kerma K_c as mentioned before. Generally, in more realistic situations CPE is not usually achieved and there are two clear instances where CPE is not expected to be achieved:

1. in the build-up region of a beam where the dose increases rapidly until electronic equilibrium is achieved at the depth d_m of maximum dose. Beyond d_m, photon attenuation results in transient electronic equilibrium (i.e., energy in is slightly greater than energy out) and a decrease in dose with depth ;

2. near the edges of a finite beam at distances between the beam edge and the point under consideration larger than the maximum secondary electron range (penumbra region).

Absorbed dose

The absorbed dose D is probably the key quantity in respect to the clinical effects of the radiation interaction with matter. This concept is relevant to all types of ionizing radiation fields, either directly ionizing, such as electrons, either indirectly ionizing, such as photons. According the ICRU Report (1980), absorbed dose is defined as the mean energy imparted dϵ by the ionizing radiation to the absorbing material of mass dm:

$$D = \frac{d\epsilon}{dm}$$

The unit for dose is the Gray (Gy).

The energy included in this definition is the energy actually transferred from the radiation, independently of its type, i.e., whereas the concept of kerma deals only with primary interactions in matter, absorbed dose deals with all the interactions taking place in the medium.

It is known that the absorption of energy does not take place at the same location as the transfer of energy described by the kerma. However, both quantities are related to each other when conditions of charged particle equilibrium (CPE) exist at the point of dose calculation, that is, when the charge entering a volume is equal to the charge leaving the same volume for each type of particle and for each energy, and under this conditions:

$$D \overset{CPE}{=} K_c$$

Exposure

Exposure, X, is defined by the ICRU as the quotient of the absolute value of the total charge of the ions of one sign produced in air (dQ) by the mass of air where all the electrons produced by photons are completely stopped (dm) , that is,

$$X = \frac{dQ}{dm}$$

The SI unit for exposure is Ckg^{-1}.

Several important concepts characterize exposure, X:

1. It is defined for all ionizations, primary and secondary, when produced and measured in air.
2. It is defined only for ionizing photons (x- and γ rays), not electrons or other particles.
3. It is properly measured only under conditions of electronic equilibrium, and it is difficult to measure for photon energies higher than 3 MeV. Above this energy the electron t range in air becomes too large for electronic equilibrium to be achieved practically.

2.1.5 General considerations of basic dosimetry

Generally, radiation dosimetry can be divided into two different procedures, namely absolute and relative dosimetry. Whereas the absolute dosimetry is based on the dose measured at a given point, in the relative dosimetry the dose measured at a point of interest under certain irradiation conditions is compared to the measured dose value obtained at a reference point under specific reference conditions. All the information provided either by ionization chamber or

other dosimeter may allow the performance of a 3D-characterization of the dose distribution for each type of radiation, material and setup. Clinically, the characterization is usually performed through Percentage Depth Dose (PDD) and transversal dose profiles. The first type of profiles are defined as the quotient, expressed as percentage, of the absorbed dose at any depth *d* to the absorbed dose at a fixed reference depth d_0, along the axis of the beam (usually, Z axis). For photon beams, the typical reference depth is taken at the position of the maximum dose, denoted as d_{max}. For radiotherapy beams, Percentage Depth Dose (PDD) are usually calculated or measured for a given field size and at a predetermined source surface distance (SSD). Typically, tables of percentage depth dose data for clinical use are provided for a variety of field sizes at a standard SSD of 100 cm.Transversal dose profiles are determined across the given field (usually, X or Y axis) at a specified depth. This type of profiles is important to determine the appropriate field size of a radiation beam and to ensure thus an adequate dosimetric coverage of the tumor. In addition to these profiles, it is also usual to obtain a 2D distribution of the dose at a given depth or location. This 2D diagrams are usually known as isodose lines maps, which gives a scheme of the points or zones in a medium that receive equal doses of radiation.

2.2 The Medical Linear Accelerator (LINAC)

For the majority of cancer treatments, radiotherapy is recommended at some stage. The Linear electron accelerator (LINAC) is by far the most common equipment used for this delivery. Here is presented a general description of the common design principles of a typical modern LINAC, remarking that some differences exists between vendors.

2.2.1 Unit composition

By heating of a tungsten filament (the electron gun), electrons are liberated and then can be accelerated using a microwave field wave-guide. Due to the need of a rotating gantry, as is the case of a conventional C-arm LINAC, the accelerator structure is constrained in direction and bending magnets are introduced to redirect the electron beam through approximately 90° in the direction of the treatment table where the patient is positioned. In this travel, the electrons collide with a target of high atomic number, usually tungsten, and, from this interaction, the high-energy bremsstrahlung X-ray photons used in treatment are generated. These photons are then collimated by a primary collimator and conformed or modulated by the jaws and the multileaf collimator (MLC).

In the typical clinical energy range (4 MV-25 MV accelerating potential), the angular distribution

of the bremsstrahlung photons is predominantly in the direction of the incident electrons. This distribution is, in general, modified by a so called 'flattening' filter (FF), designed to give an almost uniform lateral dose distribution to the patient at a specific treatment depth.

In modern clinical linear accelerator this filters typically consist of conical shaped medium/high $\mathcal{Z}$ materials, such as iron, copper or tungsten, and are specific to each particular beam energy. Bellow the flattening filter, two independent transmission ion chambers provide servo control of beam steering and dose output, and increment the patient safety preventing possible excessive radiation output.

In exit to the ionization chamber and just above the exit window of the treatment head, two pairs of opposing and movable 'jaws' are responsible for limiting the field size in orthogonal directions. Further conformation of the beam to the target shape is achieved through the multileaf collimator (MLC), consisting of 40-160 tungsten 'leaves', which can be individual positioned.

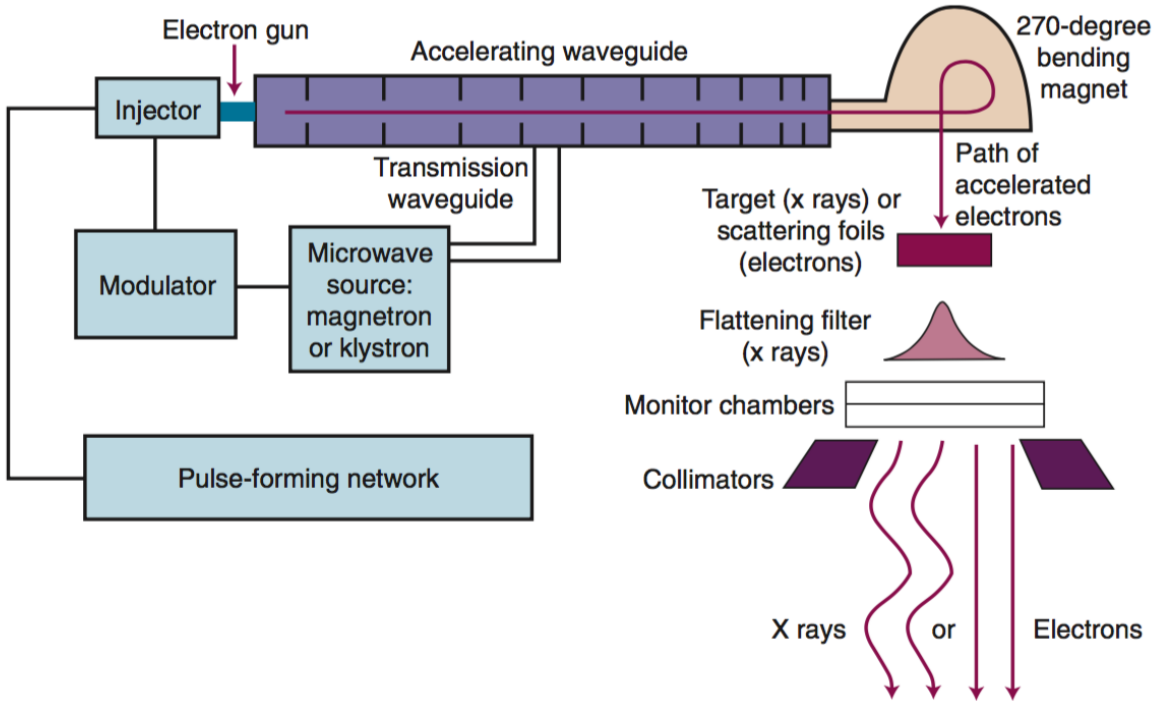

Fig. 2.4. Electron linear accelerator schematic. Key components are shown that allow a beam of electrons to be accelerated, producing a treatment beam of electrons or x-rays.

2.2.2 Removal of the flattening filter

Due to the use of the Flatness Filter (FF) some important factors can be observed. For instance, in order to achieve a uniform intensity profile across the whole extent of the beam, a large fraction of beam intensity at the central axis is removed which decreases the total output. Additionally, the filter generates scattered radiation (with photons and electrons) which contributes to undesirable dose to the patient and that can be difficult to model accurately in

the treatment planning system (TPS). Also, the photons that penetrates the flattening filter are subject to a differential amount of absorption depending on which part o the filter they pass through, leading to 'softening' of the beam energy away from the central axis (CAX), this results in a non-uniform spectral distribution and consequently a non-uniform lateral attenuation of the beam with depth.

Several studies [8][9]investigated the characteristics of non-flattened beams and compared with the conventional flattened ones. It was shown[9] that without a filter the average photon energies in a 15 MV clinical beam, measured at isocentre, only varied form 2.9 MeV at central axis to 2.5 MeV in an annular region 10-25 cm off-axis, whereas for in a conventional flattened system the mean energies were 4.11 MeV on axis an 3.3 MeV off axis, respectively. More recent studies [9] also shown that the removal of the Flatness Filter (FF) from the beam line may solve the problem of increased out-of-field dose to which the large number of photons scattered by the FF make a big contribution. The main reason why Flatness Filter Free (FFF) beams have not been widely used, is the forward peaked dose distribution or the non-uniform intensity across the field. However, this difficulty is mitigated for small fields as intensity variations are minimal over the central 1-2 centimeters of the treatment field. As field size increases, forward planning may become more challenging and in general, FFF beams are not used for large, unmodulated fields. Computer optimization, as used in inverse planning, removes the challenges of the non-uniform fluency. For instance during IMRT planning, a typical broad beam is divided into many small beamlets to provide sufficient freedom of beam intensity variations required for IMRT. FFF beams have inherent intensity variations, but these are directly incorporated into the IMRT plan optimization. In order to prevent the exit of an excessive amount of contaminating electrons from the accelerator when the flattening filter is removed, recent models with Flatness Filter Free (FFF), like the Varian 'TrueBeam' have a replacement filter of brass or copper in order to absorb these electrons.

2.3 Radiotherapy: External Beam treatments

2.3.1 General Techniques

Target depth, size, anatomic site, and proximity of critical structures influence the choice of treatment modality (photons or electrons) and the technique to be used. The technique parameters include the number of beams; beam energy; beam weight (the relative amount of dose delivered by a beam); field shape; irradiation geometry; and use of bolus, wedges, compensators, or other special devices. General practice is that photons are almost always used in a combination of two or more fields (i.e., parallel opposed, wedged pair, three field, four field,

box, or arc) and electrons are used as a single *end face* fields (perhaps in junction with other electron fields to cover a larger area). As the number of fields increases, there are two observations: The high-dose region becomes more conformal to the target, and the peripheral dose decreases but the volume of tissue covered by peripheral dose increases. Nowadays, radiotherapy is delivered by using a low number of static fields, or by increasing the complexity making use of hundreds or thousands of static sub-fields, as delivered by step&shoot IMRT. Furthermore, dynamic sliding windows IMRT and dynamic arc treatment are more complex radiotherapy treatments.

2.3.2 Advanced Modalities

3DCRT

Three-dimensional conformal radiation therapy (3DCRT) is a treatment modality in which the shape of the radiation field is fitted to the contour defined by the projection on the Planning Tumor Volume (PTV)(The PTV is the volume defined in the patient that contains the tumour, together with margin for microscopic disease spread, plus an additional safety margin for uncertainties in planning or treatment delivery)[10] . In other words, it is adjusted to the contour of the PTV as seen by an observer located at the radiation source, a perspective known as the Beam's Eye View (BEV). The field shape is set with the MLC, or custom blocks made of high density metal.

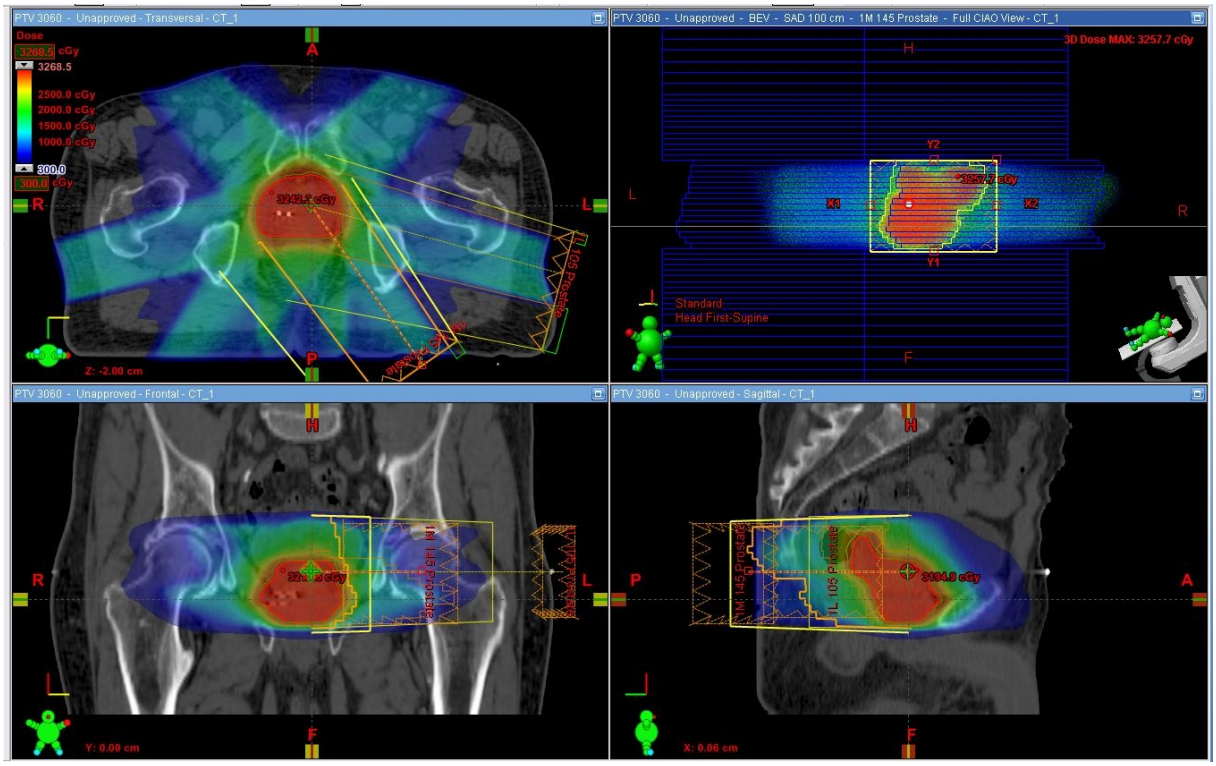

Fig. 2.5. Beam's Eye View (BEV) of a Three-dimensional conformal radiation therapy (3DCRT).

IMRT

The Intensity Modulated Radiation Therapy (IMRT) technique represents a step ahead in terms of achievable plan quality with respect to 3DCRT. Modulation can be seen as subdividing the beam in small geometrical subfields named beamlets, each with an arbitrary intensity. This can be accomplished by computed controlled positioning MLC leaves [11]. Brahme[12] showed that if the intensity is modulated across the radiation field a better dose distribution is achieved. Two alternative approaches to the delivery of IMRT using LINAC and MLC are commonly employed, they are the step-and-shoot and the sliding window techniques. The former utilizes a sequence of multiple fields (segments) of varying shape. The beam is turned on to irradiate each field when the leaves are not moving. The number of segments can be from a few to several hundred. In the sliding-windows technique leaves are continuously moving while the beam is active.

VMAT

Intensity modulated arc therapy was first proposed by Yu and Tang [13] as a generalization of the IMRT concept. It consists in delivering the intensity modulated treatment during the continuous rotation of the LINAC gantry. Yu predicted that by increasing the number of gantry angles, the number of intensity levels at each gantry angle can be reduced without degrading the plan quality. In 2008 the first commercial implementation of intensity modulated arc therapy (IMAT) was available. It appeared with the trade name of RapidArc and was marketed by Varian Medical Systems. RapidArc implements the algorithm developed by Otto [14] which includes more degrees of freedom to the dose delivery, i.e., the rotation of the gantry with variable speed and also a variable dose-rate. In addition, it uses progressive beam angle sampling to optimize a large number of apertures. The term VMAT, introduced by Otto, is widely used to identify the single-arc IMAT technique that uses variable dose-rate.

The increased complexity of the treatment requests an appropriate level of quality control to maintain safety for the patients. On the other side, an increase in the technological capability of shaping the dose to the target, allows a reduction of the doses to the organ at risk, reducing undesirable effects such as secondary induced tumors. Reducing the uncertainties during the treatment by best delivering dose to the target, allows dose escalation programs, in which a higher fractional dose is delivered in a single fraction. This approach has numerous advantages, from a radiobiological point o view and determining a lower number of treatment sessions per patient with clear benefit for the patient and for the Radiotherapy Departments schedules.

2.4 Monte Carlo

Monte Carlo (MC) is a general approach for numerical integration that is applied to several fields, from statistics to economy from medicine to physics. It is a useful technique for a wide variety of situations with a complex structure of probabilistic nature as is the case of the radiation transport in matter, where analytical approaches can be inadequate. MC is used in Radiotherapy as a numerical technique to simulate the trajectories of particles by using (pseudo)random numbers to sample the statistical distribution of the physical processes involved. The probability distributions used are derived from the underlying physical properties of the processes.

The main idea behind using Monte Carlo method is to estimate the most expected value of some variable. If this variable is obeying a uniform distribution function then this will be equivalent to finding the mean. Numerically the expected value $E(f)$ of a function $f(u)$ is calculated as:

$$E(f) = \int f(u)g(u)du$$

with $g(u)$ being the probability density function. For a uniform distribution function defined in the interval [a,b]

$$E(f) = \frac{1}{b-a}\int_a^b f(u)du$$

Considering a true random number ζ, $0 \leq \zeta \leq 1$, homogeneously distributed in the interval [0,1], the by the "law of large numbers" the expected value can be found as

$$E(f) = \frac{1}{N}\sum_{i=1}^{N} f(\zeta_i)$$

The random sequence $\zeta_i, \zeta_{i+1}, ..., \zeta_N$ must be generated using a good Random Number Generator (RNG). These generator use different techniques. One of the most used techniques is the multiplicative linear congruential RNG, which uses the formula

$$\zeta_i = (A\zeta_{i-1} + B)moduloM$$

Then with a first random number ζ_0, a seed M and constants A and B a particular sequence of random numbers can be generated.

2.4.1 Monte Carlo Method for Radiation Transport

The Monte Carlo method uses random numbers to solve problems numerically. Propagation of radiation through matter is a process in which primary particles with a given energy penetrate a material medium suffering a series of interactions in which energy is transferred to the medium and secondary particles are produced. Although the principles of the interaction of particles with matter are well known, the mathematical description of the successive interactions undergone by an ensemble of particles is a complex problem, generally solving Boltzam transport equation, but it can be easily simulated with the Monte Carlo method. The application of the Monte Carlo method for radiation transport consists of the following steps:

i) A primary particle is generated in an initial state determined by its position, flight direction and kinetic energy.

ii) The particle is moved to a new position along a straight line following the initial direction of flight (This assumption is valid in the absence of electromagnetic fields and when coherent effects are negligible), where the next interaction event is assumed to take place; the travelled distance is sampled from a decaying exponential probability distribution characterized by the mean free path of the particle in the material medium.

iii) The type of interaction is randomly selected according to the point probabilities associated to the cross sections of the considered interaction mechanisms.

iv) The interaction is simulated by changing the dynamical state of the particle and, possibly, generating secondary radiation.

v) The process starts over at step ii) .

vi) and it is repeated until the particle is locally absorbed or when it escapes the material system.

Secondary particles are subsequently simulated in the same manner. The simulation of a primary particle and its descendants is called a ‘shower’ or a ‘history’. As every numerical estimators in Monte Carlo, the solution is affected by statistical uncertainty, that is connected with the number of simulated histories and, consequently with the total calculation time.The simulation stops when a user-defined number of simulated histories or a desired level of statistical uncertainty is reached. The relevant quantities of the problem under study are tallied at the proper steps of the simulation of each particle and their averages are obtained after all histories have been completed. Owing to the stochastic nature of the Monte Carlo simulation the tallied quantities have an inherent statistical uncertainty.

The simulation algorithm described above in steps (i) to (v) is known as detailed simulation. When the mean free path between two consecutive interactions is small compared to the total distance travelled by a particle before it comes to a halt, the number of interactions to be simulated is extremely large and, therefore, detailed simulation becomes very slow. This is the situation found for charged particles, especially at high energies as those found in radiotherapy. For photons the number of interactions undergone is relatively low and detailed simulation is affordable. The problem for charged particles can be overcome by using the so-called condensed transport schemes, in which the effect of multiple interactions is described collectively in a single artificial step [40]. The total energy loss and angular deflection of the particle occurring along a step length is sampled from probability distributions obtained from multiple-scattering theories [47, 48, 75, 73]. In his seminal work Berger classified condensed-history method in two classes [12]. In class I algorithms the length of the step is predefined. This scheme may present problems at the interfaces of two different materials because some steps may not be fully contained within a single material medium, a necessary requirement for the underlying multiple scattering theories may be applicable. These limitations motivate the introduction of refinements in the algorithms such as progressively reducing the step length as the particle approaches an interface. In contradistinction, class II algorithms (Also referred to as mixed simulation schemes) select lengths stochastically. This scheme is based on classifying interactions into soft and hard events. Soft events involve energy losses and angular deflections below certain user defined cut-offs. The remaining interactions are classified as hard and they are simulated with detail, which implies that the distance between two consecutive hard events, the step length, is randomly sampled according to the usual decaying exponential distribution. The accuracy of the transport algorithm may depend on the selected step length, that is, on the selected cut-offs to distinguish hard from soft events. Usually, shorter steps imply better accuracy at the expense of a lower simulation speed.

2.4.2 Application to radiotherapy

In the radiotherapy field the Monte Carlo (MC) methods are applied with several intents like radiation dosimetry, treatment planning, quality assurance (QA) and design of treatment devices[1]. The Monte Carlo (MC) method can provide information that cannot be obtained by direct measurement or analytical calculations.

It is known that the Monte Carlo method applied to the simulation of external beam radiotherapy is capable of computing accurate absorbed dose distributions and that in general, the accuracy obtained from a Monte Carlo simulation in the dosimetry of external radiotherapy

plans of photon or electron beams is better than that yielded by treatment planning systems based on non-stochastic algorithms[15]. That is because non stochastic algorithms use simplifications to allow analytical calculations taking into account beam and dose deposition models based on measurements such as Percentage Depth Dose (PDD) and dose profiles, and introducing analytical refinement considering the non homogeneity of the treatment area in terms of density.

In Monte Carlo (MC) simulation, the history or track of a particle is viewed as a random sequence of free flight that ends with an interaction event where the particle change direction, loose energy and occasionally, produces a secondary particle [16].
To simplify the radiation transport simulation a number of considerations were adopted. At first, the force between the incident particles (electron or photon) is considered to be negligible. These particles are referred to as primary or secondary depending if they enter the medium or if they are produced inside it, respectively. Both the primary and secondary particles are supposed to move in straight lines between interactions. Each material medium is considered homogeneous and isotropic. The atoms are assumed to be randomly distributed with uniform density. To simulate radiation transport the probability of each interaction at the end of each step, dependent of energy and material electronic density is given by the cross section described before.

2.4.3 Monte Carlo codes

Several extensive reviews of the existing Monte Carlo codes were produce along the years, therefore here will be made a condensed resume based on the work of Brualla [17]. In radiation transport, a number of MC general purpose codes exist, but some of them are more adapted to the problems encountered in radiotherapy. The most known are PENELOPE , EGSnrc , MCNP and GEANT. PENELOPE and EGSnrc codes are restricted to electron/positron and photon transport, whereas MCNP and GEANT may simulate many other particles, like neutrons or protons. PENELOPE and EGSnrc are therefore focused on the particles of interest in medical physics and MCNP and GEANT have shown less accuracy and/or more sensitivity to transport parameters than those. Nonetheless, MCNP and GEANT can handle particles like neutrons and protons produced at high nominal energies (18MV or higher) in the treatment head and that may have a significant contribution to dose to the patient.

2.4.4 PENELOPE Code

PENELOPE is the code used by PRIMO for the simulation of LINACs and the estimation of the absorbed dose distribution in phantoms and CT geometries. PENELOPE simulates the coupled transport of electron, photons and positrons in the energy range form 50 eV to 1 GeV and uses a mixed simulation scheme, where a class II algorithm is used for electrons and positrons, while photons are simulated in detail.

The user defined transport parameters that control the behaviour of the mixed algorithm are:

- **C1**→ determines the average angular deflection between consecutive hard events.
- **C2**→ limits the maximum average fractional energy loss between consecutive hard events.
- **WCC**→ is the energy cutoff that separates hard from soft interactions for inelastic collisions with atomic electrons.
- **WCR**→is the energy cutoff for bremsstrahlung emission.
- **DSMAX**→ is the maximum allowed step length for charge particles.
- **EABS**→are absorption energies at which the transport of the corresponding particle (electron, photon or positron) is terminated and the remaining energy is assumed to be locally deposited.

The software package includes a set of geometry subroutines, named PENGEOM, capable of handling objects limited by quadric surfaces. The geometry is coded in a text file according to a series of syntax rules. Surfaces are defined by declaring the parameters of a quadric equation and bodies are defined by declaring their limiting surfaces. Objects can be translated and rotated arbitrarily. PENELOPE requires a main program to steer the simulation and to define sources and tallies. Several main programs are distributed with the code. PENEASY [18] is an independent main program that implements a wide variety of configurable sources, tallies and variance reduction techniques. Apart from taking advantage of the capabilities of the standard PENGEOM subroutines to simulate quadric geometries, PENEASY additionally includes a package named PENVOX which handles the transport in voxelized geometries. In PRIMO a combined system PENELOPE/PENEASY is used.

2.4.5 PRIMO system

PRIMO[19] it is a self contained software that simulates the radiation transport through the whole linac head and a binned water phantom or a CT of a patient using the general-purpose

Monte Carlo code PENELOPE2011. The system supports all the range of Varian Clinac C-series (18,21,23,iX,etc.), 600, Unique Truebeam, and Elekta SLi and MlCi series [20]. The linac geometries are part of the package, and the user is not required to enter any geometrical or physical information of the linac. Being a compiled and closed code, PRIMO does not allow to define new geometries and the user is limited to choose from those provided by the software. PRIMO can produce PHSP at the downstream end of the upper and lower parts of the linac and can import external PHSP provided they are compliant with the IAEA specification [21]. For each simulation users can assign values to the initial beam parameters which are: primary electron beam energy Full width at half maximum (FWHM) of the primary energy distribution, FWHM of the focal spot size, and beam divergence. The code provides suitable default initial parameters for most available linacs and nominal energies. Users can fine-tune these parameters to obtain a better match between the simulated and the experimentally measured depth dose and lateral profiles of reference fields. The code does not provide a beam configuration algorithm. Therefore, the user must perform several simulations varying the primary beam energy parameters until finding the most adequate ones that reproduces the experimental depth dose profiles and then vary the FWHM of the focal spot size until reproducing the lateral dose profiles. To reduce simulation time the code incorporates a number of specifically developed variance-reduction techniques [1], namely, the movable skins technique, splitting roulette, rotational splitting and fan splitting. Other variance-reduction techniques are also available such as interaction forcing in the linac target to maximize the bremsstrahlung production and standard particle splitting in the patient. Additionally, the simulation can be distributed among the cores in a computer. There are two geometry models (patient models) available for dose calculation that can be chosen in segment s3 setup, namely, a homogeneous water phantom and a computerized tomographic volume. The water phantom is the default selection. A slab phantom is another geometric possibility, and is treated by PRIMO as a CT volume. The patient representation is a binned 3D matrix created from the CT scan which is imported from a DICOM file. In the same way, phantoms of slabs and homogeneous phantoms can be created directly in the program. PRIMO includes 40 clinically relevant materials in its database, which are used to convert the Hounsfield Units (HU) into material composition. The volume segmentation is done by assigning up to 10 CT intervals from the 40 referred materials. The CT scanner calibration curve is used to assign mass densities to CT numbers. A default curve that can be edited by the user is also provided by PRIMO. The system allows to import anatomical structures from DICOM-RT STRUCT files or delineate them through the contouring functionality. The analysis tools include the creation of probability distributions from PHSP, the production of

dose-volume histograms, dose profiles and comparison of experimental dose measurements with Monte Carlo estimated dose distributions using the gamma index. All these features are wrapped under a graphical user interface and runs on Windows. PRIMO is a full Monte Carlo and a self-contained system which can be used for dose verification and research purposes. It is freely distributed from the website http://www.primoproject.net.

2.4.6 Dose assessment in the patient

The radiation field resulting from a linac simulation can be used to estimate the absorbed dose distribution in a patient CT or a phantom. Radiation transport in Monte Carlo algorithms relies on the knowledge of interaction cross sections for the material media traversed by particles, so to be able to perform the simulation in a CT geometry it is necessary to infer both the material composition and the mass density from the information provided by the CT scanner in terms of the so-called Hounsfield units HU, defined as

$$HU = 1000 \times \frac{(\mu - \mu_{water})}{\mu_{water}}$$

Where μ and μ_{water} are the average linear attenuation coefficients of the material of interest and of water, respectively, both determined for the radiation quality of the scanner.

A simple method used to inferring the material composition and mass density for each voxel is to select materials for a predefined set according to the linear mapping experimentally obtained between H and density.

Misassignment of material composition resulting from a poor CT-to-material conversion process can have an impact on the dose, with errors in the dose up to 10% for 6 and 15MV photon beams and up to 30% for a 18 MeV electron beam. From the 3D dose distribution matrix, obtained from simulation can be reported the 1D dose profiles, 2D dose maps, isodose lines and dose-volume histograms (DVHs). The dose distributions are generally compared by means of relative differences and with the gamma index. The increasing clinical application of Monte Carlo method has raised the question of whether the dose-to-medium D_m, which is the dose estimated by Monte Carlo codes, or the dose-to-water D_w, the one historically calculated by treatment planning systems, should be specified. Relative differences between D_m and D_w are given by unrestricted mass collision stopping power of water to medium (S/ρ) and are of the order of 1%-2%, hence considered not clinically relevant for tissues with media composition similar to water, with the exception of bone, where differences can be as high as 15%. Statistical uncertainties are inherent to dose distributions estimated with the Monte Carlo method and consequently isodose lines exhibit a jagged appearance that may confound visual evalu-

ation of the dose distribution. Integral dose quantities such as DVHs are less affected by the uncertainty, however steep DVHs, such as those of PTVs, are significantly smoothed when calculated from distributions with a large uncertainty. This effect is less pronounced in DVHs of critical structures due to their shallower slopes. When analysing dose limits to critical organs, for instance, the level of acceptable uncertainty is relative to the biological effect produced by the dose on a particular organ. The biological effect on serial organs, such as the spinal cord, is exclusively dependent on maximum dose values, therefore demanding a low statistical uncertainty for their estimation. In contradistinction, biological effects on parallel organs, such as the lungs depend on mean doses. It has been suggested that a relative statistical uncertainty of 2% of the maximum dose (D_{max}) is acceptable in evaluating a Monte Carlo base treatment plan. However, the uncertainty of a single voxel is a poor measure for the uncertainty of a treatment plan and have been proposed the mean uncertainty of a volume determined by all voxels accumulating a dose greater than $D_{max}/2$ as a convenient indicator of the overall uncertainty of a dose distribution. Where for estimating the mean statistical uncertainty σV of a region V the summation in quadrature of the relative uncertainties of all voxels in V is done,

$$\bar{\sigma}_V = \sqrt{\frac{1}{k}\sum_{k=1}^{K}\sigma^2}$$

where K is the number of voxels in V and σ_k is the relative statistical uncertainty of the dose in voxel k.

2.5 Simulation of Linear Accelerators

The description of the radiation beam leaving a medical linear accelerator can be obtained by two approaches:

1. Based on the so called virtual source model, which approximate the particle fluence downstream the head assembly by considering the major linac components as separate particle sources. The virtual source models are classified into three groups: (i) those that solely use pre-calculated data from Monte Carlo simulations, (ii) hybrid models in which the planar fluences and energy distribution derived from Monte Carlo simulations are adapted to match measured dose profilesand (iii) those based on measurements.

2. Performing a full Monte Carlo simulation of radiation transport through a detailed model of the linac head. In principle, virtual source models are less accurate than Monte Carlo approach.

In the Monte Carlo approach the simulation of a linac starts by modelling the primary source of particles as a narrow beam of electrons exiting the acceleration structures and entering the head assembly. Knowledge of the characteristics of the initial particle states (i.e., energy distribution, spatial distribution and angular divergence) is necessary for accurately reproducing the actual treatment beam. The simplest model assumes that a monoenergetic and collimated electron point source is located at the top surface of the target and directed downstream along the treatment head central axis. A more elaborate model assumes that the energy particles of an electron beam have Gaussian distributed energy, with defined mean and FWHM. In addition, the model assumes that the particles are directed with an angular divergence distribution. A suitable configuration of the primary electron source can be found in an iterative trial-and-error procedure in which dose profiles estimated in simulations are compared to measurements water phantom. Primary beam information provided by manufacturers might be used as a starting guess in this iterative procedure and some Monte Carlo treatment planning systems incorporate algorithms to try to avoid the application of this trial-and-error procedure.

To compute the dose distribution in the patient, particles must be transported through the upper structures of the linac, the patient dependent beam modifiers and, finally, through the computerized tomography (CT) or phantom. However, this may be an inefficient method. In principle, a more efficient approach is to simulate the upper part of the linac, from the primary beam downstream to a plane situated just upstream the jaws, and to save the state of particles reaching that plane in a file. This simulation has to be performed only once per beam. The file tallied at the aforementioned plane, which is known as the phase-space file PHSP, is used as a source of particles for subsequent simulations. It is not infrequent that a second PHSP is tallied at treatment head exit and used for dose estimation in the patient.

In general, the simulation of a linac can be divided into three parts:

i) the simulation of the linac components located upstream the movable collimator (upper part);

ii) the simulation of the linac components located upstream the movable collimator (upper part) and the simulation of the movable collimators themselves and all other linac components downstream them (lower part);

iii) computation of the distributed dose through the computerized tomography (CT) representing the patient.

A full Monte Carlo system simulates all the three parts while the virtual source models only simulate the radiation transport through the CT, item iii).

2.5.1 Phase Space Files

A phase space file (PHSP) contains all the information relative to the particles passing through a specific plane. It is a database that stores the state of the particles in terms of type of particle (electron, photon, positron, etc.), energy, position in Cartesian coordinates (x, y, z) and direction cosines (u, v, w) are always stored[21]. As each user can define its own PHSP structure the IAEA proposed a unifying standard structure as in Table 2.1. As for this standard, the minimum space occupied in the binary file by the information relative to one particle is 25 bytes. Optionally, some other information may be stored as is the case of the incremental shower number that permits to create a relation between a particle and its history for further statistical uncertainty calculation. This number indicates how many histories (showers) were simulated between each tallied particle and the previous one in the sequence of particles in the PHSP. For example, if two consecutive particles in the PHSP belong to same history, the second particle will have its incremental shower number equal to zero. This approach allows separating information about primary and secondary particles.The summation of all incremental shower numbers in a PHSP yields the number of simulated histories. Another approach to relate each particle with its history number is to tag each particle in the PHSP with a flag that indicates when a change of history has occurred, and to provide with the PHSP the number of simulated histories that was used for its computation. This approach yields the same accuracy than the incremental shower number in the estimation of the statistical uncertainty of quantities tallied using the PHSP as radiation source, provided the whole PHSP is used. If only a fraction of the PHSP is used an approximation to the statistical uncertainty can be obtained by assuming that all histories have contributed with the same number of particles to the PHSP. The finite size of a PHSP imposes a lower bound to the statistical uncertainty of observables tallied with it, and the minimum statistical uncertainty that can be asymptotically reached using a given PHSP is called the latent variance. Reusing particles in a PHSP is a way to approximate the uncertainty of the estimated quantities to the latent variance of the PHSP, however, when recycling a PHSP, it is critical to maintain the correlation between particles pertaining to the same history, otherwise uncertainties will be erroneously underestimated. A convenient way to reuse τ times a PHSP without loosing the correlation of the particles of one history is to split τ times the particle entering the simulation and to treat the original particle and the clones as pertaining to the same history, as seen before in the particle splitting Variance Reduction Technique (VRT). As each code has its own proprietary phase space file (PHSP) format, for the purpose of consistency an effort to standardize it was made by the International Atomic Energy Agency (IAEA) that has defined as PHSP format used in their PHSP database [21]. The IAEA

specification consists of two files, a header file that contains general information (such as the number of histories that were simulated to produce the PHSP, the number of particles stored and the byte order) about the way the related binary file stores the data for every particle tallied. The IAEA has made available a library of subroutines written in the C/C++ language to handle its PHSP format by the main Monte Carlo codes.

Variable	Meaning	Type of variable returned
x	Position in X direction in cm	Real*4
y	Position in Y direction in cm	Real*4
z	Position in Z direction in cm	Real*4
U	Direction cosine along X	Real*4
V	Direction cosine along Y	Real*4
E	Kinetic energy in MeV	Real*4
Statistical_Weight	Particle statistical weight	Real*4
Particle_Type	Type of the particle	Integer*2
Sign_of_W	Sign of W (direction cosine in Z)	Logical*1
Is_new_history	Signifies if particle belongs to new history	Logical*1
Integer_extra	Extra storage space for variables(e.g., EGS LATCH, incremental history number,PENELOPE ILB, etc.)	n*(Integer*4) (n≥0)
Float_extra	Extra storage space for variables(e.g., EGS ZLAST)	m*(Real*4) (m≥0)

Table 2.1: Information to be returned from a PHSP

As a general rule IAEA recommends to use about 10000 primary particles per unit area of interest to obtain an approximate 1% statistical uncertainty and that the minimum number of particles per unit area for radiation therapy fields should be around 2500 particles/mm^2 at the isocentre plane. The actual number of particles to use requires additional investigation with respect to the latent variance (the minimum statistical uncertainty that can be asymptotically reached using a given finite size PHSP).

2.5.2 Variance Reduction

The efficiency η of computational calculations is defined by the following equation:

$$\eta = \frac{1}{\sigma^2 T}$$

where T is the calculation time and σ^2 is the variance. In Monte Carlo calculations, the variance is proportional to the inverse of the number of histories N and can be written as

$$\sigma^2 = \frac{\sum_{i=1}^{N}(X_i - \bar{X})^2}{N}$$

So there are two possibilities in order to increase the efficiency, reduce T or σ. For most of the Monte Carlo algorithms T is constant and can be reduced only by changing the algorithm implementation, so the alternative is to reduce the variance which is achieved through the use of the so called Variance Reduction Technique (VRT). This techniques are time consuming and can affect the accuracy of the evaluated tally therefore its use must be balanced.

In many cases there is no interest in following a particle that go outside a user-defined volume of interest and stopping the tracking when it exit from such a volume reduce te computational time. When VRT are used, a statistical weight is associated to each particle. As an example, when using interaction forcing *n*, so that a particle interaction with production of secondaries (as is the case of photon production by electron-target interaction) the statistical weight of each of the secondaries is $1/n$. This means that every secondary photon produced by the same primary counts conts for $1/n$. In some cases, it is preferable to discard from tracking the particles that get statistical weight under a predefined threshold. As a further example, this criterion is active when executing the Russian Roulette technique, where the idea is to eliminate the particles with specific probability and depending on their positions, direction or weight. When this particles are removed the weight of the remaining are increased in order to maintain fixed the statistical weight of a history.

Other methods to reduce variance is to force a particle to go through the volumes of interest. One way to achieve this is to copy a number of particles with suitable position and direction and using them in simulation, this is called particle splitting technique. In this technique, the copied particles, although with the same starting position and energy of the original will propagate through a new random path. The statistical weight is divided between the original and copied particles to keep the statistical balance of the simulation.

In the interaction forcing VRT technique , the particles are forced to interact with specific probability when they pass through the volume of interest, which is an efficient technique to increase the bremsstrahlung radiation resulting from the electron interaction with the target.

some techniques of VRT rely on the true physics instead of random sampling, as is the case of the exponential transform techniques in which the path lengths are adopted according to the rule of exponential attenuation of particles instead of its random sampling.

For any simulation there is a level of particle energy under which the interactions of particles has no important contribution for the evaluated tally and in addition, the number of interactions to compute is still high. Therefore a cutt-off energy value is defined to reduce time and particles are not tracked anymore when reaching energy below such value. In order to keep energy conservation, the remaining energy is assumed to be deposited in the last step of the particle

or, in other cases the continuous slowing down can be assumed. This VRT introduces a bias in the final estimation of tallied energy deposition in a point.

2.5.3 Evaluation of results of a numerical MC calculation with respect to experimental measurements

Gamma Function

To evaluate if a plan is adequate it is necessary to compare quantitatively way the calculated dose with a reference. The background to this approach is that MC makes use of models to simulate interactions, geometries, particles and physical properties. A model can be close to reality and give good results or far from being real and give not acceptable results. The basic idea behind the Gamma Function approach is that a reference is considered as the truth, while the MC model is an attempt to reproduce the reality. In Radiotherapy, if the evaluation is done during the plan elaboration, the reference dose will be the prescribed, i.e., it will be the dose indicated by the radio-oncologist. In other cases, e.g. validation of Monte Carlo (MC), the reference dose is obtained from the experimental measurements and the calculated dose results from the MC simulation. In either case, the objective is to compare the calculated and reference dose distributions.

For this evaluation is usually used the so-called the Gamma index and has been used to evaluate the algorithms for dose calculation against the dosimetric measurements since its introduction[22]. The gamma criterion is based on the definition of an acceptance region that is represented by an ellipsoid defined by

$$\Gamma(\vec{r_c}, D_c) = \sqrt{\frac{\Delta r^2}{\Delta d_M^2} + \frac{\Delta D^2}{\Delta D_M^2}} = 1$$

where $\Delta r = |\vec{r_r} - \vec{r_c}|$ is the distance between the calculated and the reference points and $\Delta D = D(\vec{r_c}) - D(\vec{r_r})$ is the doses difference. In order to the evaluated distribution coincides with the reference its necessary that at least one point verifies $\Gamma(\vec{r_c}, D_c) \leq 1$. considering the quality factor, as the minimum value, i.e.,

$$\gamma(\vec{r_r}) = min\{\Gamma(\vec{r_r}, D_c)\}\forall\{\vec{r_c}\}$$

the acceptance-rejection criteria becomes:

- $\gamma(\vec{r_r}) \leq 1$, the dose compares adequately with the reference
- $\gamma(\vec{r_r}) > 1$, the evaluated dose is not equivalent to the reference.

The Distance To Agreement (DTA) is the distance between the point that is being evaluated and the closest point of the reference dose distribution and this concept was introduced because dose difference in the high dose regions can be large but of little importance compared with other uncertainties. The dose difference and the DTA are complementary parameters and so an evaluation can be considered adequate not only if it has a low dose difference but also if it has a relative high dose difference but at the same time a DTA that is inferior to the treatment precision or to the security margins defined. The Gamma criterion combines in a single indicator the dose difference and the DTA where the acceptance criterion is the difference (or distance) in the multidimensional space of dose and physical distance between the points. The gamma analysis index (γ) is sensible to the statistical noise [23], which means that special care must be taken in computation with the use of small voxel sizes with high statistical uncertainties. This can lead to improperly accept a plan that would fail the test in a no-noise condition or vice-versa.

2.6 Monte Carlo simulation of IMRT and VMAT

IMRT and VMAT techniques involves dramatically different approaches in treatment planning and dose delivery. Thus, conventional dose calculation methods based on scatter summation and water-phantom measurements are becoming inadequate for obtaining accurate dose distributions for this dynamic modalities. On the other hand, with the fast growing computer technology, methods based on the first principles of radiation transport, such as Monte Carlo simulation, are evolving into the standard of practice for the need of more sophisticated dosimetry tools. Several research efforts have been focused particularly on Monte Carlo simulation for the IMRT in order to answer a full range of questions from three-dimensional treatment planning to clinical dosimetry [24] [25][26]and more recently a complete QA system worflow for VMAT [27] and a PRIMO IMRT implementation study [28].

2.6.1 The dynamic motion of the MLC - SCS and PPS approaches

An additional challenge to radiation dosimetry posed by IMRT and VMAT techniques, including for Monte Carlo simulation, is the time dependent factor that may have to be incorporated in dose calculation and measurement for these dynamic beam delivery systems. To approach this issue there are two approaches to this problem with Monte Carlo in order to simulate the motion of the collimators, for intensity modulated (IM) or dynamic fields. A more rudimentary method referred to as the Static Component Simulation (SCS), is based on the simulation of each sub-beam segment of a sequence of static configurations individually, as in the case of

step-and-shoot IMRT, and integrating the results from all component fields in the end. For IM fields with a large number of segments that could exceed 100, this method may become cumbersome in order to track results from all the segments. Alternatively, a Position Probability Sampling (PPS) approach can be used to represent the motion of the dynamic components by randomizing its position during a simulation[5]. This technique was first proposed in a work for modelling dynamic wedges delivered by sweeping the collimator jaws [2]. Compared to the SCS method, the PPS method is more automated and efficient from an operational point of view and the principle of the PPS method can be extended to simulate other dynamic motions, and in particular, sliding windows intensity-modulated beams using multileaf collimators, with the advantage that a PPS method simulation can be accomplished in one single run, improving the operational efficiency, and the degree of fidelity of the simulations in the condition of continuous dynamic collimator motion.

3. Implementation

After the previous work [28] done in the simulation of IMRT with PRIMO software, realized at IPO, the current work aimed at extending the results to the VMAT treatment modality and to design a workflow that allowed to introduce the simulation in the clinical practice. This would involve the development of an application that would help to configure, with the aid of a graphical user interface, the PRIMO system with the wanted modulation to simulate.
As of the starting of this work a new Varian TrueBeam Linac, with the Flatness Filter Free (FFF) operation mode had been installed and commissioned at IPO and no MC model existed, all the work was conducted in order to that this linac would be the main equipment and so all the MC modelling and the respective validation tests to be performed become another inevitable objective of this work.

3.1 Materials

3.1.1 Varian TrueBeam Linac

TrueBeam is a clinical linear accelerator, manufactured by Varian. The system dynamically synchronizes imaging, patient positioning, motion management, and treatment delivery. It is a versatile platform which can be used for all forms of advanced radiotherapy modalities including Image Image Guided Radiotherapy (IGRT) and Image Guided Radiosurgery (IGRS), Intensity Modulated Radiation Therapy (IMRT), Volumetric Intensity Modulated Arc Therapy (Rapid Arc) and Stereotactic Body Radiotherapy (SBRT) along with conventional and 3-D conformal radiotherapy. Adding to this has the possibility of operate in Flatness Filter Free (FFF), or ”High Intensity Mode” as Varian refers to it, at the 6MV and 10MV energies.
This linac is equipped with a 120 HD MLC system.

3.1.2 PRIMO

As described in 2.4.5 PRIMO is a software that simulates clinical linear accelerators (linacs) and estimates absorbed dose distributions in water phantoms and computed tomography (CT).

It combines a graphical user interface and a computation engine based on the MC code PENELOPE, generating all the necessary input files need by this one for simulating a variety of linacs. The version 0.1.5.1307 of PRIMO was used through this work.

3.1.3 treatment planning system (TPS)

The treatment plans used in the various simulations were done using the Eclipse TPS system.

3.1.4 The Control Point

The representation of a dynamic treatment by a calculator poses the problem of representing a continuous motion using discrete states. The most intuitive and straightforward approach is to use a number of discrete configurations to represent the system trajectory. These points are known as the Control Points (CP), assumed as snapshots of the system at discrete time conditions. The sequence of the control points represents the system trajectory. In Radiotherapy a control point consists on information on gantry angle, jaws position and one value per each leaves of the MLC as function of time. In the case of radiotherapy systems, the time axis flowing is replaced by another quantity that is the MU_{index}. The MU_{index} is the cumulative monitor unit value normalized to the total of MUs at specific control points. Consequently, MU_{index} is a value that runs between 0.0 at begin of the treatment and 1.0 at the end and it is directly related to the time only in the case of fixed dose rate. A CP can be viewed as the source of trajectory information or as the source of configuration itself. The MC based TPS calculate the dose at the planned control points, but alternative algorithms can be developed, in order to redefine the steps between the MU_{index} of consecutive CPs or to randomize the sampling method of CPs as by the PPS approach.

3.1.5 DICOM plan file

The TPS communicate with the LINAC and the Record and Verify systems through DICOM files. The plan informations are stored in a DICOM file usually name as RP.*xxx*.dcm. Once open with specific software, it is shaped as a structure with registered information allocated in specific cells. This structure contains the geometric and dosimetric data specifying a course of external beam, e.g., the number of beams, beam angles, collimator openings, beam modifiers and the control points sequence.

3.1.6 mlc modulation file

The TPS calculates the MLC motion and offers the possibility to the user to export a file, which contains information on the motion of every single leaf during the delivery. This file simpler than the RP DICOM file as it does not contain any information on other components as the jaws or the gantry. This file can be used as a modulation information source when the gantry is fixed as in the case of IMRT procedures. It is structured in a sequence of positions, one per leaf at specific moments during the treatment.

3.1.7 Trajectory log file

During treatment, the TrueBeam system records actual axis positions and MU delivered. After the treatment is completed, this information is stored to a trajectory log file so that the information can be retrieved and evaluated. The output file is binary with snapshots of the system with a sampling interval of 20ms.

3.1.8 Workstation

All the simulations were performed with a worksation present at the IPO research lab with a Intel(R) Xeon(R) CPU E5-2660 v3 @ 2.60GHz with 16GB of RAM and with 32 CPU cores available.

3.1.9 Measurement materials

For the measurements, two types of phantom were used. For the static and IMRT type fields, a multislab RW3 box was constructed. For the case of VMAT the OCTAVIUS4D®phantom was used. In either case Gafchromic films were inserted between two slabs at a specific depth in the phantoms to allow comparison between simulations and experimental dose distributions. The Dose distribution images were obtained by scanning the Gafchromic film with an Expression 10000XL scanner (Seiko Epson Corp., Nagano, Japan). The conversion from Optical Density (OD) to absorbed dose was done with DOSELAB®from PTW, using 24h pre-calibrated curves.

3.1.10 Matlab®

All the modules of the in house developed application were coded with Matlab R2016a from Mathworks®. MATLAB®(matrix laboratory) is a multi-paradigm numerical computing environment and fourth-generation programming language. A proprietary programming language developed by MathWorks®, it allows matrix manipulations, plotting of functions and data, im-

plementation of algorithms, creation of user interfaces, GPU and parallel processing as well as interfacing with programs written in other languages.

3.2 Method

3.2.1 Verification and Validation

Beam

The first step in order to proceed with the work is to get a validated model of the beams produced by the linac. For that, the first approach was to use the linac model FAKEBEAM included in PRIMO as the good results showed in (Belosi)[29]. The first iteration values used for the requested parameters such as the number of histories, energy and space Full width at half maximum (FWHM) and beam divergence, were the same as those of the [29](Belosi et al.) study. After this the process consisted in a successive parameters refinement in a cyclical model tuning.

A different workflow is offered by the IAEA, which provides some PHSP free to download for the MC community through the open IAEA database. PRIMO allows to import such IAEA PHSP s1 stage in standard format as discussed in 2.5.1. The import of the IAEA PHSP files requested to adapt the files into a specific format. As mentioned before, the PRIMO is based on PENELOPE and is able to track only electrons, positrons and photons. The IAEA PHSP may be produced by another code (e.g., in this case with GEANT4), which are able to deal with other types of particle. Ann in-house code was developed to delete the undesirable particles form the PHSP in order to use it in PRIMO. The fraction of deleted particles was negligible. Unfortunately, although PRIMO successfully imported the files it always gave an error when trying to simulate the s2 stage. Following this approach the set of PHSP files provided by Varian were download from Varian site. There were about 50 files available for each of the energies, 6FFF, 10FFF and 15X with sizes of around 1GB each. These PHSP were collected above the movable jaws. The Table 3.1 gives a summary of the contents of the stored Phase Space, as extracted from the respective accompanying header files.

Later, a new project was created for each energy and choosing the model Varian 2100 in PRIMO as recommended in the PRIMO manual. Only a number of 5 PHSP files were used in all the three cases. The statistics using this number of files is well higher than the the minimum number of histories recommended by the IAEA, and above the 2×10^9 number of histories benchmark of other studies [29].

A first consistency check was done with this resulting phase space, running a simulation

through the stages s2 and s3 with the largest field possible ($40 \times 40cm^2$) in a water phantom. Comparison with the reference measured dataset available from the linac commissioning were performed. After this starting point, the beam model was commissioned with respect to a larger dataset. The whole dataset included several collimation conditions defining the beam size: 2x2, 3x3,4x4, 6x6, 8x8, 10x10, 15x15, 20x20, 30x30 and 40x40 cm^2. Different energies were considered: 6, 10 and 15 MeV. The comparison was based on the PDD and dose profiles at different depths in water tank under reference conditions.
After this process the phase spaces were considered a valid model of the installed TrueBeam unit and used thereafter in all the simulations during this work.

Table 3.1: Summary of the characteristics of the initial electron sources, as described in the header files of Varian phase space file (PHSP)

	6FFF	**10FFF**	**15X**
Stored position Z	26,7 cm	26,7 cm	26,7 cm
Number of original histories	$6,5 \times 10^7$	$3,24 \times 10^8$	6×10^8
Mean energy	5,9 MeV	10,2 MeV	13,5 MeV
Energy sigma	0,051 MeV	0,2 MeV	0,27 MeV
Energy FWHM	0,12 MeV	0,2 MeV	0,27 MeV
sigma X	0,6645 mm	0,8118 mm	0,6415 mm
sigma Y	0,7274 mm	0,8001 mm	0,5768 mm
Beam divergence	1 mrad	1mrad	1 mrad

The Collimator

As the collimator was extensively used during the work in order to simulate their modulation effect on the radiation beam, a test was made in order to give an answer to whether the MLC model furnished by PRIMO is acceptable and a user can be confident on it. For the validation of the modelled multileaf collimator (MLC) an irregular shape conformed by the MLC was simulated, Figure 3.1. The same leaves configuration was irradiated in a phantom constituted by a set of slabs of RW3, constituting a box of 15 cm of height. The measure was taken making use of a Gaphcromic film placed at 5cm depth from the surface of the top slab, 100cm SAD set-up. This procedure was repeated for the 6FFF and 10FFF energies.

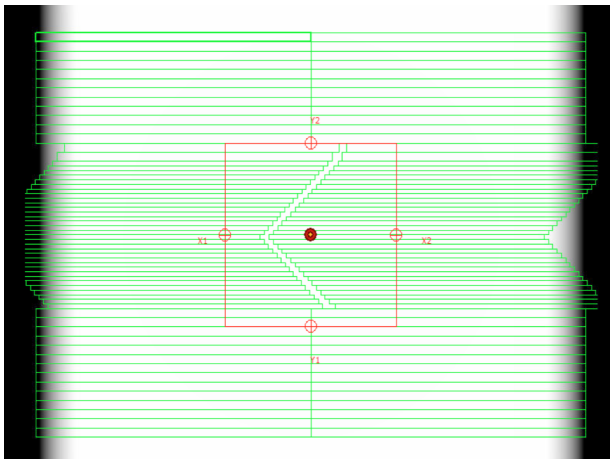

Fig. 3.1. Leaves configuration used in MLC validation.

3.2.2 Simulation of dynamics procedures

With the machine model validation complete the following step was to validate the sampling algorithm. As PRIMO does not have intrinsically the functionality of IMR or VMAT simulation, a suitable algorithm had to be developed in order to drive the software to simulate a dynamic procedure. In this context an in house graphical application was developed to assist the standardized configuration of PRIMO.This application is referred as APP. Several modules had to be included in the application, each one dealing with a specific purpose, Figure 3.2. Firstly, the module to allow PRIMO to interface with the TPS was developed to allow importing dynamic information, relative to component motion during the procedure. This step was conducted making use of either the DICOM plan file or the *mlc* modulation files, both downloadable by the TPS. Since both the DICOM and the *mlc* files are structured in a sequence of discrete control points which contains the data sampled from the treatment delivery planned, the data relative to each control point (e.g., the beam modifiers positions and the correspondent MUs delivered) are extracted from the TPS files and processed, followed by the generation of the fields to use in the simulation through random sampling and subsequent interpolation. This fields are then written to a PRIMO configuration file for posterior simulation execution.

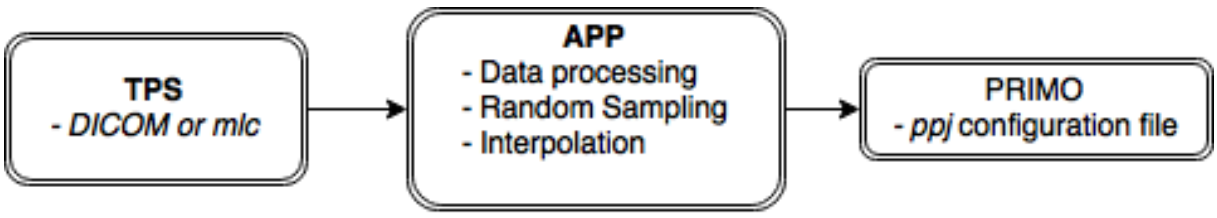

Fig. 3.2. Block diagram of the workflow.

Sampling algorithm

From what discussed in 2.6, in this work, a stochastic method was developed to model the dynamic motion of the beam modifiers with the Monte Carlo simulation of the IM fields. The simulation of the elements motion was accomplished by the Probability-Position-Sampling (PPS) method, in which MU$_index$ array of the CPs to simulate was randomized. As a consequence, the number of particles being simulated for each sampled segment was considered proportional to the MUs or dose delivered for that segment or position. In order to deal with the time dependence on the four-dimensional dose calculation a transformation of the factor of time into the MUs or dose being delivered was done, because of their direct correlation. Consequently, the length of time can be more naturally folded into MC simulation by batching the number of histories or dose according to the MUs. From the number of segments for the IM fields, beam modifiers position in the segment and the MU index of each segment the sampling algorithm generates random IM fields that try to resemble the movement. From the input data, DICOM or mlc files, the dynamic trajectory of all the components are calculated. The PRIMO, as all the software, works by finite states configurations and the motion is modelled by considering a number of static configurations. The position of all the components are interpolated from the trajectory at specific time fraction as defined by the randomly generated MU. The MU index is the incremental or cumulative MUs that will be delivered up to the completion of the current segment and its delivery will depend on the operation mode, i.e., step-and-shoot or sweeping-leaf. In the context of present work only the last was considered however the algorithm works similarly in the former case. The MU index of the IM field can be seen as the Cumulative Probability Distribution Function (CPDF) of each segment or beam modifier position. Therefore the positions can be randomized from the MUs that in turn have a direct relation with dose delivered by segment [2]. Somehow, the positions are sampled from the predetermined trajectories specified in the mlc or DICOM file, depending of the origin, with the probability position governed by the CPDF. The sampling algorithm works as following:

1. A set of *n-1*random numbers, where n is the number of final IM sub-fields desired are generated.

2. 0.0 at the begin and 1.0 at the end are added to the random number sequence. This *n+1* random numbers represent the extremes of the *n* wanted IM random fields in terms of MU$_index$.

3. The system configuration is interpolated at the value of MU$_index$ correspondent to the center of the interval.

4. A weight proportional to the MU fraction of the correspondent interval is attributed to each of the sampled IM field. Finally, the sum of the intervals will be 1 and the final dose can be computed as the weighted sum of the doses of the IM sub-fields simulated.

As a side note, some brief tests were conducted to assess the error introduced by interpolating at the center of the interval, or at the mos probable position inside the interval, especially in the case of the existence of a great modulation inside the interval. The observed differences for the case of a large number of fields,i.e, small interval widths, were negligible and don't justify the cost time consuming operation to iterate the most probable position inside the interval by randomization.

Dynamic MLC with Gantry fixed

A standard dynamic MLC procedure, known as the "Gap" was planned using the TPS and transferred to the LINAC for irradiation. The mlc file of this plan was extracted from the TPS for elaboration and simulation of this configuration. This mlc file, with 13 control points was imported into the APP and a sampling of 180 randomly interpolated fields was generated. The resulted sampling was exported to the corresponding ".ppj" project file created for this simulation. The simulation was taken in a 2 steps way, first, the validated phase space at s1 was used as the radiation source for the s2 stage. The simulation of the s2 was carried out followed by the s3 stage of dose deposition calculation in a multislab RW3 solid water phantom, with the surface placed at 95 cm from the LINAC source position. The same procedure was delivered at the LINAC stage and the measurement performed with a gafchromic film at a depth of 5 cm from the surface of the top slab.

Dynamic MLC and Gantry

As in the last case, a 6FFF pre-planned test VMAT, with 16 control points was imported from a DICOM format into the APP, sampled and exported to PRIMO for simulation. Again the simulation was executed following the steps described but in this case the phantom used was an OCTAVIUS4D ®. A CT scan of the phantom was imported in PRIMO and treated as a homogeneous RW3 material. The same plan in the same set-up was irradiated with a film at the referred position. As the available CT of the phantom did not have the slabs used for sandwich the film, in the middle of the phantom, this was processed with Matlab, where the HU values in that region were replaced by the HU value corresponding to RW3.

TB machine movement log simulation

In order to simulate the real movement of the beam modifiers first of all a module that could read the binary file was coded, implementing the header specifications supplied by Varian, where the TrueBeam (TB) stores the information. Later, the usual steps of sampling the maximum 180 randomly interpolated fields, PRIMO export and PRIMO simulation and doses integration operations were carried on.

Clinical case study

Without a priori constraints, an available VMAT treatment plan made for TrueBeam with energy 6 MeV FFF was chosen to test the whole workflow as enumerated below and with a graphical view in Appendix A.1. The original treatment consisted of 2 dynamic arcs. Arc 1 with CC gantry rotation and arc 2 with CW rotation. Each arc was originally defined with 98 control points.

1. Export the selected plan from the TPS in DICOM format.
2. Import the DICOM file in the VMAT_APP.
3. Select arc 1 and choose the number of random fields wanted to sample the dynamic treatment. The choice was the 180 maximum number of fields allowed by PRIMO in order to not under-sample the dynamic trajectory of the system.
4. Export the sampled fields to the PRIMO configuration file. This process generates a joint file with the relative weight of each sampled field to use in later dose integration.
5. Repeat steps 3 and 4 for the remaining arcs. In this case Arc number 2.
6. Open PRIMO with the first configuration file.
7. Import CT and set the isocenter.
8. Simulate s2 and Simulate s3.
9. Close PRIMO and move the output calculated dose files to a backup folder.
10. Replace configuration file with the one of the Arc 2.
11. Reopen PRIMO and repeat step 8.
12. With VMAT_APP integrate calculated dose files for Arc 1 using the corresponding weight file.

13. Repeat the integration for the calculated dose files of Arc 2.

14. Integrate the 2 output files from 12 and 13, using weights equal to 1 for each, in teh case that the total monitor units are equally divided between the two arcs.

15. Generate DICOM for all slices or only for the depth of interest from the integrated dose file.

16. Compare this output with the dose calculated by the TPS. This was done using Verisoft and the RD DICOM file exported from the TPS.

MC calculated doses evaluation

With exception of the Clinal case(s), all the other simulations were compared with the real measurements performed with the TB. Each Gafchromic film irradiated was scanned and processed with DoseLab®from PTW where the corresponding calibration curve was applied in order to obtain the dose distributions. On the other hand from the PRIMO simulations the accessible result was not a unique distribution but several with the dose deposited by each of the 180 fields simulated. To overcome this a module was coded that imported this files, applied the respective weight and produced a unique dose file. From the resulting integrating dose distribution a slice corresponding to the desired depth was extracted the and exported to DICOM.
The exported DICOM and a DICOM generated from the tif Gafchromic digitalized dose distribution from DoseLab, were imported into the Verisoft PTW software for a gamma 2D evaluation. All the dose distributions originated from the simulation, film measurement and TPS calculation were compared with each other in Verisoft.

4. Results and Discussion

The results from the several steps taken in the implementation phase as described along the chapter 3, are exposed in this chapter. Firstly, the results for the simulation of the TrueBeam linac model for the desired energies, i.e. 6MV and 10MV operating in Flatness Filter Free (FFF), and the respective validation through the gamma comparisons with the respective measurements of reference from the linac commissioning work are shown. Later, a subsection is dedicated to the results of the simulation used to validate the multileaf collimator (MLC) HD120 mounted in the TrueBeam linac is equipment.
In addition, the results of the dynamic simulations, of algorithm sampling validation to the the workflow application to dynamic treatments, including a TrueBeam "TrajectoryMachineLog" and a real clinical case are shown. Finally the GUI Matlab application built is described and explained.

4.1 Validation

4.1.1 Beam

Phase Spaces

The use of PRIMO for the beam simulations showed to be able, on one hand to generate models of the Varian Trubeam Linac machine and to the other, to validate the PHSP files available from Varian repository. Both ways are viable options to get a functional model of the LINAC, although the latter option should be preferred as it is less time consuming, since the first option involved to generate a PHSP with PRIMO using the FakeBeam model, which results in longer simulation times and very large files which will induce longer times in the subsequent s2 stage simulations.

Results of the analysis within PRIMO of the Phase Space used for the 6MV FFF that resulted from the Varian PHSP import are shown in Figure 4.1 and 4.2. Energy spectra and angular distribution of particles crossing the PHSP are shown for each kind of particles PRIMO is able to deal with, photons, electrons and positrons.

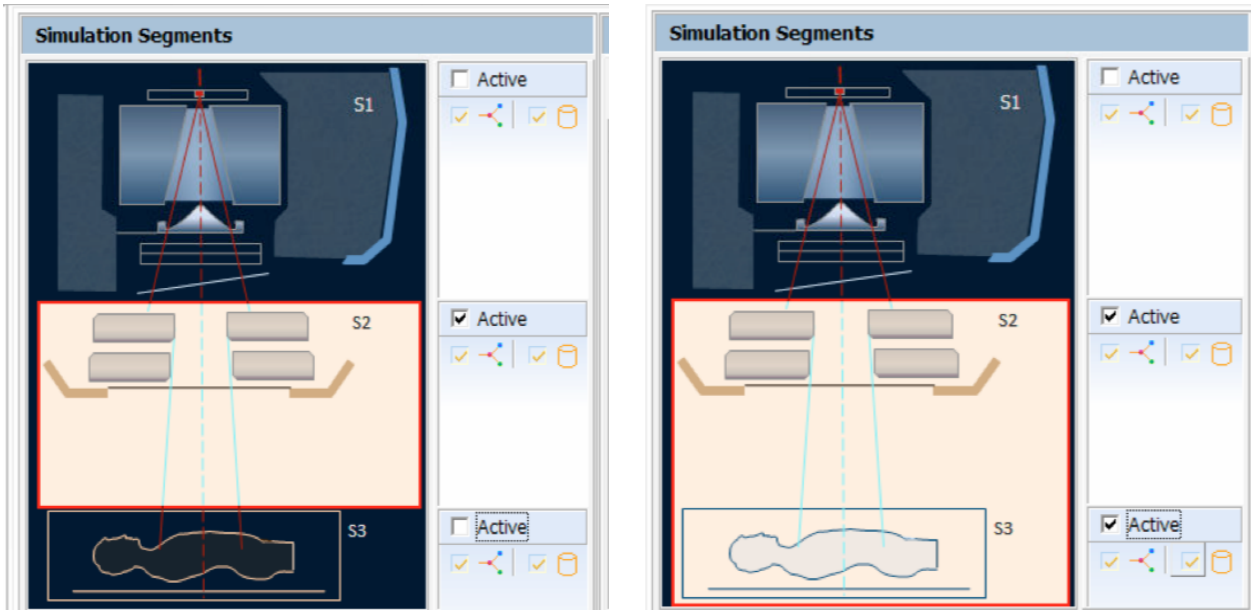

Fig. 4.1. Varian Phase Space as a valid model of the linac head and as the source of particle for the subsequent s2 stage of the simulation through jaws and MLC.

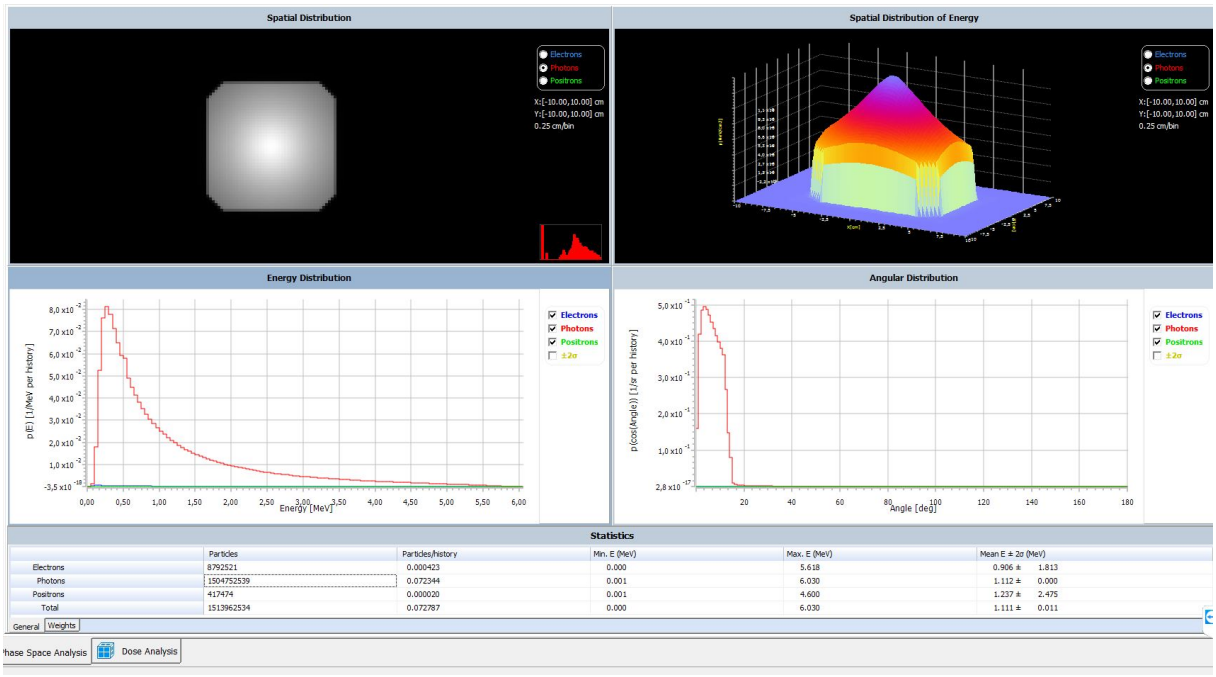

Fig. 4.2. PRIMO analysis of the Phase Space used as source for the 6MV Flatness Filter Free (FFF) beam.

The calculated PDDs and Lateral Profiles

The normalized curves obtained from the simulation of the different field sizes, different depths and energies, used for the comparison with the reference values that resulted from the commissioning of the TrueBeam are shown. Square fields are considered, from 2x2 cm^2 to 40x40 cm^2 and the curves plotted for the lateral profiles were extracted from PRIMO, at each desired depth, with the tool for dose inspection, accessible after the s3 stage calculation.

The 6MV-FFF The Percentage Depth Dose profiles

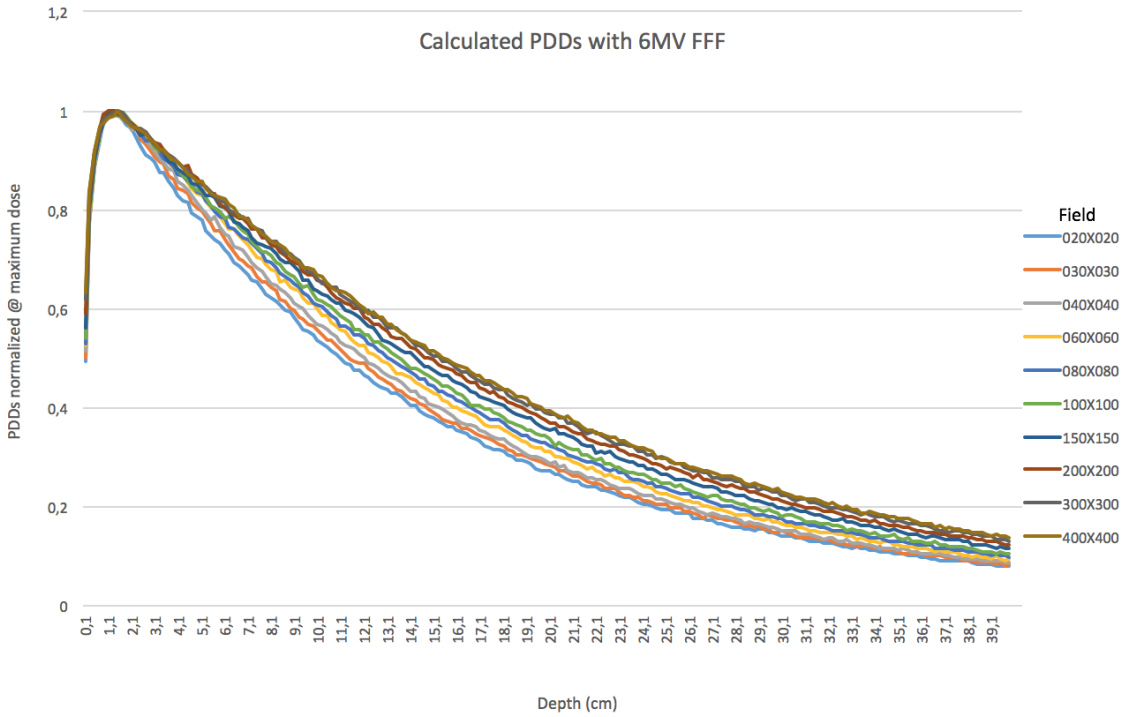

Fig. 4.3. 6MV FFF - normalized PDDs to each PDD maximum dose depth

In Figure 4.3 the PDD are shown, each one normalized to its specific maximum. As a general note, for this energy a build up region of approximately 14 mm is calculated, in line with measurements, where the maximum dose can be found. For greater depths is observed that to a larger field corresponds a higher absolute dose with depth.

The 6MVFFF lateral profiles at different depths obtained with the various open field sizes.

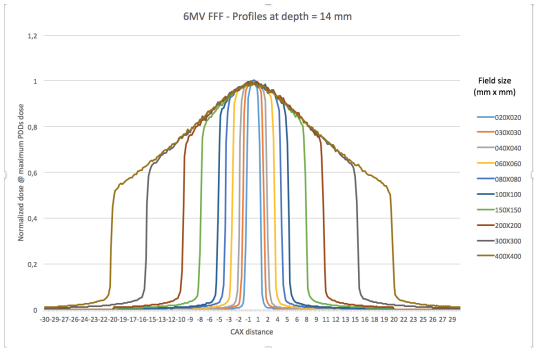

(a) 6MV FFF - normalized lateral profiles at depth 14 mm

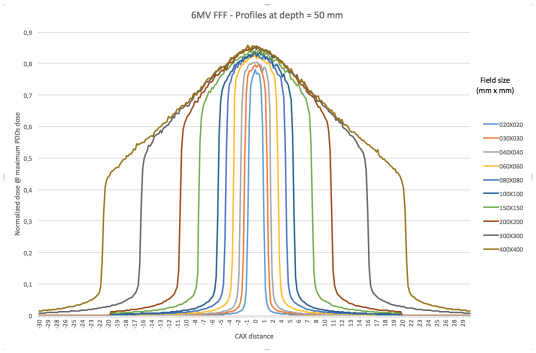

(b) 6MV FFF - normalized lateral profiles at depth 50 mm

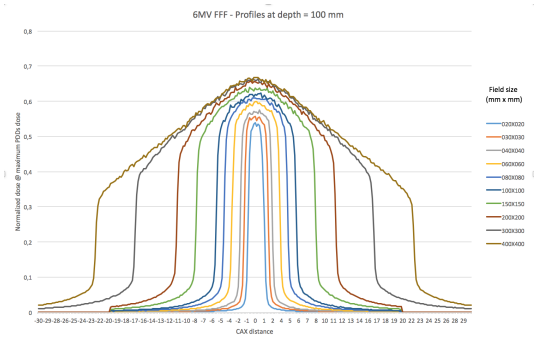

(c) 6MV FFF - normalized lateral profiles at depth 100 mm

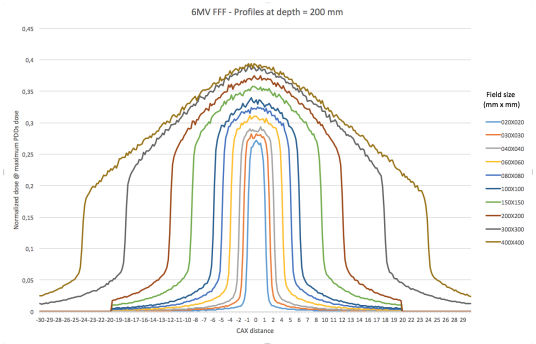

(d) 6MV FFF - normalized lateral profiles at depth 200 mm

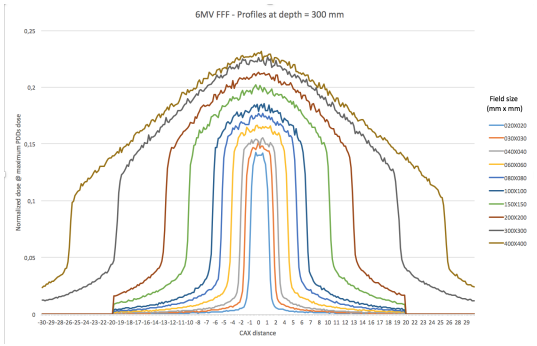

(e) 6MV FFF - normalized lateral profiles at depth 300 mm

Fig. 4.4. 6 MV FFF lateral profiles

Figure 4.4 shows the lateral dose profiles when open fields with different size are used. The data are normalized to the maximum value of the PDD, in order to keep the absolute normalization between different fields. The data show that the larger the field the higher the absolute value. This is due to scattering effects, which depend of the field size as the lateral contribution increases while increasing the field size.

The 6 MV FFF lateral profiles for different field sizes at the various commissioned depths.

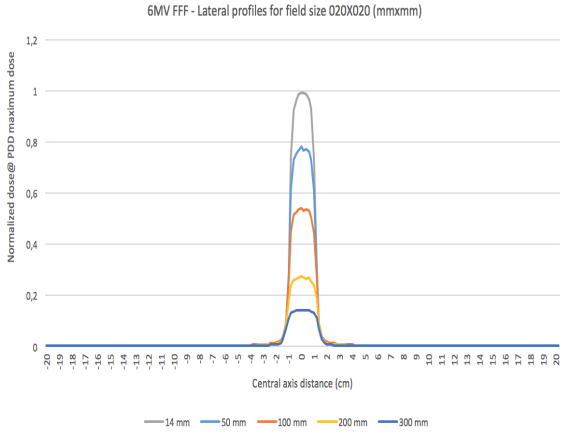

(a) 6MV FFF - normalized lateral profiles for 20X20 (mmxmm) field size

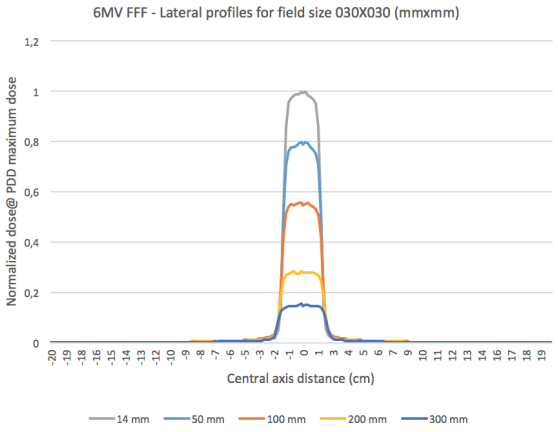

(b) 6MV FFF - normalized lateral profiles for 30X30 (mmxmm) field size

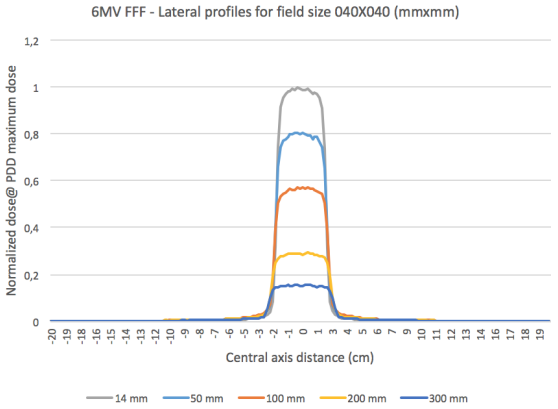

(c) 6MV FFF - normalized lateral profiles for 40X40 (mmxmm) field size

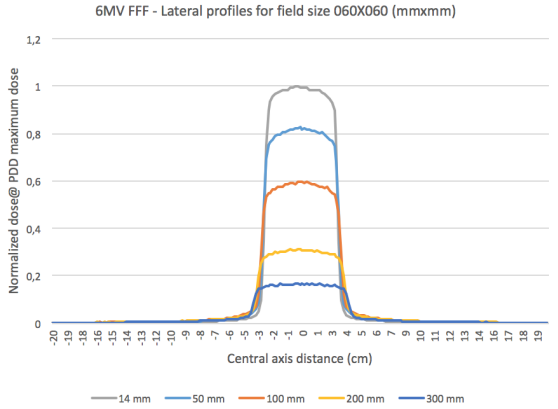

(d) 6MV FFF - normalized lateral profiles for 60X60 (mmxmm) field size

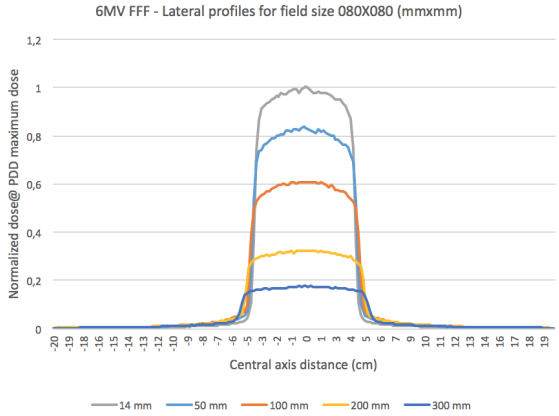

(e) 6MV FFF - normalized lateral profiles for 80X80 (mmxmm) field size

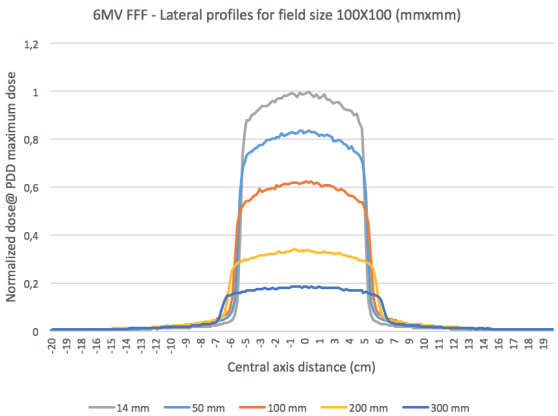

(f) 6MV FFF - normalized lateral profiles for 100X100 (mmxmm) field size

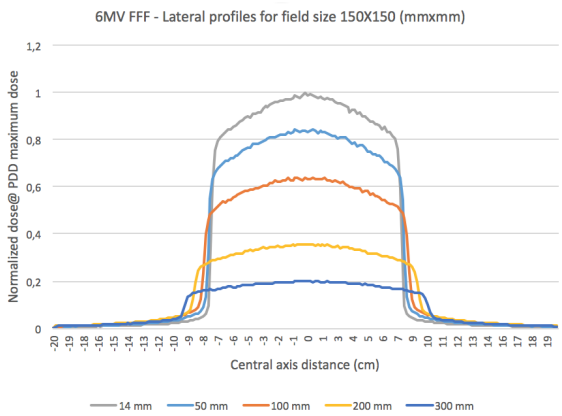

(g) 6MV FFF - normalized lateral profiles for 150X150 (mmxmm) field size

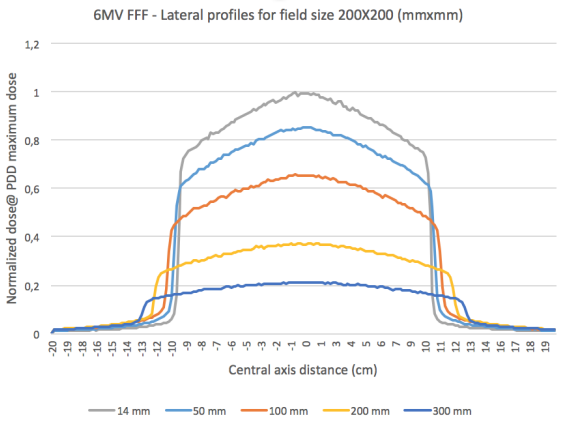

(h) 6MV FFF - normalized lateral profiles for 200X200 (mmxmm) field size

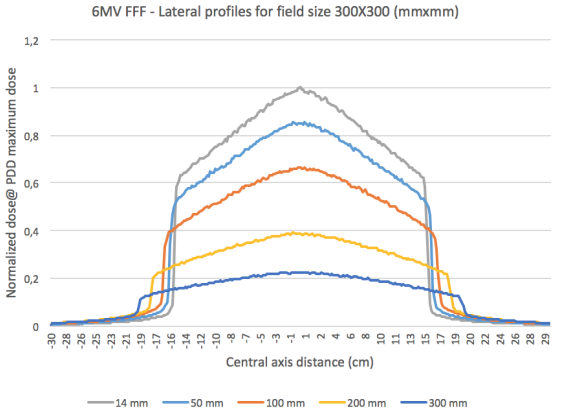

(i) 6MV FFF - normalized lateral profiles for 300X300 (mmxmm) field size

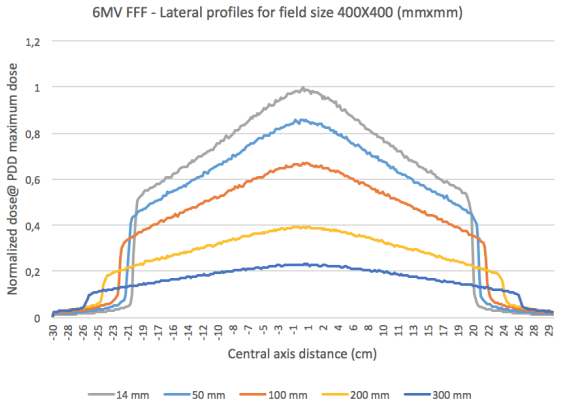

(j) 6MV FFF - normalized lateral profiles for 400X400 (mmxmm) field size

Fig. 4.5. 6 MV FFF lateral profiles

Figure 4.5 shows the lateral profile at different depths when a fixed beam size is considered. The absolute normalization is kept, that is the data are normalized with respect to the maximum dose value. While increasing the depth of the profile at a fixed beam size two features can be observed. Firstly, the beam enlarges with depth. The effect is given by the aperture of the beam and by scattering effects. Secondly, the maximum normalized value depends on the depth and decrease for deeper profiles.

The 10MV-FFF Percentage Depth Dose Profiles

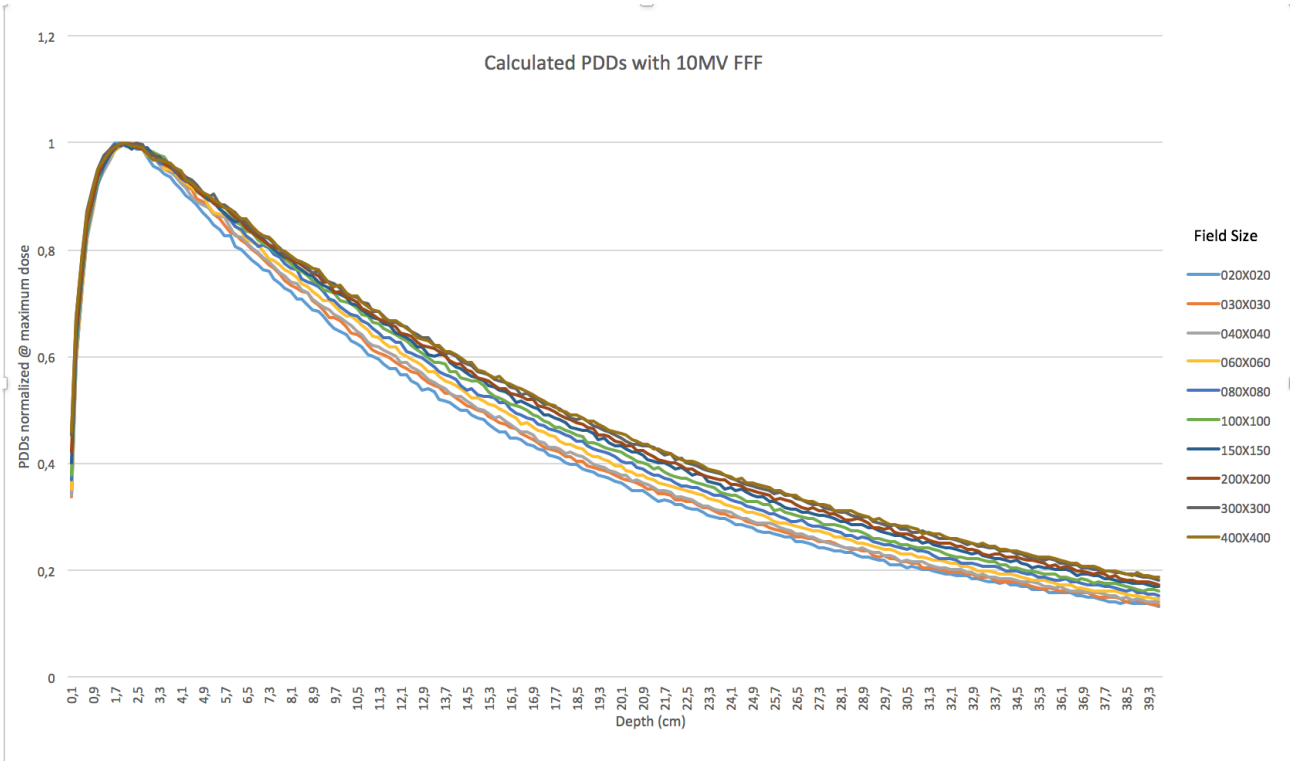

Fig. 4.6. 10MV FFF - normalized PDDs to each PDD maximum dose depth

The 10MVFFF lateral profiles at different depths obtained with the various open field sizes.

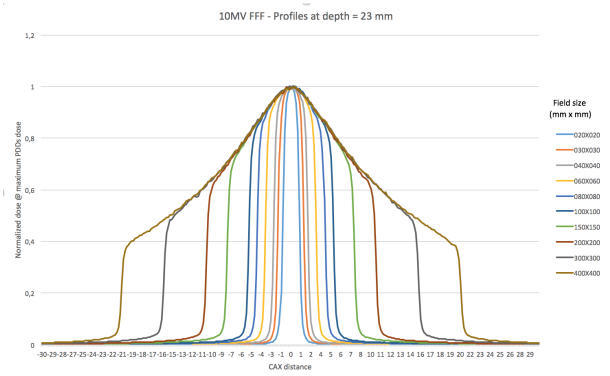

(a) 10MV FFF - normalized lateral profiles at depth 23mm

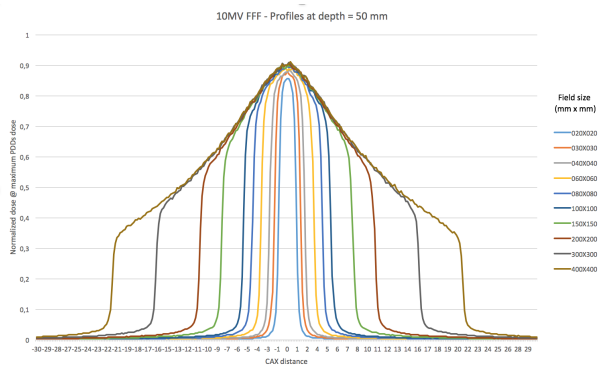

(b) 10MV FFF - normalized lateral profiles at depth 50mm

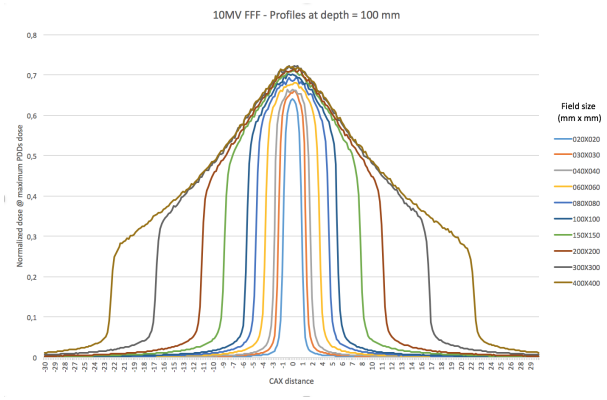

(c) 10MV FFF - normalized lateral profiles at depth 100mm

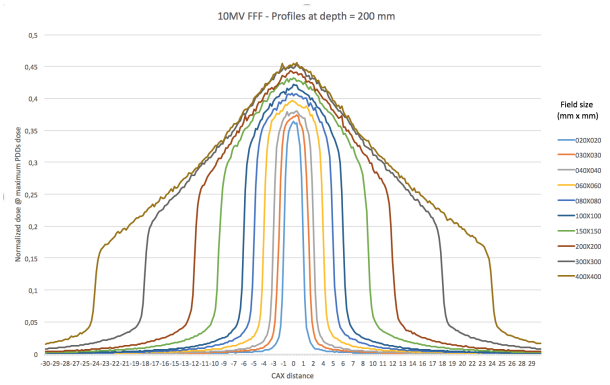

(d) 10MV FFF - normalized lateral profiles at depth 200mm

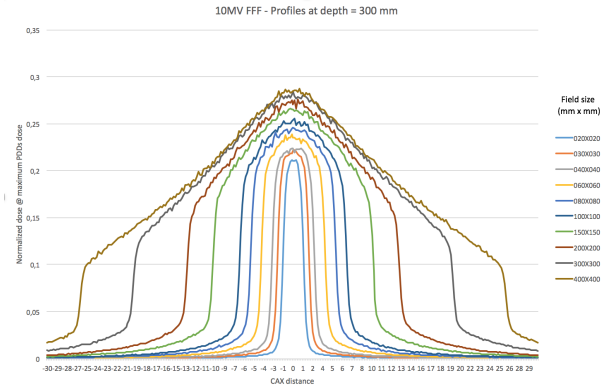

(e) 10MV FFF - normalized lateral profiles at depth 300mm

Fig. 4.7. 10 MV FFF Normalized lateral profiles

10 MV FFF lateral profiles obtained with the different field sizes used.

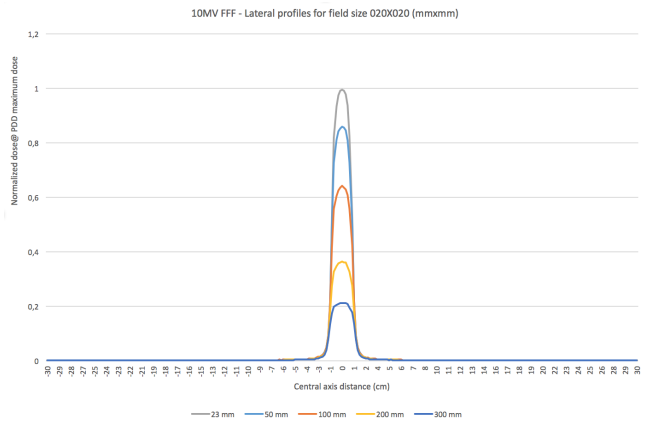

(a) 10MV FFF - normalized lateral profiles for 20X20 (mmxmm) field size

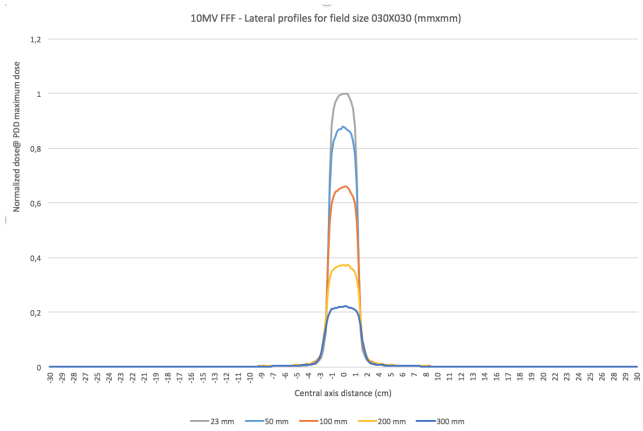

(b) 10MV FFF - normalized lateral profiles for 30X30 (mmxmm) field size

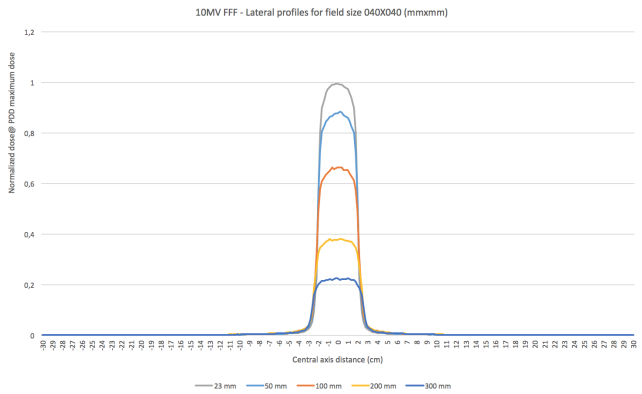

(c) 10MV FFF - normalized lateral profiles for 40X40 (mmxmm) field size

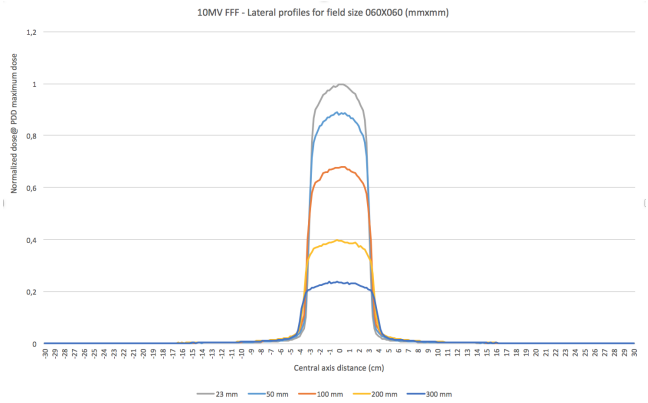

(d) 10MV FFF - normalized lateral profiles for 60X60 (mmxmm) field size

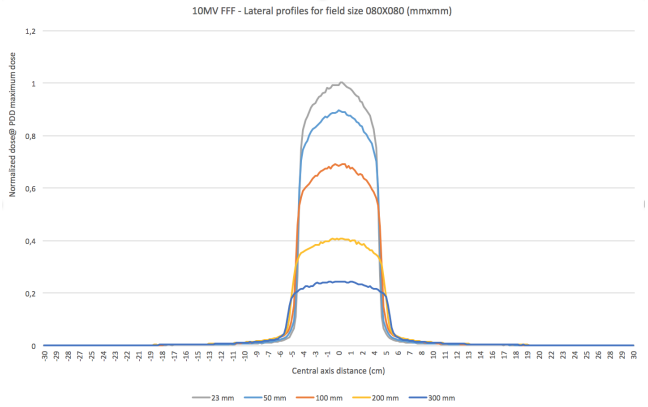

(e) 10MV FFF - normalized lateral profiles for 80X80 (mmxmm) field size

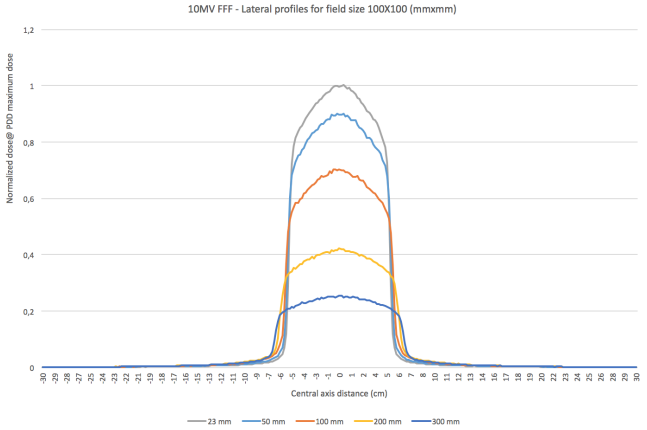

(f) 10MV FFF - normalized lateral profiles for 100X100 (mmxmm)

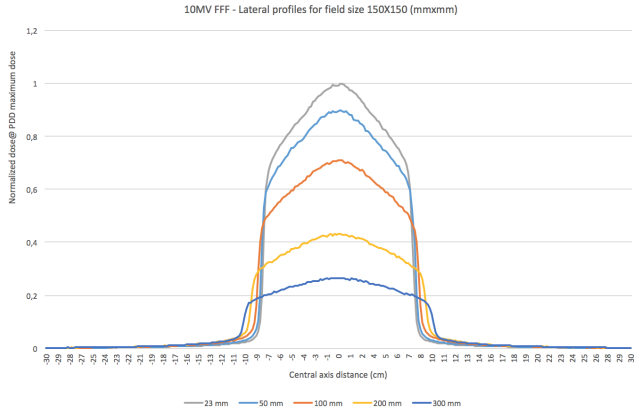

(g) 10MV FFF - normalized lateral profiles for 150X150 (mmxmm)

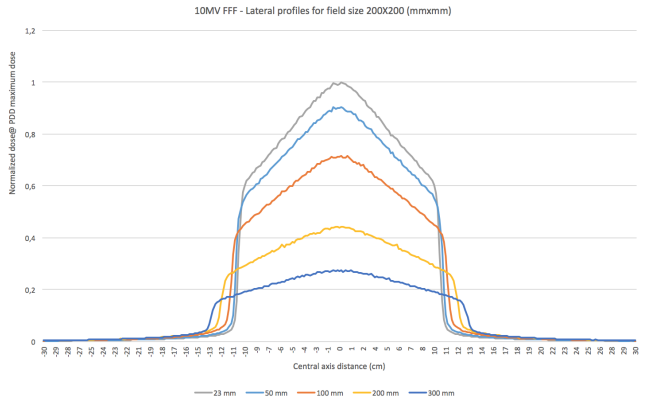

(h) 10MV FFF - normalized lateral profiles for 200X200 (mmxmm)

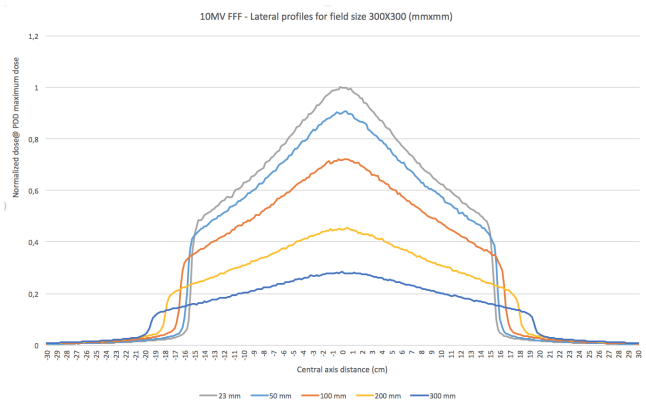

(i) 10MV FFF - normalized lateral profiles for 300X300 (mmxmm)

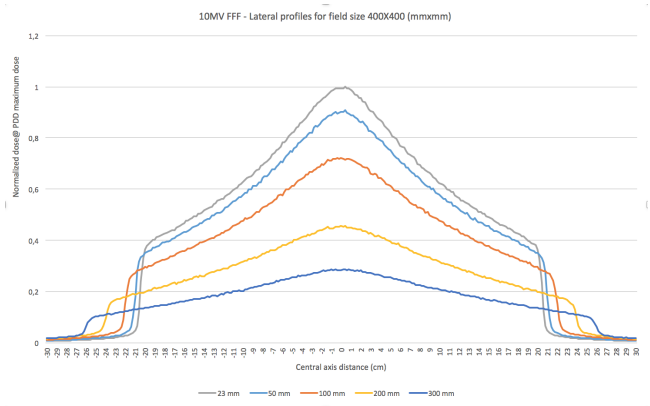

(j) 10MV FFF - normalized lateral profiles for 400X400 (mmxmm)

Fig. 4.8. 10 MV FFF lateral profiles obtained with the different field sizes used.

The 15X MV- working in FF mode. Percentage Depth Dose profiles

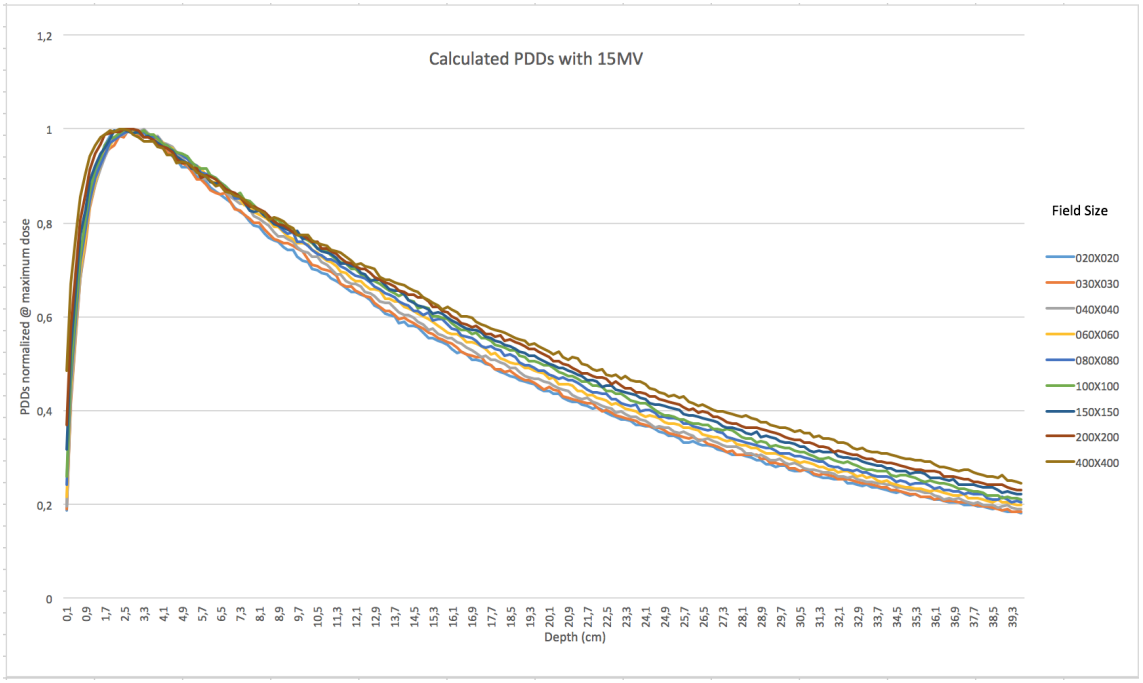

Fig. 4.9. 15X MV, working in FF, normalized PDDs to each PDD maximum dose depth

Figure 4.9 show the PDDs for the 15MV energy and working in Flatness Filter (FF). The build up region is of approximately 28mm.

PRIMO Gamma index evaluation results

The Figures 4.10, 4.11, 4.12 and 4.13 illustrates the PRIMO functionality that allows to perform the gamma analysis of the MC calculations with respect to the measured reference values. In Figure 4.10 the comparisons between experimental and simulated PDD are shown, while Figure 4.11 reports the same analysis for lateral profiles at the depth of maximum central axis (CAX) dose for each energy and for the typical 100X100 mm^2 field size. The data refers to 6 MV radiation beam.

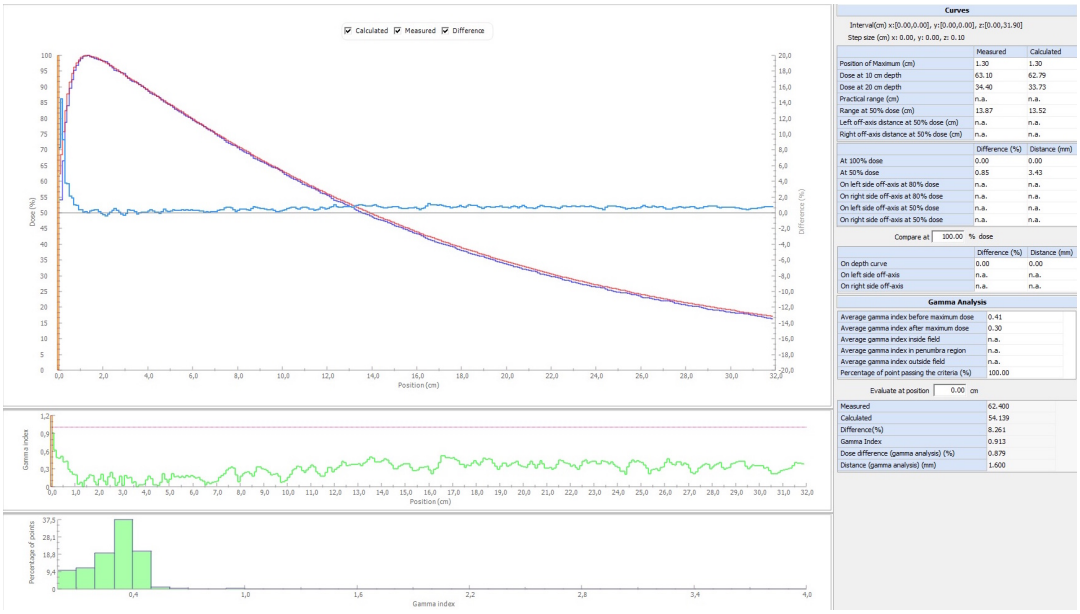

Fig. 4.10. Gamma PDD comparison for the case of a 100X100 mm field size and energy 6MV Flatness Filter Free (FFF)

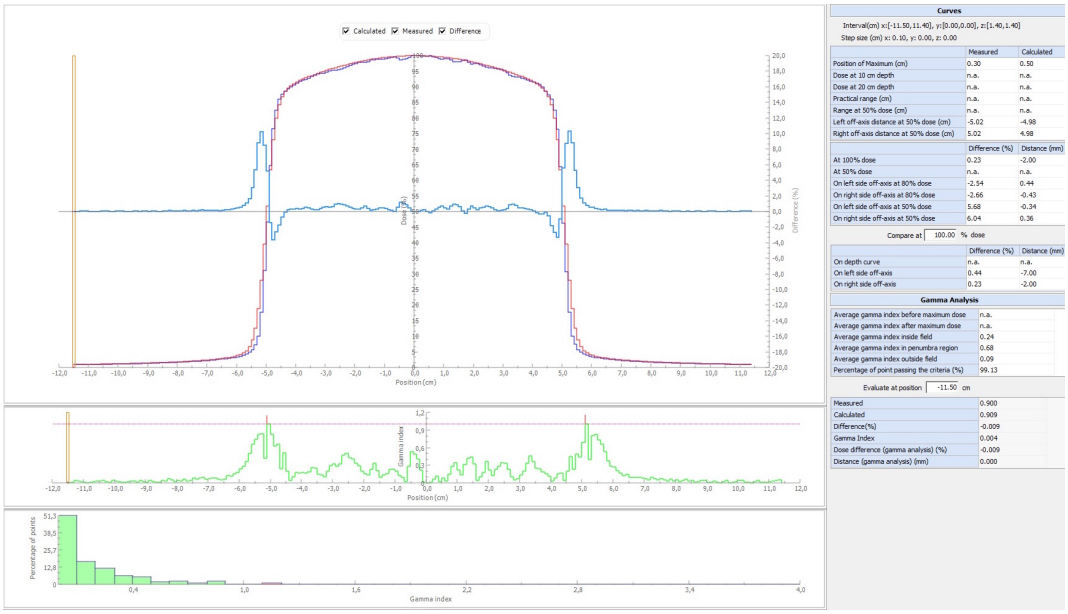

Fig. 4.11. Gamma Lateral profile comparison for the case of a 100X100 mm field size and energy 6MV Flatness Filter Free (FFF) at 14mm depth

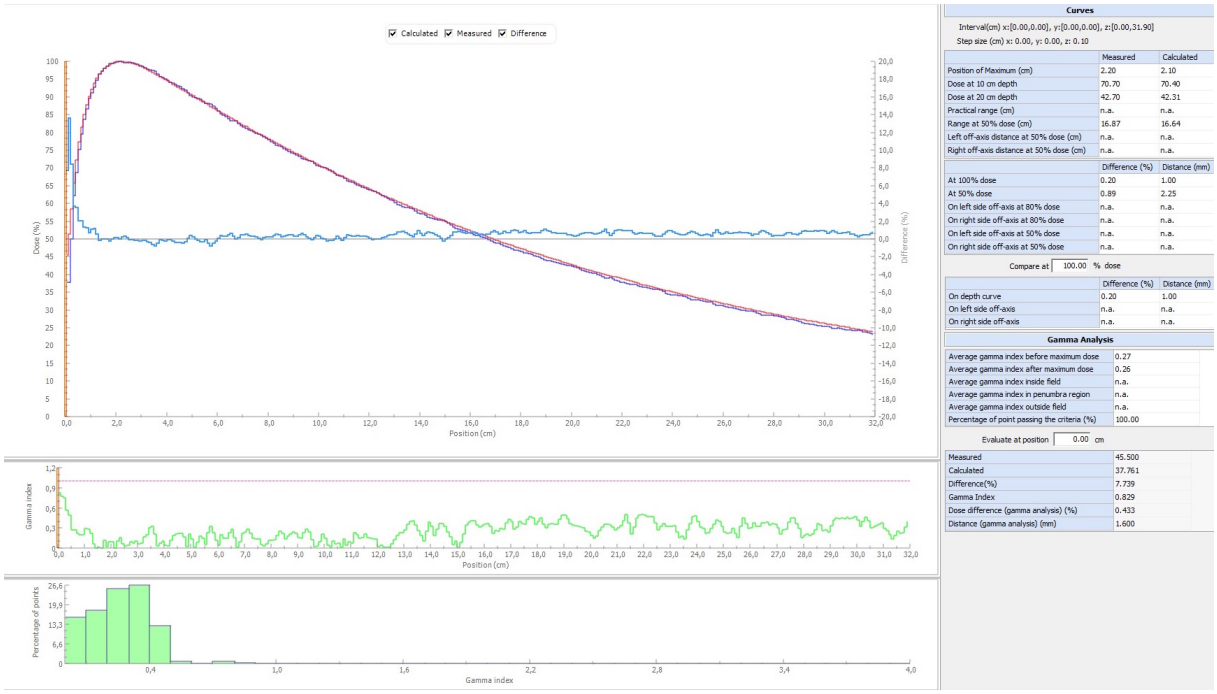

Fig. 4.12. Gamma PDD comparison for the case of a 100X100 mm field size and energy 10 Flatness Filter (FF)

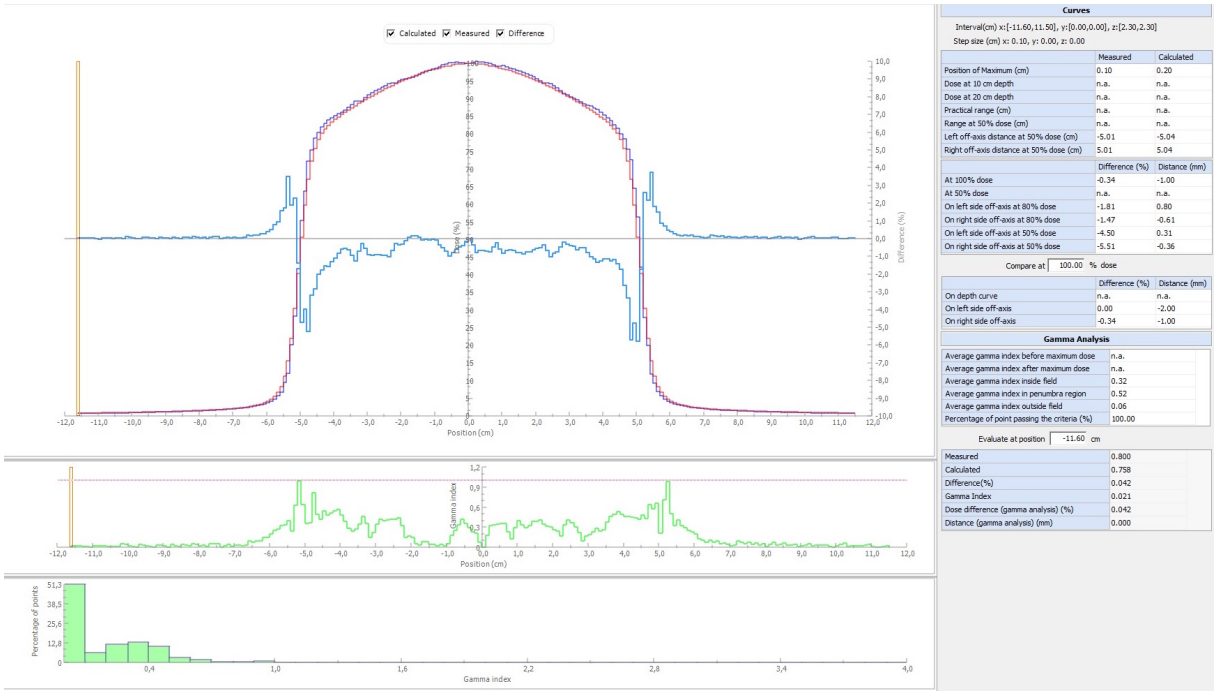

Fig. 4.13. Gamma Lateral profile comparison for the case of a 100X100 mm field size and energy 10MV Flatness Filter Free (FFF) at 23mm depth

Figures 4.12 and 4.13 show the Gamma analysis for the 10MV beam. As a general feature, it is observed that the gamma function assumes higher value in coincidence with steep gradient region, that is the build-up region of the PDD and the edge regions of the dose profiles. Even if some gamma points are higher than one, in all the cases the gamma pass/fail criteria is respected.

The Tables 4.1, 4.2 and 4.3 numerically resume the results from the gamma comparison, with a criteria of 2%-2mm, for the PDDs and lateral profiles of all the fields sizes calculated and measured for the simulated energies of 6MV FFF, 10MV FFF and 15MV, respectively.

Table 4.1: Gamma index results for energy 6MV Flatness Filter Free (FFF) - values in (%) percentage of passing points

Field Size (mmxmm)	PDD	Depth (mm)				
		14	50	100	200	300
020 x 020	99.06	97.33	96.75	96.30	97.73	99.48
030 x 030	99.69	97.50	97.56	97.67	98.40	98.53
040 x 040	99.69	96.47	96.59	98.37	99.00	99.08
060 x 060	99.69	100.00	97.96	99.03	99.11	99.59
080 x 080	99.06	97.14	100.00	99.12	100.00	100.00
100 x 100	100.00	99.13	100.00	98.40	99.63	100.00
150 x 150	100.00	97.14	96.55	98.68	99.10	98.61
200 x 200	100.00	96.39	97.67	97.78	97.19	97.75
300 x 300	100.00	99.54	100.00	100.00	100.00	100.00
400 x 400	100.00	100.00	100.00	100.00	100.00	100.00

Table 4.2: Gamma index results for energy 10MV Flatness Filter Free (FFF) - values in (%) percentage of passing points

Field Size (mmxmm)	PDD	Depth (mm)				
		23	50	100	200	300
020 x 020	99.06	97.33	98.70	98.77	98.30	100.00
030 x 030	99.69	98.13	98.78	98.84	98.40	99.51
040 x 040	99.69	97.65	99.43	98.91	100.00	99.54
060 x 060	99.69	97.92	100.00	99.51	99.55	100.00
080 x 080	99.38	99.06	100.00	99.12	100.00	100.00
100 x 100	100.00	100.00	100.00	100.00	100.00	100.00
150 x 150	100.00	100.00	100.00	100.00	100.00	100.00
200 x 200	100.00	100.00	100.00	100.00	100.00	100.00
300 x 300	100.00	100.00	100.00	100.00	100.00	100.00
400 x 400	100.00	100.00	100.00	100.00	100.00	100.00

Table 4.3: Gamma index results for energy 15MV - values in (%) percentage of passing points

Field Size (mmxmm)	PDD	Depth (mm)				
		28	50	100	200	300
020 x 020	99.38	98.68	98.70	100.00	98.86	97.62
030 x 030	99.38	98.77	97.56	98.84	99.47	99.51
040 x 040	100.00	98.26	98.86	98.37	99.50	99.54
060 x 060	100.00	97.40	98.98	99.03	99.11	99.59
080 x 080	100.00	99.06	99.54	99.56	99.19	99.63
100 x 100	99.69	100.00	98.74	99.20	100.00	100.00
150 x 150	99.38	100.00	100.00	99.67	100.00	100.00
200 x 200	99.69	100.00	100.00	100.00	100.00	100.00
300 x 300	99.38	100.00	100.00	100.00	100.00	NA
400 x 400	99.69	100.00	100.00	100.00	100.00	99.50

As can bee seen from the results presented in the tables, in all the cases reported more than 95% of gamma points passed the acceptance criteria, 2%-2mm as the Gamma parameters. In general, small size fields show a lower number of gamma points accepted on the beam profiles, while 10MV and 15MV show better agreement than 6MV.

Hereafter, the validated PHSP of the PRIMO linac model can be confidently used for all the MC in future simulations related to this machine and these validated energies.

4.1.2 Collimator validation

The MLC model within PRIMO was validated with respect to measurements making use of the 2D Gamma analysis, 2% - 2 mm, and 95% as the minimum fraction of gamma points accepted as pass/fail criteria. This result allowed the use of the MLC model in the MC simulations of intensity modulated fields. The gamma 2D analysis on the 6MV case showed 94.9% of Gamma points accepted using the usual 2% - 2mm gamma parameters, while increasing the parameters to 3% - 3mm, the Gamma accepted points increased to 98.7%. The correspondent values for the TPS calculation are 89.8% and 93.9%, which reveal a worse agreement with the measurement than the MC.

Considering the same analysis on the 10MV simulation case, were obtained 98.0% and 99.3% accepted points with 2% - 2mm and 3% - 3mm respectively, while the TPS showed 93.7% and 96.9% Gamma points lower than 1, confirming the worse calculation capability of TPS in this particular field shape condition.

PTW Verisoft was here used to calculate 2D Gamma distributions, as PRIMO does not provide yet such advanced calculation tools. A data manipulation was required in order to import PRIMO output into Verisoft as the PRIMO output are written in specific format. The core routines for this task were inherited from previous works done at IPO and incorporated in the APP, with the introduction of the automatic detection of the type of PRIMO dose file, i.e. water tank phantom or CT, feature.

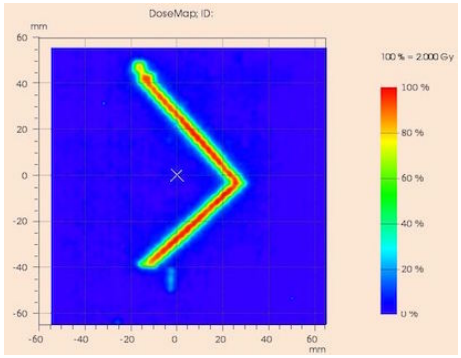

(a) Gaphchromic measure

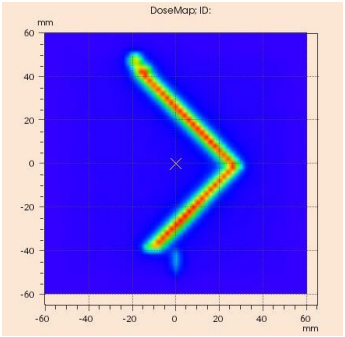

(b) Monte Carlo (MC) calculation

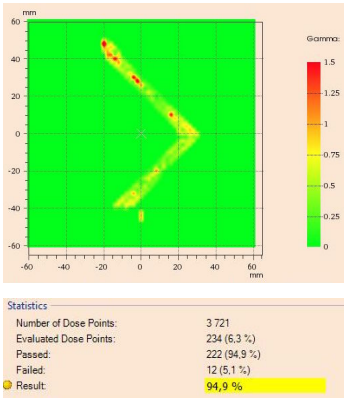

(c) MC Gamma 2% 2mm comparison

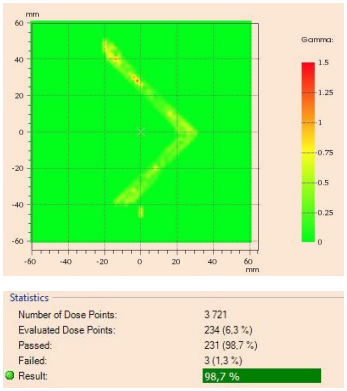

(d) MC Gamma 3% 3mm comparison

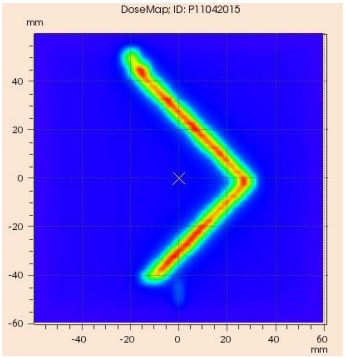

(e) treatment planning system (TPS) calculation

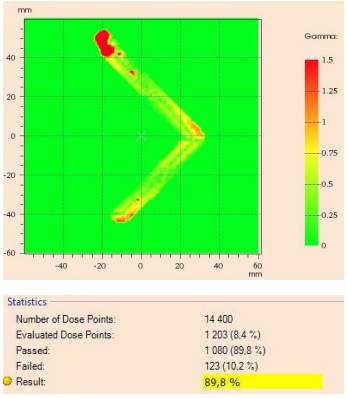

(f) TPS Gamma 2% 2mm comparison

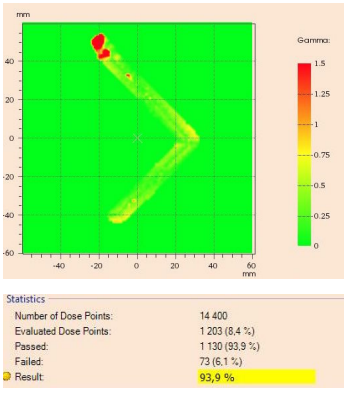

(g) TPS Gamma 3% 3mm comparison

Fig. 4.14. Results for the MLC validation with 6 MV FFF. Gamma comparison between MC calculation and Measurement and between TPS and measurement, respectively, obtained with Verisoft PTW.

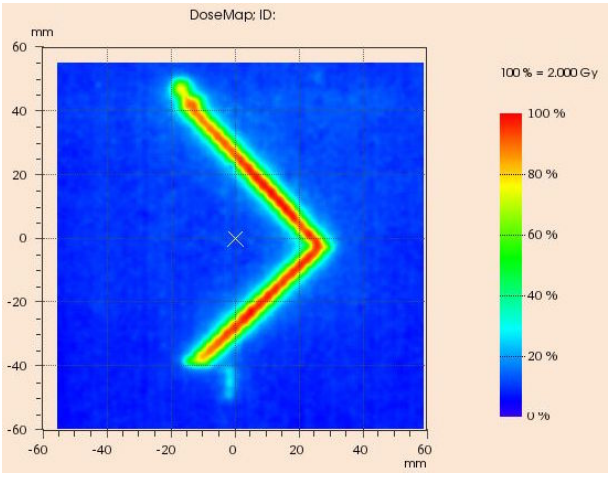

(a) Gaphchromic measure

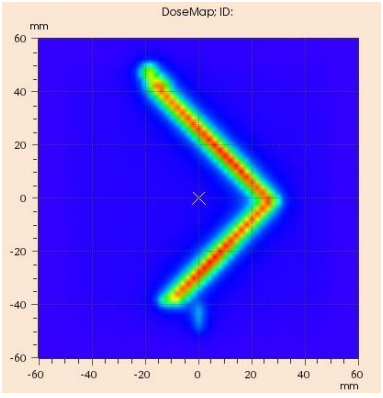

(b) Monte Carlo (MC) calculation

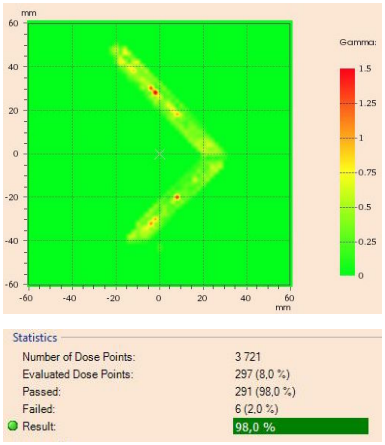

(c) MC Gamma 2% 2mm comparison

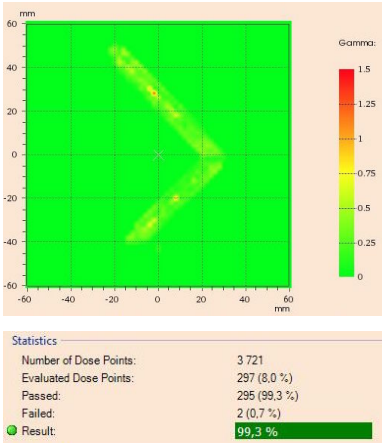

(d) MC Gamma 3% 3mm comparison

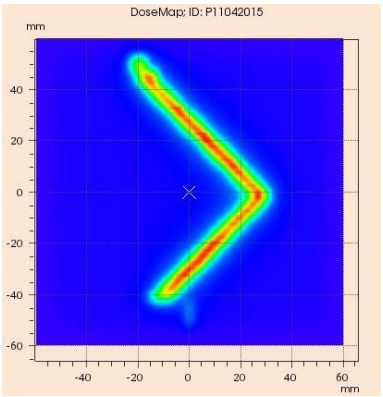

(e) treatment planning system (TPS) calculation

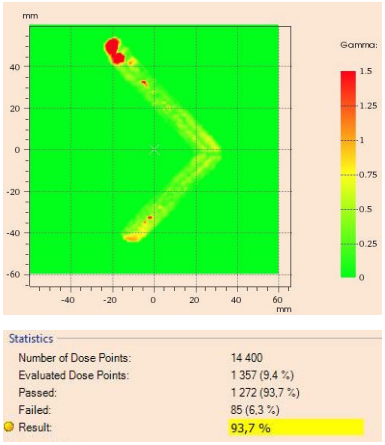

(f) TPS Gamma 2% 2mm comparison

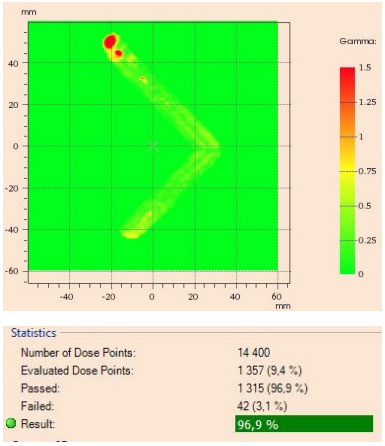

(g) TPS Gamma 3% 3mm comparison

Fig. 4.15. Results for the MLC validation with 10 MV FFF. Gamma comparison between MC calculation and Measurement and between TPS and measurement, respectively, obtained with Verisoft PTW.

4.1.3 Sampling algorithm

The continuous intensity modulation with time was assessed through the implementation of an algorithm that executes a probabilistic sampling of the position of the different beam modifiers, based on the cumulative MUs, following the Position Probability Sampling (PPS) approach.
The first test performed to test the algorithm consisted of simulating the MLC movement and keeping the Gantry fixed as shown in Figure 4.16. The requirement for the planned MLC movements was to create a homogeneous dose area in a definite treatment area. Agreement between the MC simulation and the Gaphchromic is confirmed by 94.0% with 2% - 2 mm and of 99,2% with 3% - 3mm Gamma points lower than 1. As for the case of the TPS, for the same criteria, the results shown an agreement with the Gaphchromic measured of 94,7% and 99,6% respectively. The same kind of tests, keeping the same criteria for the Gamma comparisons, included the movement of the Gantry, as shown in Figure 4.17. An agreement of 92,2% for the 2% - 2mm and 97,1% for the 3% - 3mm between the MC simulation and the Gaphchromic, revealed reliability in the sampling method. The same analysis between the TPS calculation and the Gaphchromic measurement showed 96,1% of 2% - 2mm accepted Gamma points and 99,8% accepted 3% - 3mm Gamma points.

As for the test of the reverse engineering process for reconstruction of the dose distribution from the snapshots stored in the TrajectoryLog, for the IMRT like case, i.e. gantry fixed and MLC dynamic, the agreement achieved between MC simulation and Gaphchromic was of 90.4% with 2% - 2mm and of 97.6% with 3% - 3mm Gamma points < 1, respectively. For the VMAT like case, i.e., both gantry and MLC allowed to move dynamically, the agreement achieved between the MC simulation and the Ghaphcromic measurement using the Octavius phantom was of 82.6% Gamma points < 1 with criteria 2% - 2mm and of 92.8% of Gamma < 1 with criteria 3% - 3mm. These results suggests that the introduction of the degree of freedom corresponding to the gantry movement and consequently of higher modulation fluence delivered may need a greater number of fields to represent it with the desired level of accuracy.

IMRT - Dynamic MLC with fixed Gantry

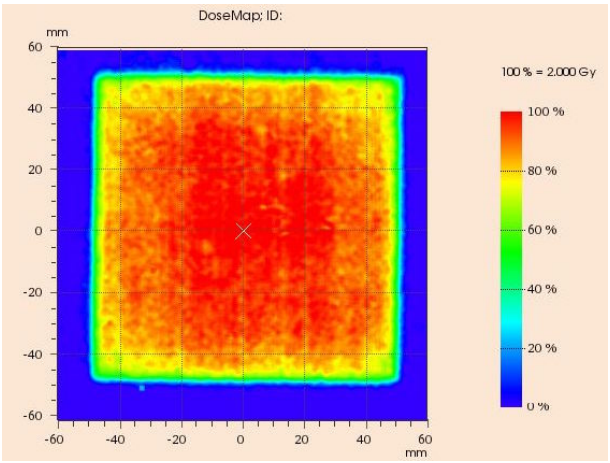

(a) Gaphchromic measure

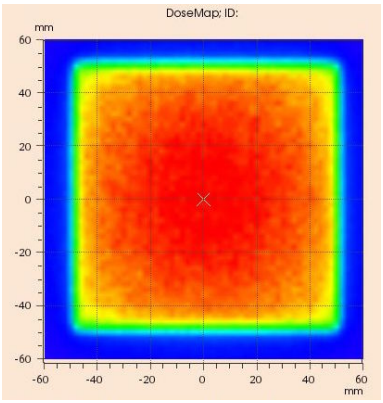

(b) Monte Carlo (MC) calculation

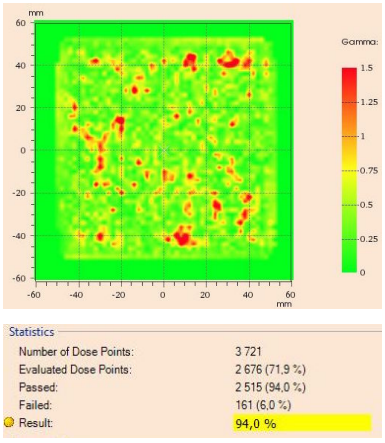

(c) MC Gamma 2% 2mm comparison

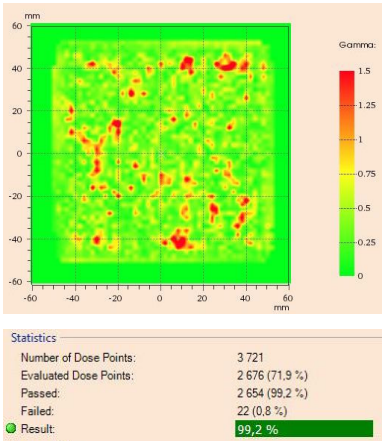

(d) MC Gamma 3% 3mm comparison

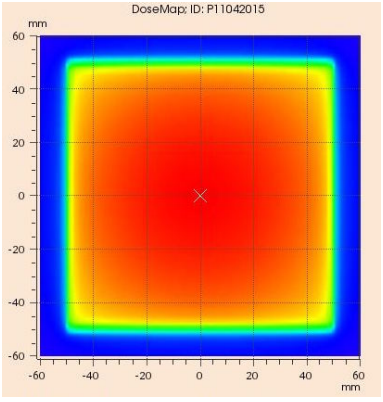

(e) treatment planning system (TPS) calculation

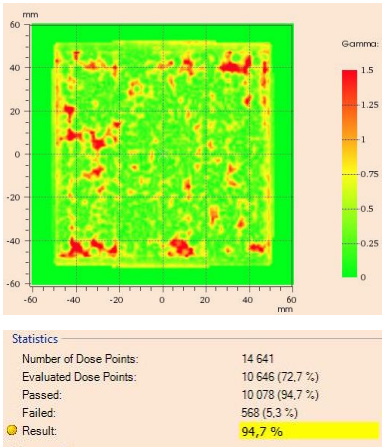

(f) TPS Gamma 2% 2mm comparison

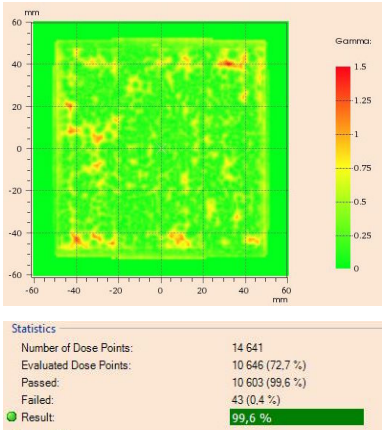

(g) TPS Gamma 3% 3mm comparison

Fig. 4.16. Results for the IMRT sampling algorithm validation with 6 MV FFF. Gamma comparison between MC calculation and Measurement and between TPS and measurement, respectively, obtained with Verisoft PTW.

VMAT - Dynamic MLC with moving Gantry

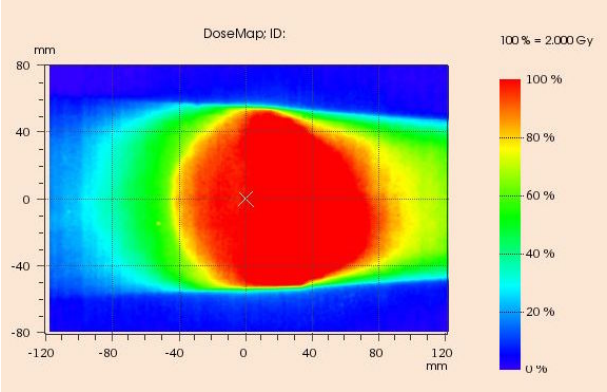

(a) Gaphchromic measure

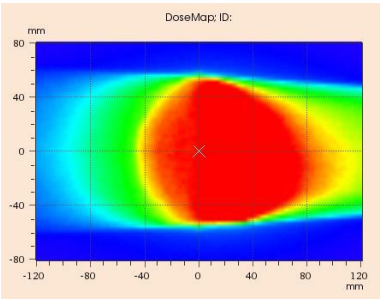

(b) Monte Carlo (MC) calculation

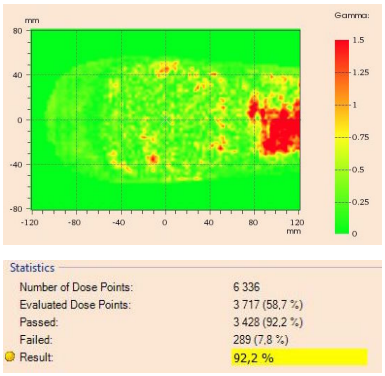

(c) MC Gamma 2% 2mm comparison

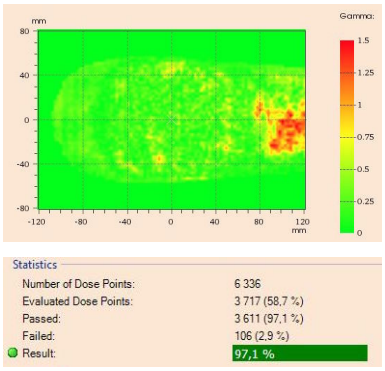

(d) MC Gamma 3% 3mm comparison

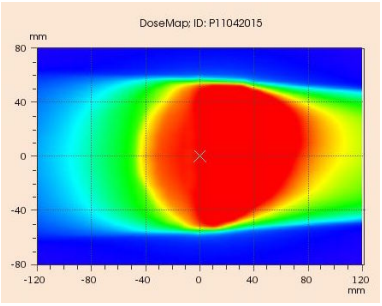

(e) treatment planning system (TPS) calculation

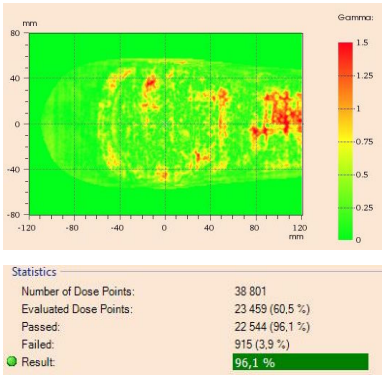

(f) TPS Gamma 2% 2mm comparison

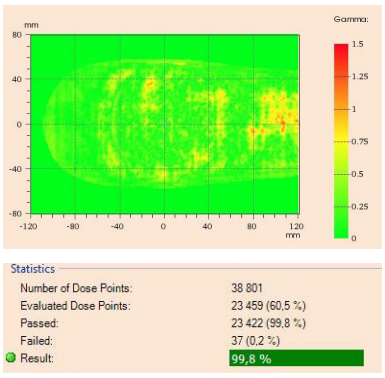

(g) TPS Gamma 3% 3mm comparison

Fig. 4.17. Results for the VMAT sampling algorithm validation with 6 MV FFF. Gamma comparison between MC calculation and Measurement and between TPS and measurement, respectively, obtained with Verisoft PTW.

IMRT - Trajectory Log simulation

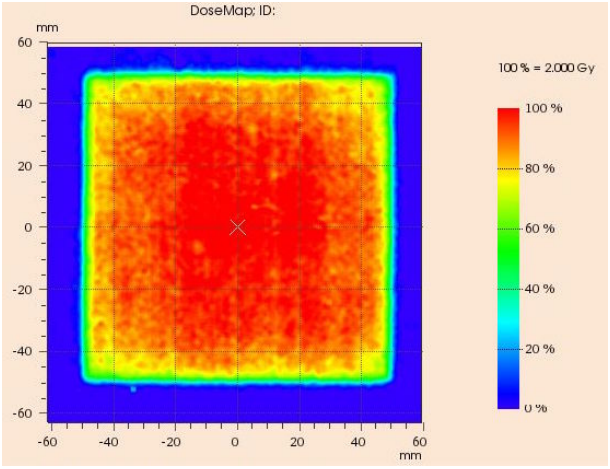

(a) Gaphcromic measure

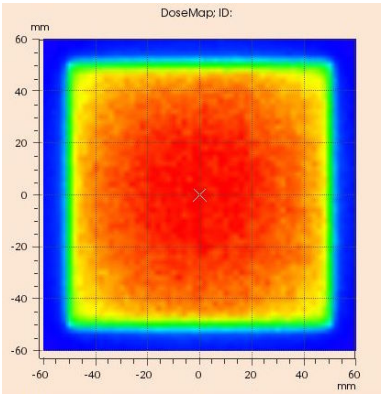

(b) Monte Carlo (MC) calculation

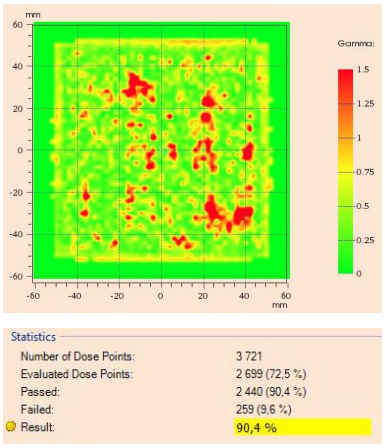

(c) MC Gamma 2% 2mm comparison

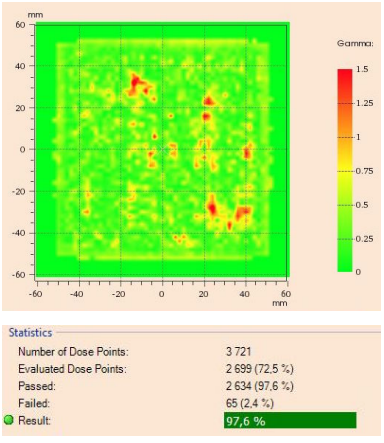

(d) MC Gamma 3% 3mm comparison

Fig. 4.18. Results for the IMRT trajectory log sampling algorithm validation with 6 MV FFF. Gamma comparison between MC calculation of the trajectory log and Measurement, obtained with Verisoft PTW.

VMAT - Trajectory Log Simulation

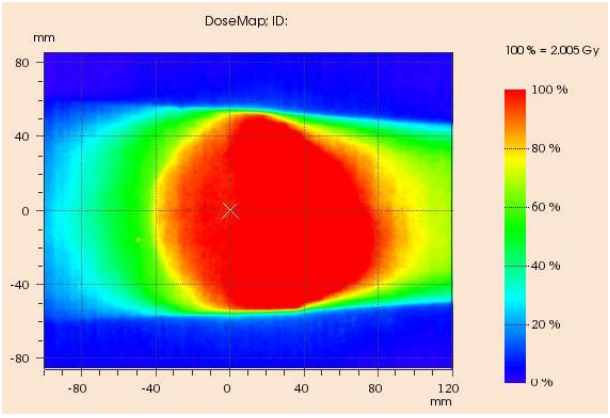

(a) Gaphchromic measure

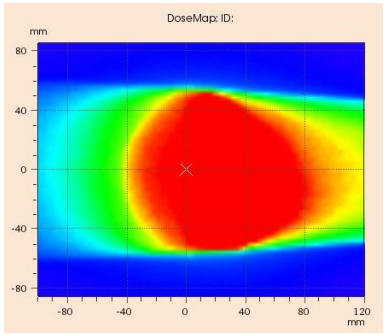

(b) Monte Carlo (MC) calculation

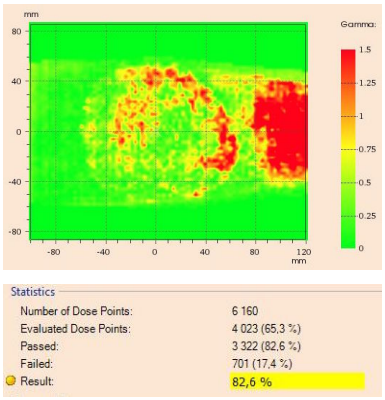

(c) MC Gamma 2% 2mm comparison

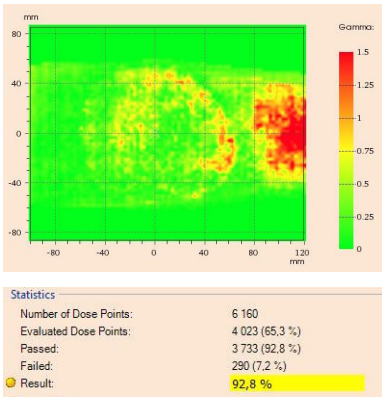

(d) MC Gamma 3% 3mm comparison

Fig. 4.19. Results for the VMAT trajectory log sampling algorithm validation with 6 MV FFF. Gamma comparison between MC calculation of the trajectory log and Measurement, obtained with Verisoft PTW.

All these results gave support to the viability of using PRIMO to simulate the dynamic treatments as was the premise of the start of this work.

Although the encouraging results the necessary operations to implement the whole strategy were not simple and very dispersed, so a workflow was designed to simplify the introduction of PRIMO MC simulations for dynamic treatments. To implement this workflow an application was developed exposing a graphical interface that encapsulated the several tasks to perform, including the data processing and data preparation needed for the simulations and for the calculation evaluations.

4.2 Matlab Application

Although the PRIMO system offers a graphical user interface that allows to easily and quickly overcome several tedious tasks common to any MC simulation, it does not include by default the possibility of simulate dynamic fields like IMRT or VMAT treatments. PRIMO allows to simulate up to a maximum number of 180 static fields, but to set up each one of them by hand can be a cumbersome task. Besides this, although the final resulting dose distribution calculated by PRIMO can be visually accessed, this final result cannot be extracted to further comparison with the reference distribution in external software. What is stored by PRIMO is the individual result for each one of the simulated fields. In order to build a work-flow capable of integrating the use of MC to simulate the dynamic treatments, and following the PRIMO approach as a user-friendly software, one of the principal objectives of this work was to build an application that would expose an easy to use Graphical User Interface (GUI) and put in the background and automatize the routine tasks. The principal routine tasks identified were: the reading of the TPS Dicom or ".mlc" files, the Machine log files, the sampling of the fields to simulate, the construction of the PRIMO ".ppj" configuration file, the reading and integration of the dose files generated by PRIMO and the generation of the Dicom files that could be used to compare with the reference distribution in external 3rd party software, e.g. VeriSoft PTW, Friburg. In a first approach several functions already developed at IPO in previous works were used and a deep work of optimization was done, trying to vectorize where possible to reduce the matrix manipulation times. Whenever possible the redundant tasks spread by different functions were condensed, mainly through the introduction of parsing functionality and regular expressions. A Graphical User Interface necessary to the present work was designed and constructed. Finally a work of code encapsulation into classes was done in order to get a more modular, maintainable and reusable code. The resulting application is composed by the following principal components (View Classes diagram A.2):

- **VMAT_APP**, is the entry point for the application and is responsible for managing the access to the principal components of the application. From the Menu the different modules can be called as needed, Figure 4.20.

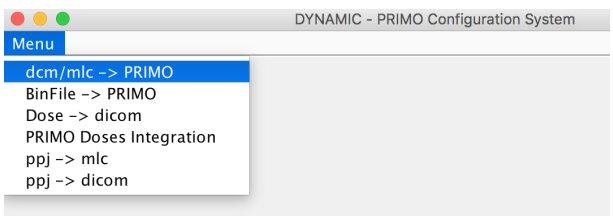

Fig. 4.20. APP Main Menu

- **TPSFile**, this module manages the operations related with the files originated from the treatment planning system (TPS) in format DICOM (dcm extension) or mlc.

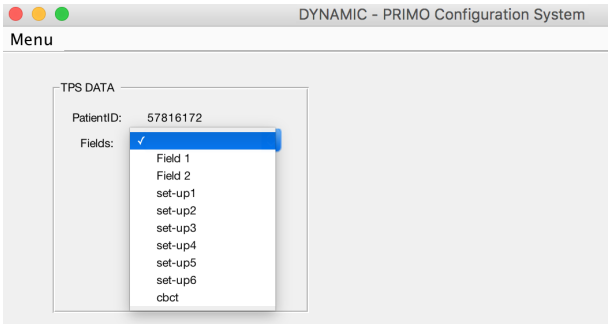

(a) Selection of the beam to sample. Although all present beams in the DICOM are shown, only the dynamic ones are processed, in this case Field 1 and Field 2.

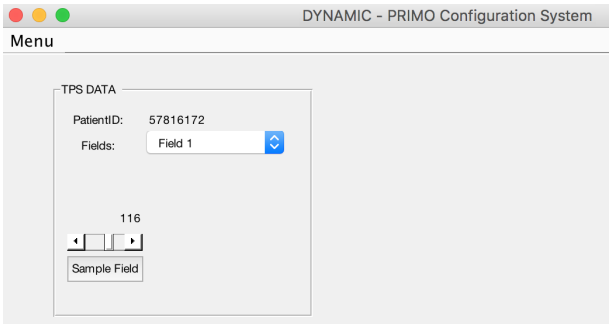

(b) Choosing the number of fields to sample. Minimum 3 and maximum 180.

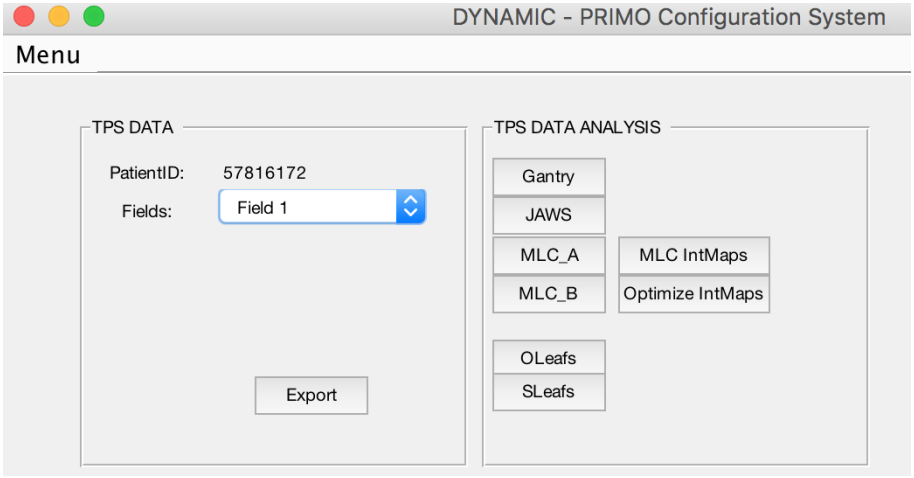

(c) Available options after successful sampling

Fig. 4.21. APP TPSFile - Beam selection, sampling and results options layouts.

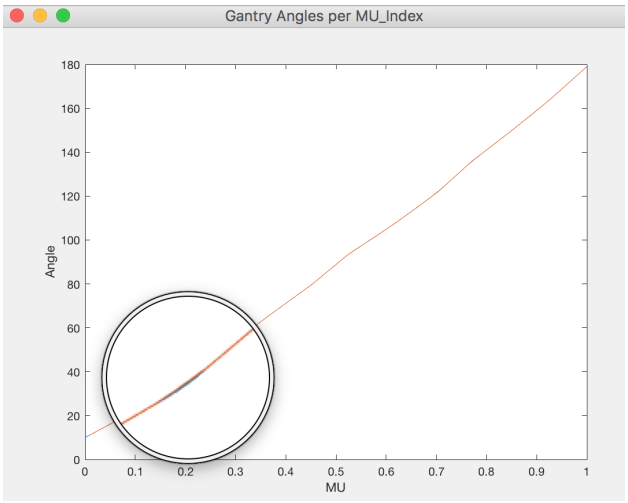

(a) Inspection of the result of the Gantry movement sampling. Magnifier pretends to show the difference between original (blue) and sampled (orange) movements

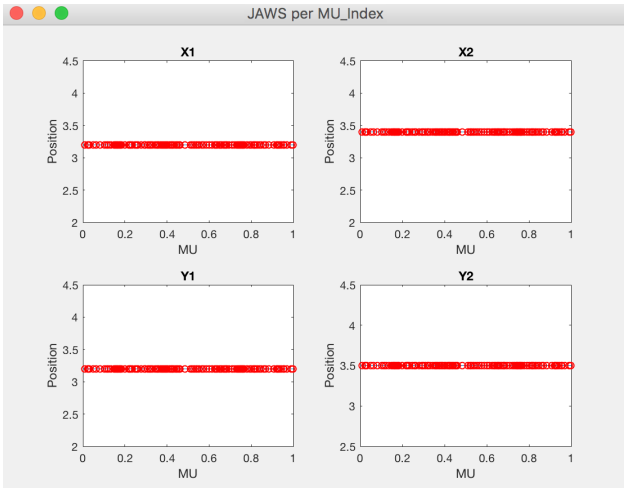

(b) inspection of the result of the sampling of the Jaws movement.

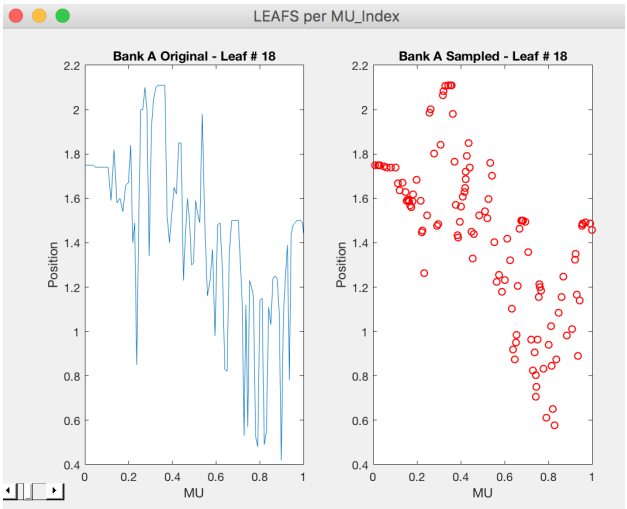

(c) example of a view of the result of sampling of the MLC (Leaf 18 Bank A)

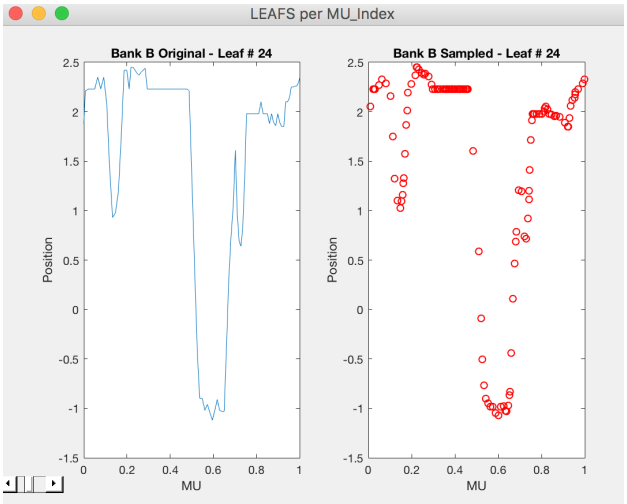

(d) example of a view of the result of sampling of the MLC (Leaf 24 Bank B)

Fig. 4.22. APP TPSFile - Inspection of the results for the sampled Gantry, Jaws and MLC leafs movement.

Figure 4.22 exemplifies the functionality implemented to help visualize the end result of the random sampling of movement process, showing the new positions as a function of the Monitor Units. For this particular case tested, (a) refers to the sampling of the gantry angle and the magnifier was used to show a that there are actually two different curves, the original (blue) and the sampled one (orange); (b) shows the resulting X and Y jaws sampled positions; (c) and (d) refers to the MLC leafs sampling, in concrete to the leaf 18 of the Bank A and to the leaf 24 of the Bank B, respectively. The Blue line represents the original motion and the red circles the sampled points. The slider at the bottom left corner allows to navigate through the leafs of the respective Bank.

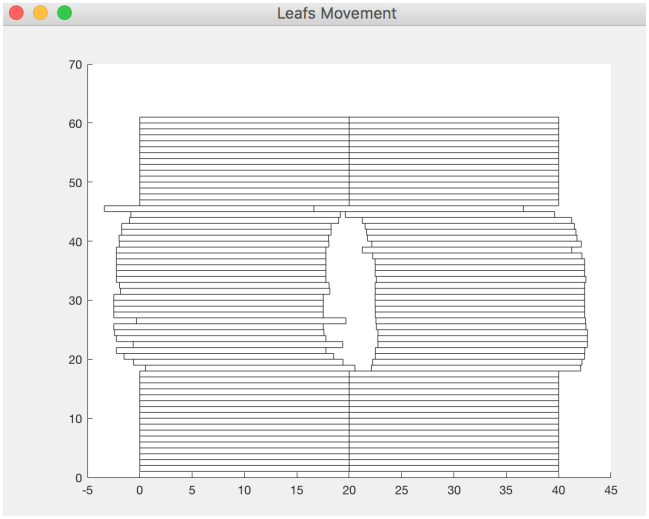

(a) Oleaf and Sleaf allows a preview, for inspection, of the original and sampled leafs movement.

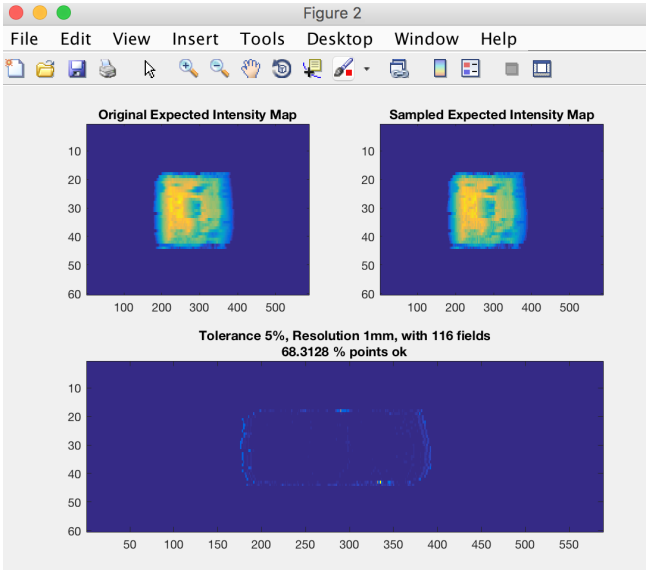

(b) Functionality for comparison between original and sampled estimated Intensity Maps, with tolerance of 5% difference between them point by point (1mm).

Fig. 4.23. Implemented functionality for inspection of segments of leaf movement and expected fluence maps.

- **Sampling** this module implements the random sampling algorithm of the dynamic treatment.
- **PRIMOFile** In this class the read and write mechanisms related with the PRIMO project configuration files, with extension ".ppj" are implemented.
- **BINFile** this is the equivalent module to TPSFile but for the case of the binary trajectory log files originated by the TrueBeam linac, with extension ".bin".
- **DosePRIMO** this module operates the reading of a dose file with PRIMO format and extension ".f#", where # is an integer number. This class builds the dose matrix from the files read and allows exporting the slices of interest in dicom format, to use, for instance in further comparisons with the reference distributions with a third program like Verisoft PTW.

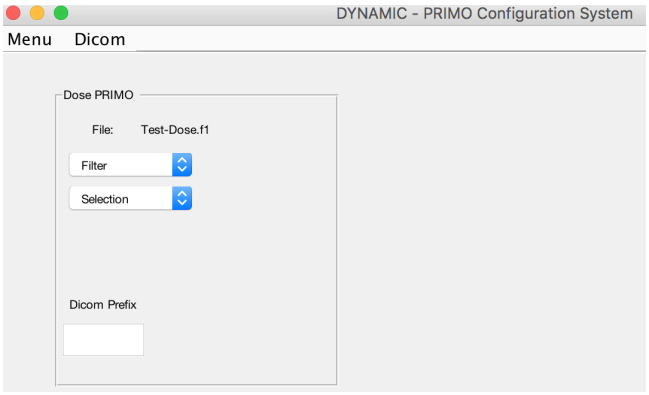

(a) Entry point for the DosePrimo Module after dose file is choosen.

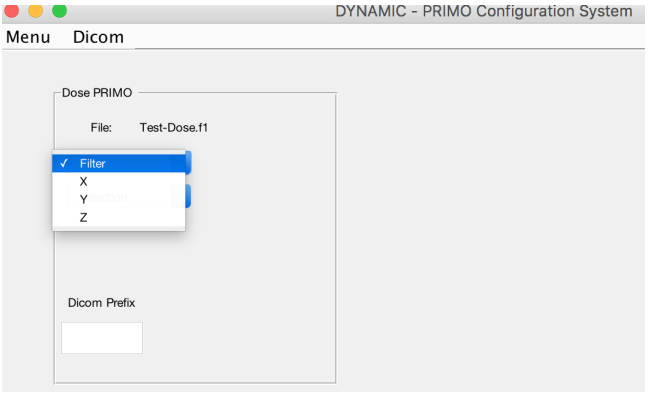

(b) The slices can be selected by index or by position.

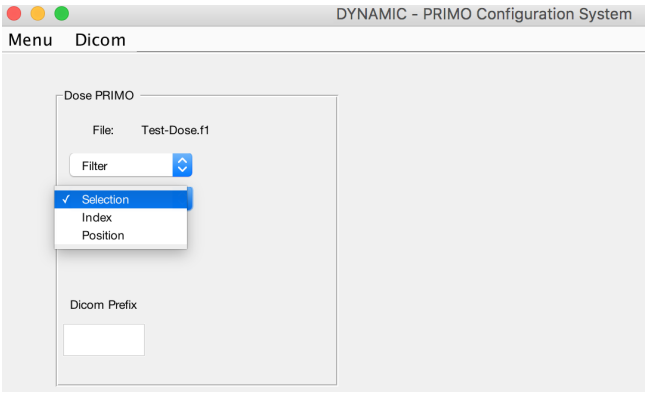

(c) The slices can be selected by index or by position.

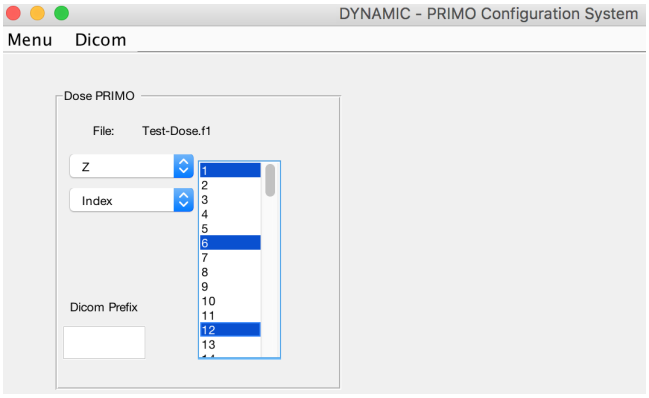

(d) Multi slices selection is possible.

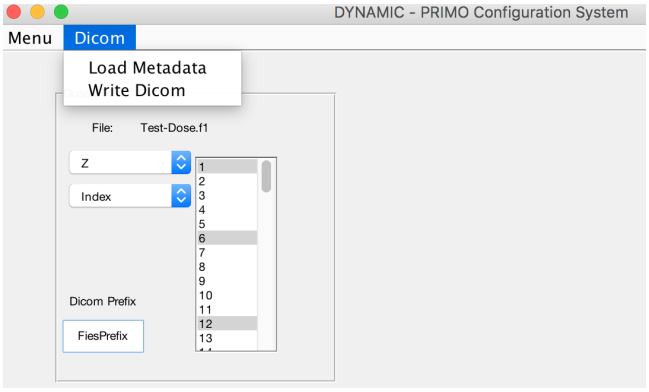

(e) Given the Prefix the dicom files are generated through the Dicom Menu.

Fig. 4.24. APP DosePRIMO Module functions

- **DoseIntegrator** reads a set of PRIMO dose files and allows to attribute weights to each one of them and produces a single file with the weighted calculated doses. The weights can be loaded from a file, e.g. the file generated by the PRIMOFile:: exportPRIMOFile APP module, or from the clipboard through the copy&past mechanism that this class implements.

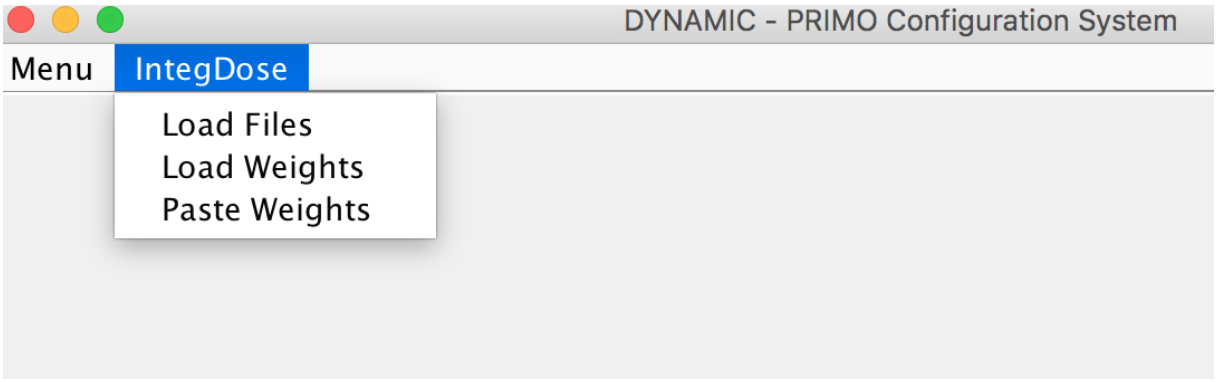

(a) Dose files to integrate and weight from file or clipboard are loaded.

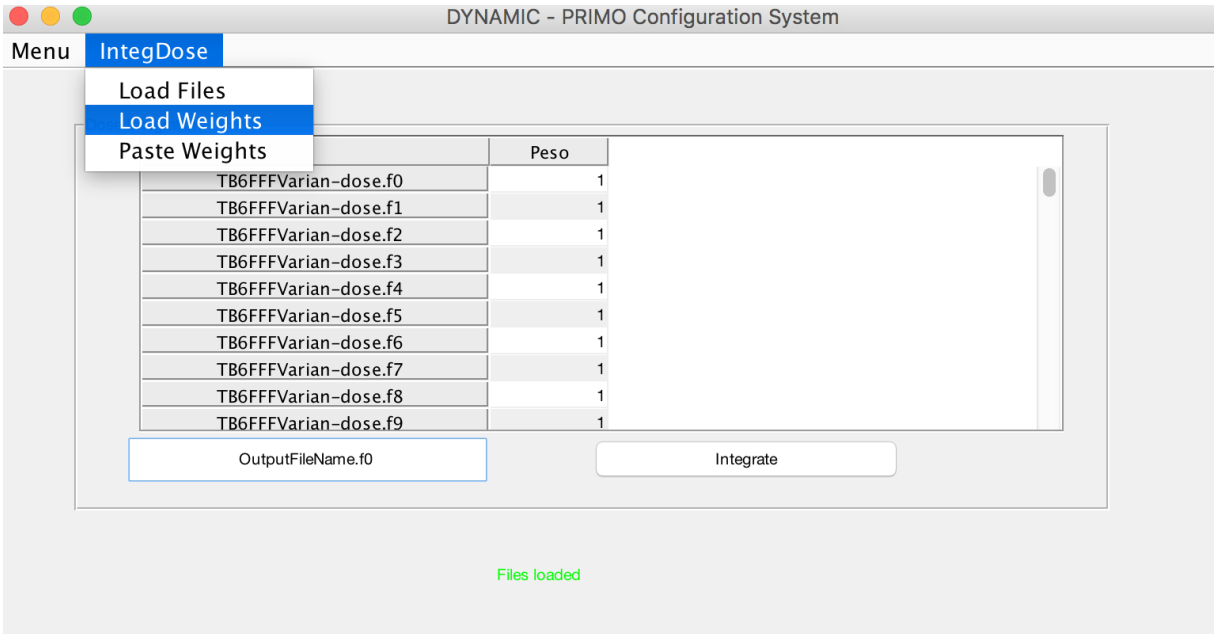

(b) The integrate button starts the integrating process that results in a one file with name choosen.

Fig. 4.25. APP DoseIntegrator Module functions

- **FluenceTest** module responsible for the comparison between the expected original and sampled Intensity Maps, and is used as an accessory tool for the number of fields optimization, view Figure 4.23(b).

  This tool was also used to study the relationship between the number of fields and the expected result from the sampled fields.

  The algorithm that performs the expected fluences comparison and number of fields optimization works as follows:

1. It sets a spatial grid with a size that covers all the incident fluence and with a resolution of 1 mm x 1 mm. In case of the fixed gantry is set to 200 mm x 200 mm. In the case of a moving gantry the grid have size (max angle - min angle) mm x 200 mm.

2. For each control point the respective MUs are accumulated in the respective original or sampled grid and in the corresponding position with the referred 1 mm X 1mm resolution.

3. The comparison between the original and sampled fluences is made by subtracting one from the other and dividing the absolute value by the original value. This operation is performed pixel by pixel, where the pixel dimension is defined by the resolution that is chosen by the user.

4. The evaluation takes in consideration the user criteria, i.e., the space resolution and fluence difference tolerance. In the end overall evaluation is given as the percentage of points inside the criteria over the total number of points evaluated.

5. The optimizer uses this algorithm as an inverse optimization to iteratively sample the original control points until it finds a configuration that shows a comparison with a percentage number of passing points greater or equal to the objective value. The convergence is obtained when the agreement between the expected fluence and the sampled Control points integrated fluence shows the objectives for the percentage points and tolerance defined by the user. While the convergence is not obtained, a new sampling operation is iterated increasing the number of sampling projection by 1.

The relationship between the number of sampled fields and the resolution obtained. Are 180 fields enough?

Using the FluenceTest module some tests were conducted to understand the influence of the number of sampled fields. First test conducted consisted in generating 100 runs with independent configurations from 3 to 180 fields and assessing the resulted predicted accuracy, Figure 4.26(a). A second test consisted in 100 runs with the objective of finding the minimum number of fields needed to achieve a pre-defined objective, Figure 4.26(b). In this case within each run, starting at 3 fields, a new independent configuration with one more field was added until the pre-defined objective was achieved.
With the validity domain of the modulation used, for the first test, can be noted that the expected accuracy increases as the number of fields used increases but at approximately 100 fields can be found the elbow where it enters at a plateau and asymptotically approaches the objective. As for the second test conducted the results show that for the degree of agreement pre-defined of 97,5% of the pixels with maximum difference of 5% the number of fields required always exceeded the 180 maximum available at PRIMO, although the great proportion of times it was not far, at around 190 fields needed.

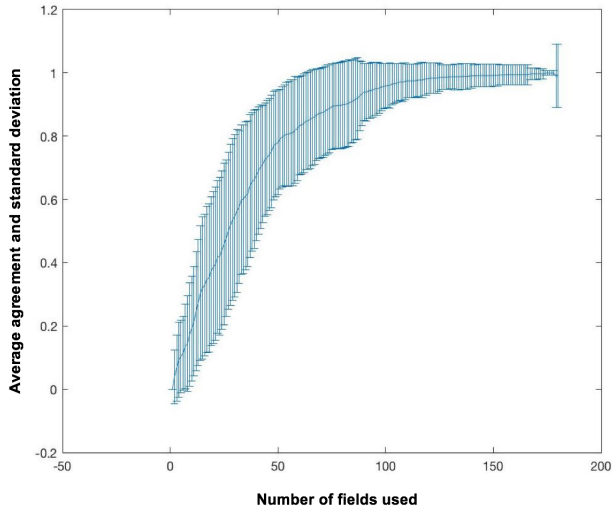

(a) Relationship between the number of fields sampled and the best match expected

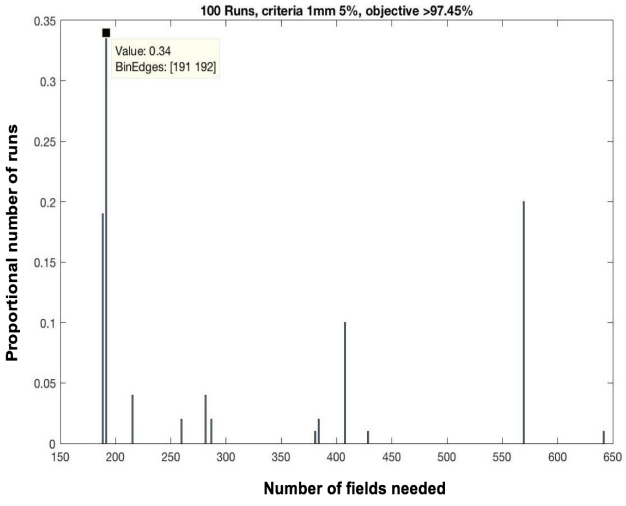

(b) Number of fields needed to achieve the requested point-to-point matching objective of 97.5% with a 5% difference in tolerance.

Fig. 4.26. Tests made with the FluenceTest module with the objective of assessing the number of sampled fields influence.

4.3 Clinical Case

The real VMAT case tested shown an agreement between the PRIMO MC calculation and the TPS calculation of 98,4% with criteria 2% / 2 mm for the Arc 1. As for the Arc 2 resulted 95,8% for the same criteria. When considering both arcs the integral treatment, gave the result of 97,2% points with gamma $<$ 1 with the same 2% - 2mm criteria. Adding to the possibility of the simulation and evaluation of a TPS calculation for a dynamic treatment, the workflow and application also contemplate the possibility of simulation of the Trubeam trajectory logs which allows to assess the real deposited dose distribution and compare with the expected one.

Arc 1 - Calculation results

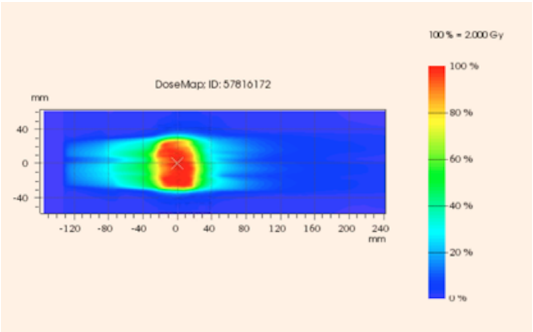

(a) Arc 1 TPS calculation

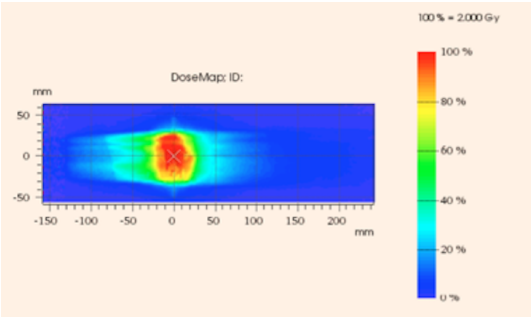

(b) Arc 1 MC Calculation

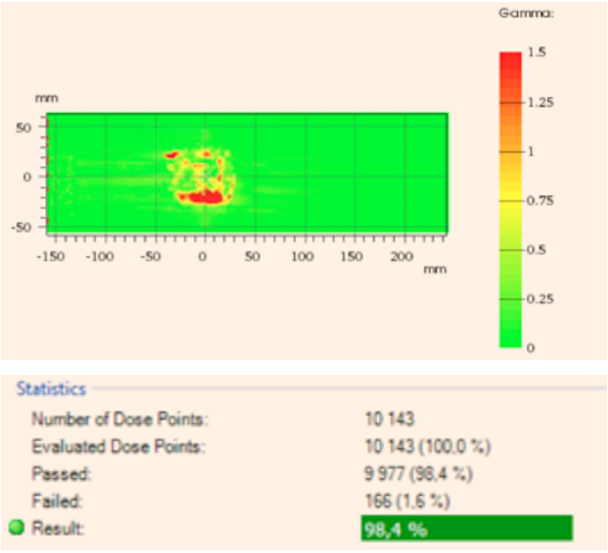

(c) Gamma evaluation

Fig. 4.27. Arc 1 - Gamma evaluation 2% 2mm between TPS calculation and MC simulation.

Arc 2 - Calculation results

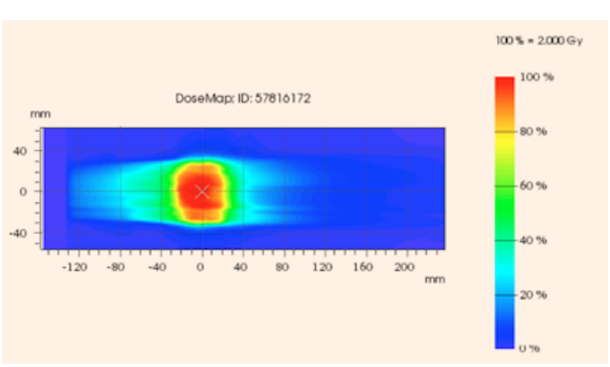

(a) Arc 2 TPS calculation

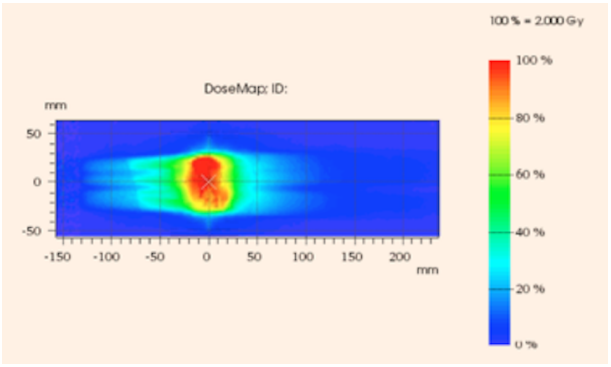

(b) Arc 2 MC Calculation

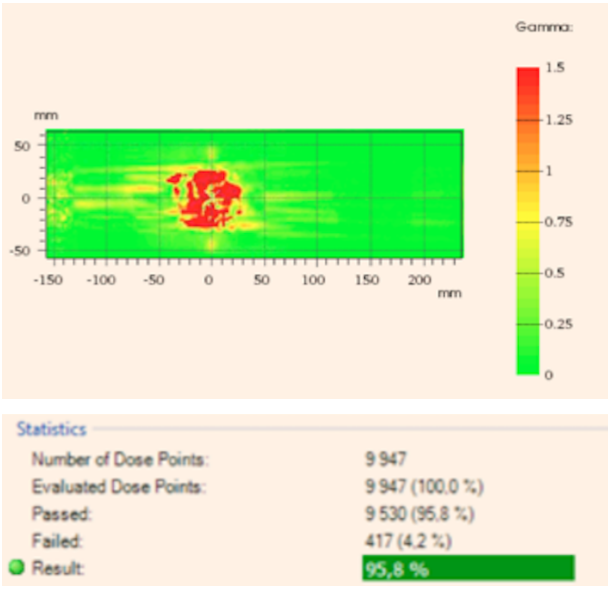

(c) Gamma evaluation

Fig. 4.28. Arc 2 - Gamma evaluation 2% 2mm between TPS calculation and MC simulation.

Complete Integrated treatment calculation results

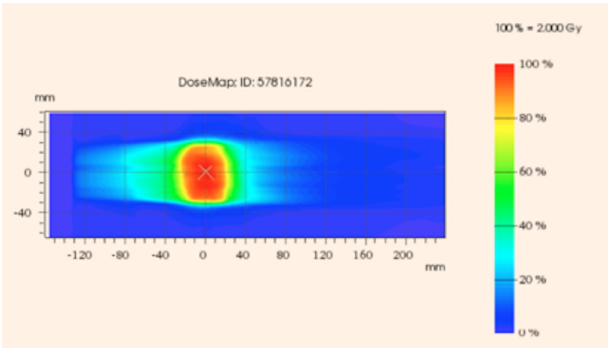

(a) Total treatment TPS calculation

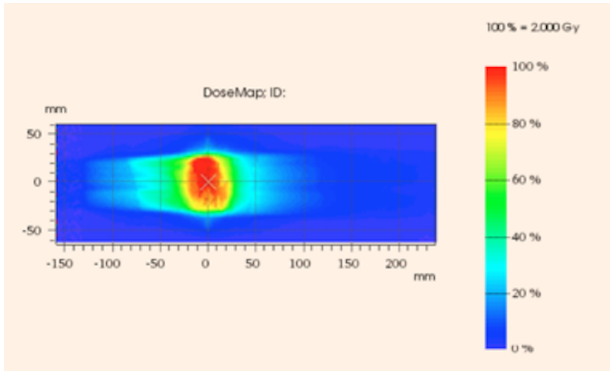

(b) Total treatment MC Calculation

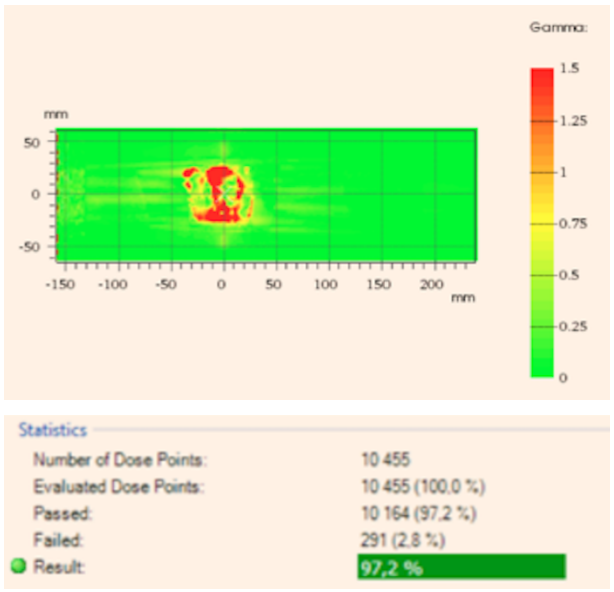

(c) Gamma evaluation

Fig. 4.29. Total treatment - Gamma evaluation 2% 2mm between TPS calculation and MC simulation.

Although the results obtained can in general be considered very good, an eternal issue that always comes to the talk when dealing with MC arose, i.e., the time needed to perform the calculations. The larger the field, the higher the number of particles to be tracked passing through the collimator and hitting the phantom, and the longer the time needed to complete the simulation. Adding to these ”natural time” to perform the simulation itself, the way PRIMO manages data files is not optimized. The time the operating systems consumes writing and managing large size files is still a possible obstacle for the daily use of this methodology and workflow. The time spent in calculating is compensated, especially in conditions, where commercial algorithms performances are critical, by the quality od the calculation, that in turns allows to minimize the risks of due to algorithm calculation bias.

5. Conclusions and Future Work

5.1 Achievements

TrueBeam Machine phase space validation allows its use for the 6FFF, 10FFF and 15MeV Monte Carlo simulation.In addition, the validation of the MLC model and of the probabilistic sampling algorithm developed allows simulating dynamic treatments with intensity modulation. Finally the GUI developed and in conjunction with PRIMO allows implementing a workflow that simplifies the application of the Monte Carlo method for the simulation of dynamic treatments in the daily practice.

5.2 Future Work

Of course one case doesn't make the whole history, and so, much more clinical cases should be tested in order to check for consistency and limitations.
As the users begin to use the GUI and Workflow from their feedback a continuous improvement process will start.
As a general statement, the number of fields should not be influenced by the number of geometries to be simulated. In other words, the total number of radiation beam particles is fixed. The condition for this statement to be true is that the time needed by the operating system to perform operations of read/write with large files is negligible with respect to the tracking time. In PRIMO each field creates large text files, each one associated to a parallel process. At the end of each beam, a post-process time is dedicated to integrate the output matrix file from each process, and this operation can be very time consuming. Consequently, a future improvement should be addressed to study the performance of PRIMO simulating multi-field treatments as the case of dynamic procedures and, possibly, to minimize the number of fields to sample, once the desired accuracy is defined. A first optimization algorithm was already implemented within the APP but it still needs refinements.
Currently, even with the use of the APP, the workflow still implies switching between different applications to perform some tasks. It would be a great improvement to get a higher degree of

automation to the point of executing the whole process within the same program, ideally this could be done within PRIMO.

Finally, in the view of the future clinical implementation of the APP, in order to assist the clinical Medical Physicists to simulate dynamic RT procedures in the daily practice, a number of training sessions should be dedicated to the explanation of the APP functionality and the algorithms, working through the whole simulation configuration process.
The results of this work has been presented at the last International Conference on Monte Carlo Techniques for Medical Applications (MCMA2017) in Naples as a poster and a collaboration is ongoing with the development group of PRIMO. The collaboration aims to setup benchmark conditions for the dynamic simulations, in the view of release of future version of PRIMO.

Bibliography

[1] Frank Verhaegen Joao Seco. *Monte Carlo Techniques in Radiation Therapy*. CRC Press.

[2] Frank Verhaegen and H Helen Liu. Incorporating dynamic collimator motion in monte carlo simulations: an application in modelling a dynamic wedge. *Physics in Medicine and Biology*, 2001.

[3] D. Schaart W. van der Zee M. Tomsej C. van Vliet-Vroegindeweij J. Jansen M. Coghe C. De Wagter B. Heijmen N. Reynaert, S. van der Marck. Monte carlo treatment planning. Technical report, Netherlands Commission on Radiation Dosimetry, 2006.

[4] miguel lázaro rodríguez castillo. *Automation of the Monte Carlo simulation of medical linear accelerators*. PhD thesis, Universitat Politecnica de Cataluna, 2015.

[5] Frank Verhaegen H Helen Liu and Lei Dong. A method of simulating dynamic multileaf collimators using monte carlo techniques for intensity-modulated radiation therapy. *Physics in Medicine and Biology*, 46:2283–2298, 2001.

[6] X. Allen Li Rompin Shih and James C. H. Chu. Dynamic wedge versus physical wedge: A monte carlo study. *Medical Physics*, 28(4):612–619, April 2001.

[7] Frank Herbert Attix. *Introduction to Radiological Physics and Radiation Dosimetry*. WILEY, 2004.

[8] Richard Popple Ellen Yorke Niko Papanikolaou Sotirios Stathakis Ping Xia Saiful Huq-John Bayouth James Galvin Fang-Fang Yin Ying Xiao, Stephen F. Kry. Flattening lter-free accelerators: a report from the aapm therapy emerging technology assessment work group. *Journal of Applied Medical Physics*, 16(3), 2015.

[9] Oleg N Vassiliev Stephen F Kry and Radhe Mohan. Out-of-field photon dose following removal of the flattening filter from a medical accelerator. *Physics in Medicine and Biology*, (55):2155–2166, 2010.

[10] ICRU. Prescribing, recording, and reporting photon beam therapy. Technical report, International Comission on Radiation Units and Measurements.

[11] D. J. Convery and M. E. Rosenbloom. The generation of intensity-modulated fields for conformal radiotherapy by dy- namic collimation. *Physics in Medicine and Biology*, 37: 1359–1374, 1992.

[12] A. Brahme. Optimization of stationary and moving beam radi- ation therapy techniques. *Radiation Oncology*, 12:129–140, 1988.

[13] C. X. Yu and G. Tang. ntensity-modulated arc therapy: principles, technologies and clinical implementation. *Physics in Medicine and Biology*, 56, 2011.

[14] K. Otto. Volumetric modulated arc therapy: Imrt in a single gantry arc. *Medical Physics*, 35:310–317, 2008.

[15] Jeffrey Siebers Pamela Garmon Larry Cox Mark R. Arnfield, Christine Hartmann Siantar and Radhe Mohan. The impact of electron transport on the accuracy of computed dose. *Medical Physics*, 27(6):1266–1274, June 2000.

[16] Laura K. Methods for dose calculation and beam characterization in external photon beam radiotherapy. Master's thesis, Helsinki University of Technology, 2009.

[17] Antonio M. Lallena Lorenzo Brualla, Miguel Rodriguez. Monte carlo systems used for treatment planning and dose verification. *Strahlenther. Onkol.*, 2016.

[18] Lorenzo Brualla Josep Sempau, Andreu Badal. A penelope-based system for the automated monte carlo simulation of clinacs and voxelized geometries—application to far-from-axis fields. *Medical Physics*, 38(11):5887–5895, November 2011.

[19] J. Sempau M. Rodríguez and L. Brualla. Primo: A graphical environment for the monte carlo simulation of varian and elekta linacs. *Strahlenther. Onkol.*, 1889:881–886, 2013.

[20] Sempau Brualla, Rodriguez. *PRIMO User's Manual - SOFTWARE VERSION 0.1.5.1202*.

[21] C.-M. Ma D.W.O. Rogers F. Sánchez-Doblado J. Sempau J. Seuntjens J. V. Siebers R. Capote, R. Jeraj. Phase-space database for external beam radiotherapy. Technical report, IAEA - International Atomic Energy Agency, 2005.

[22] Sasa Mutic Daniel A. Low, William B. Harms and James A. Purdy. A technique for the quantitative evaluation of dose distributions. *Medical Physics*, 25(5):656–661, May 1998.

[23] Daniel A. Low and James F. Dempsey. Evaluation of the gamma dose distribution comparison method. *Medical Physics*, 30(9):2455–2464, September 2003.

[24] Jong O. Kim Qiuwen Wu-Paul J. Keall Mark R. Arnfield, Jeffrey V. Siebers and Radhe Mohan. A method for determining multileaf collimator transmission and scatter for dynamic intensity modulated radiotherapy. *Medical Physics*, 2000.

[25] Jeffrey V. Siebers and Charlie Ma. Monte carlo applications in imrt planning and quality assurance. Technical report, American Association of Physcists in Medicine, 1991.

[26] M Arnfield J O Kim P J Keall, J V Siebers and R Mohan. Monte carlo dose calculations for dynamic imrt treatments. *Physics in Medicine and Biology*, 46:929–941, 2001.

[27] P. Andersson M. Krantz R. Chakarova, R. Cronholm. Monte carlo patient-speci c pretreatment qa system for volumetric modulated arc therapy. Technical report, Swedish Radiation Safety Authority, 2017.

[28] Alessandro Esposito. Primo software as a tool for monte carlo simulations of intensity modulated radiotherapy: A feasibility study primo software as a tool for monte carlo simulations of intensity modulated radiotherapy: A feasibility study. .

[29] Antonella Fogliata Luca Cozzi Josep Sempau-Alessandro Clivio Giorgia Nicolini Eugenio Vanetti Harald Krauss Catherine Khamphan Pascal Fenoglietto Josep Puxeu David Fedele Pietro Mancosu Maria F. Belosi, Miguel Rodriguez and Lorenzo Brualla. Monte carlo simulation of truebeam flattening-filter-free beams using varian phase-space files: Comparison with experimental data. *Medical Physics*, (41), 2014.

A. Simulation Workflow

A.1 Workflow Diagram

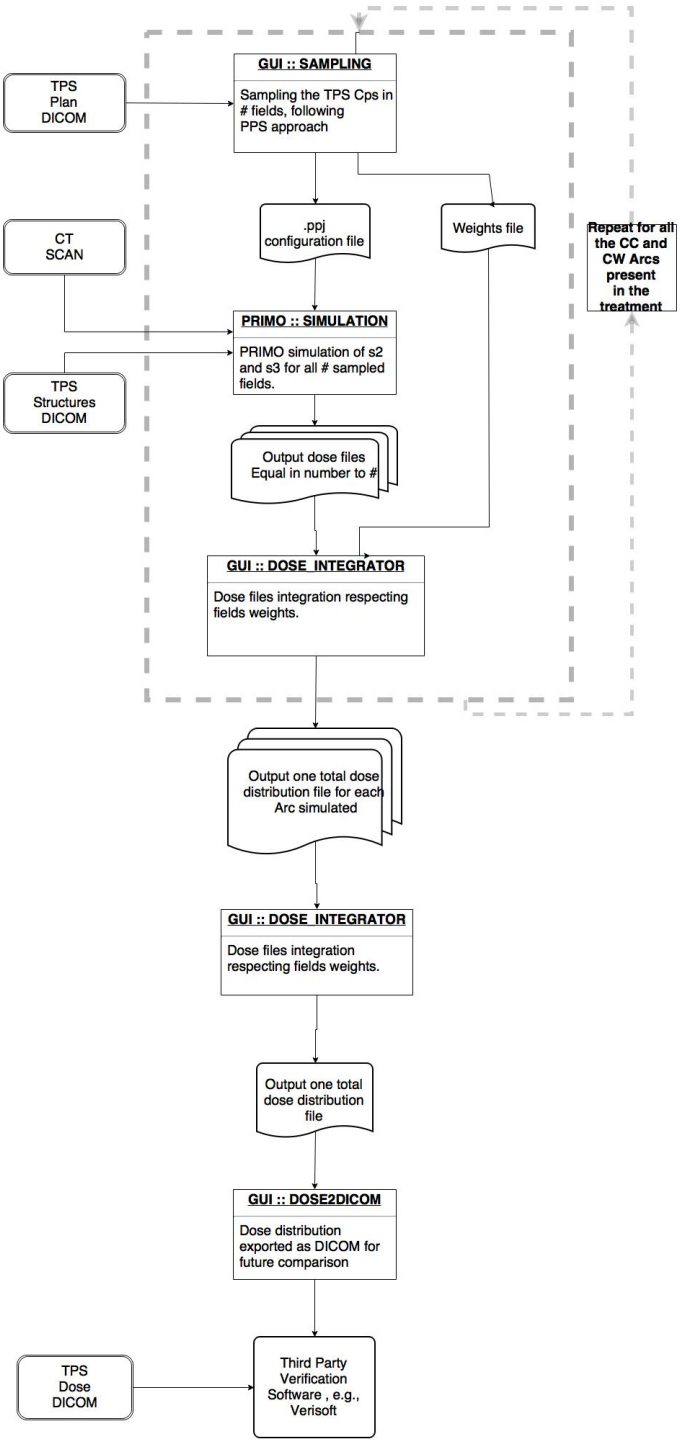

Fig. A.1. Workflow proposed for the MC simulation of a VMAT treatment.

A.2 VMAT_APP: Classes diagram

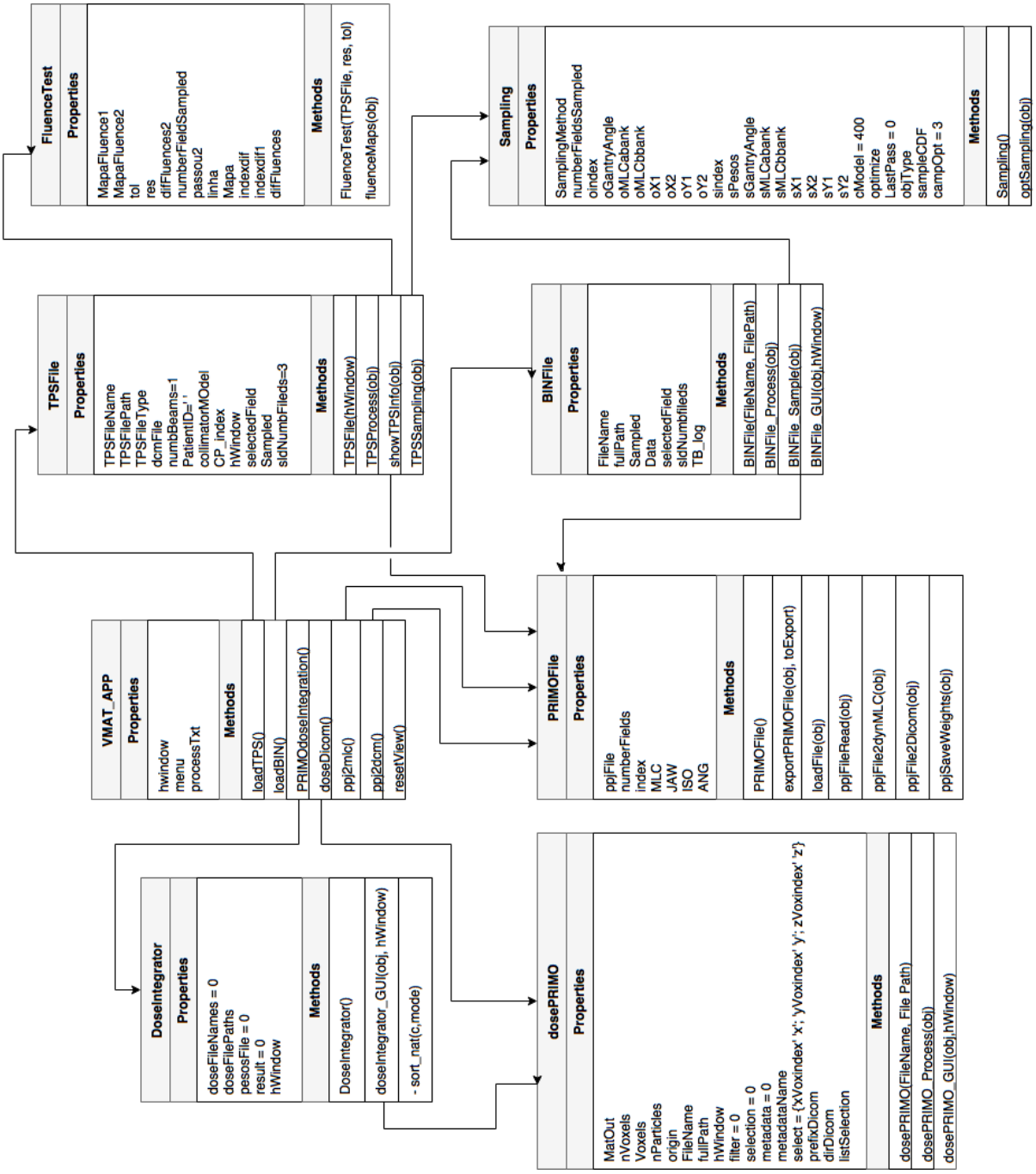

Fig. A.2. Classes diagram for the VMAT_APP